ABSTRACT

ABIT, SERGIO JR. Hydrologic Effects on Subsurface Fates and Transport of Contaminants. (Under the direction of Dr. Aziz Amoozegar and Dr. Michael Vepraskas.)

Concerns over contamination of ground water (GW) and its subsequent effect on surface water quality underscore the need for an improved understanding of the fate and transport of the contaminants in the subsurface. Among the contaminants that are harmful to humans and the environment are nutrient pollutants [e.g., nitrogen (N) and phosphorus (P)] and microbes. The general goal of this research was to evaluate the subsurface fates and transport of contaminants in a vadose zone-GW continuum under various simulated hydrologic conditions through a series of laboratory-scale studies.

The first study, which aimed to visually evaluate the effects of GW velocity and water table (WT) fluctuation on the fate and extent of horizontal transport of solutes and microbes in the capillary fringe (CF) and GW, was conducted in a sand-packed flow cell. Subsurface transport of surface-applied solutes and microbes tended to be isolated in the CF at a higher pore-water velocity. A rise in WT resulting from surface recharge of contaminated water occurred without the contaminants reaching the original water table. Subsequent drainage did not effectively leach contaminants that were initially in the CF into the GW.

The second study assessed the effect of pore-water velocity on the development of reduced conditions in a vadose zone-GW continuum. Reduction potential (Eh) was monitored at various locations in flow cells packed with Ponzer (Terric Haplosaprists), Lynchburg (Aeric Paleaquult), and Leon (Aeric Alaquod) soil materials that were subjected to different lateral pore-water velocities. Regardless of organic carbon (OC) content of the soil materials (12.4 to 195 g kg^{-1}), locations close to the WT became reduced within 14 days.

In contrast, the upper portions of the CF remained oxic. Increasing the pore-water velocity also slowed the development of reducing conditions especially in soils with low OC content.

The third study was conducted to evaluate the effect of pore-water velocity on the fate and transport of nitrate (NO_3^-) in a simulated vadose zone-GW continuum. This was conducted in flow cells packed with soils of various OC content (0.3 to 35 g kg^{-1}) that were subjected to different horizontal water velocities. Nitrate and bromide (Br) concentrations as well as Eh at various locations along the flow path of an applied NO_3^- and Br^- solution were monitored. Results show that in the presence of sufficient OC, NO_3^- was lost under reducing conditions below the WT but persisted while in transport in aerobic regions in the CF. Increasing GW flow pore-water velocity from 3.5 to 28 cm d^{-1} reduced the degree of NO_3^- removal from solution. High flow velocity also tended to limit the horizontal transport of surface-applied NO_3^- only in the upper regions of the CF.

The fourth study was conducted to evaluate the dissolution of phosphorus (P) in pore-water flowing through the vadose zone-GW continuum. Distilled water was allowed to flow horizontally at different pore-water velocities through flow cells packed with an organic soil material (from Ponzer series). Extensive P dissolution was detected below and just above the WT. Phosphorus dissolution at the upper portion of the CF was relatively limited.

The results obtained in this study suggest the following: a) the non-detection of contaminants below the WT down-gradient from a source does not definitively indicate that contaminants are not being transported horizontally in the subsurface as they can be transported in the CF, b) collection of samples from the CF should be considered when monitoring the subsurface transport of contaminants, and c) the hydrology of a system could be managed to improve nitrate removal from solution or to limit P dissolution.

Hydrologic Effects on Subsurface Fates and Transport of Contaminants

by
Sergio Manacpo Abit Jr.

A dissertation submitted to the Graduate Faculty of
North Carolina State University
in partial fulfillment of the
requirements for the Degree of
Doctor of Philosophy

Soil Science

Raleigh, North Carolina

2009

APPROVED BY:

_____	_____
Aziz Amoozegar Co-Chair of Advisory Committee	Michael J. Vepraskas Co-Chair of Advisory Committee
_____	_____
Wei Shi Committee Member	Owen W. Duckworth Committee Member
_____	
William J. Showers Committee Member	

DEDICATION

To Pam and Andre,

my special reasons to chase a dream…

BIOGRAPHY

Sergio Manacpo Abit Jr. was born on August 28, 1975 in Baybay, Leyte, Philippines. He is the 5th of a brood of five of Sergio E. Abit Sr. and Adelaida Manacpo-Abit. He is married to the former Ms. Pamela Milan Po with whom he has a son, Serge Andre. He completed a Bachelor of Science degree in Agriculture, with a major in Soil Science, from the Visayas State College of Agriculture (now Visayas State University or VSU), in Baybay, Leyte, Philippines. He is connected to the Department of Agronomy and Soil Science at VSU. In 2003, he was awarded a full scholarship by the Fulbright-Philippine Agriculture Scholarship Program to pursue graduate studies in Soil Science. In the fall of 2005, he received his Master of Science degree in the Department of Soil Science at North Carolina State University (NSU), Raleigh, North Carolina, where he specialized in environmental soil physics under the guidance of Dr. Aziz Amoozegar and Dr. Michael J. Vepraskas. He then pursued his Ph.D. in Soil Science at NCSU beginning in the fall of 2006 under the guidance of the same professors. He specialized in environmental soil physics and minored in hydrogeology. Sergio is a member of the Phi Kappa Phi Honor Society, the Gamma Sigma Delta Honor Society, the Sigma Xi Honor Society, the Soil Science Society of North Carolina, the Society of Wetland Scientists, the Soil Science Society of America and the American Society of Agronomy.

ACKNOWLEDGEMENTS

I was blessed with the privilege to work with an outstanding group of people without whom this research project would have never been possible. My sincerest thanks goes to Dr. Aziz Amoozegar, my major professor, mentor and co-Chair of my research committee, for advising me through this research, guiding me in writing manuscripts, directing me through my coursework and helping me deepen my appreciation of soil physics. Sincere thanks also goes to Dr. Michael Vepraskas, my co-mentor and co-Chair of my research committee, for his guidance, valuable suggestions and instilling in me the value of always considering the practical impacts of a research endeavor. I also thank Dr. Wei Shi, Dr. Owen Duckworth and Dr. William Showers, members of my advisory committee, for their comments and suggestions that lead to the improvement of my research.

Special thanks to Christopher Niewoehner, research assistant of the Hydropedology Group, for providing all the logistical support I needed in this research. Thanks also to Dr. Alexandra Graves and Dr. Dean Hesterberg for their willingness to help me with my research. I also would like to express my gratitude to Emily Dell, Brad Robinson, Guillermo Ramirez, Kim Hutchison, Lori Saal, Lisa Lentz, Roberta Miller-Haraway, Christopher Stall, Colby Moorberg and Amanda Zelasko-Morris for their assistance. To the Soil Science family at the North Carolina State University (NCSU), thank you for treating me as you own.

I would like to express my deepest gratitude to the North Carolina Department of Transportation for funding this research. I also would like to acknowledge the support of my

home institution, the Visayas State University (LSU) and to the Department of Agronomy and Soil Science at VSU for allowing to me go on study leave to pursue my Doctorate.

Special thanks go to my wife and best friend, Pamela Po Abit, for her unwavering support and understanding, and to my son, Serge Andre, for providing me the daily drive to work harder. Thanks also to my parents Tatay Serge and Nanay Deling, my brother, sisters and extended families for their prayers. Finally, to the Lord Almighty, thanks for the wisdom and strength!

TABLE OF CONTENTS

LIST OF TABLES

CHAPTER 2

CHAPTER 3

CHAPTER 4

CHAPTER 5

LIST OF FIGURES

CHAPTER 1

CHAPTER 2

CHAPTER 3

Chapter 4

CHAPTER 5

CHAPTER 1

Hydrologic Effects on Subsurface Transport of Surface-Applied Solutes and Microbes in a Vadose Zone-Shallow Ground Water Continuum

Abstract

Better understanding of the processes governing the subsurface transport of contaminants is vital to their proper monitoring and treatment. This study was conducted to evaluate the effects of ground water (GW) velocity and water table (WT) fluctuation on the fate and extent of horizontal transport of solutes and microbes in the capillary fringe (CF) and GW. A set of experiments was conducted using medium sand packed in a 90 × 50 × 3.5 cm flow cell to visually evaluate the transport of a surface-applied dye solution and fluorescent *Escherichia coli* suspension in the vadose zone and GW under various simulated hydrologic conditions. To simulate GW and CF, the bottom 12 cm of the flow cell was saturated and lateral GW flow or static WT was established by manipulating the water levels on the left and right sides of the flow cell. A solution containing acid-red dye or *E. coli* was applied to a small area on the surface of the flow cell and the path of the dye or *E. coli* was visually monitored with time. Surface-applied solutes and microorganisms tended to be transported vertically in the vadose zone until reaching the CF before being transported horizontally above the WT. At a relatively high flow velocity, horizontal transports of surface-applied contaminants were confined to the upper portion of the CF. With a decrease in the lateral GW flow velocity the dye and microbes tended to move deeper in the CF and

eventually entered the saturated zone below the WT. Surface recharge with water containing dye and microbes showed a rise in WT before the contaminants could reach the original WT. Subsequent drainage resulted in a drop in WT without appreciably leaching vertically the dye and microbes that were in the CF prior to drainage. Because solutes and microbes in the CF can be transported horizontally in the presence of horizontal GW flow, their non-detection below the WT does not indicate that the surface-applied chemicals and microbes are not transported horizontally in the subsurface. Monitoring of the vadose zone, particularly the CF, should be considered when monitoring the horizontal transport of soluble chemicals and suspended microbes in the subsurface.

1. Introduction

Concerns over microbial and chemical contamination of GW and its subsequent effect on surface water quality highlight the need for an improved understanding of the fate and transport of microbes and solutes in the subsurface. Interest in subsurface fate of microbes is rooted from known cases of microbial contamination of both surface waters (USEPA, 2004) and subsurface drinking water sources (USEPA, 2006), and from the role that microbes play in the restoration of contaminated aquifers (Lee et al., 1988; Lovley, 1995; Scow and Hicks, 2005). Attention has also been directed to chemical contaminants as they pose a hazard to the environment (Correll, 1998) while some may cause diseases in humans and animals (Gerba, 1996). Contaminant solutes and microbes may be introduced to the soil via planned activities, such as concentrated animal feeding operations; through accidental spills and storage leakage; and from faulty waste treatment infrastructure, such as leaky sewer pipes, landfills and septic systems (Bedient et al., 1997).

Various chemical and physical properties affect the fates of soluble chemical and microbial contaminants in the soil. Properties of chemical pollutants; including their net charge, ability to be taken up by plants and microbes, and redox properties; determine whether a given chemical is sorbed to the porous media, transformed, utilized by plants and microbes, or remains in solution for transport (Bedient et al., 1997). Microbial properties; such as size, shape, hydrophobicity, and electrostatic charge; determine whether a microbe is transported, sorbed, or strained/filtered in the soil (Ginn et al., 2002). In addition, microbial ability to compete for growth factors in the subsurface affects their survival (Coyne, 1999).

It is common knowledge that when soluble chemical and microbial contaminants are applied to the soil in improper schemes and amount, they can exceed the attenuation capacity of the soil and remain available for transport in the subsurface. When available for transport, their fate in the subsurface becomes largely determined by the hydrology of the system.

On a field or watershed scale where a contaminant plume had traveled for hundreds of meters after years of transport, the plume is usually tongue-shaped and deeper in the aquifer at the advancing plume front than at locations closer to the source (Frind and Hokkanen, 1987; LeBlanc, 1984). The dip in the plume front is largely attributed to years of recharge mainly resulting from precipitation that pile on the advancing plume, pushing it downward as it moves horizontally. On a local scale, i.e., where a contaminant source is near the location of interest (e.g., stream, ditch, drinking water well), downward movement of the plume is most likely less extensive. This is because the plume could reach the location of interest before extensive surface recharge is able to push the contaminants effectively into the aquifer. It is in this case or transport scale that horizontal transport in the vadose zone, mainly in the CF, could be a major contribution to the overall subsurface horizontal transport of the contaminants.

Transport of solute and microbial contaminants in the vadose zone and shallow groundwater has been studied for many years. Surface applied solutes have been described to move vertically down rather uniformly or in fingers at regions in the vadose zone with low water content (Jawitz et al., 1998; Martin and Kroener, 1984). However, at regions in the vadose zone with high water content, such as the CF, solute transport shifts from

predominantly vertical to a predominantly horizontal direction, as demonstrated in sand-packed flow cell experiments (Silliman et al., 2002). In addition, laboratory scale simulations have shown that up to 100% of surface-applied solutes can be transported horizontally in the CF without intersecting the WT (Amoozegar et al., 2006; Henry and Smith, 2002; Silliman et al., 2002). Heterogeneity of the porous media in the CF also affects horizontal transport. In a flow cell experiment, coarser lenses in the CF with higher hydraulic conductivity provided transport routes above the WT for accelerated horizontal transport of solutes (Silliman et al., 2002). Horizontal transport in the CF was also demonstrated to appreciably contribute to the subsurface transport of solutes under field conditions (Abit at al., 2008a,b).

Horizontal transport of bacteria in the CF has also been demonstrated in a laboratory scale experiment where green fluorescent protein (GFP)-transformed *Escherichia coli* were transported via advection from below the WT to the CF (Dunn et al., 2004). The said experiment also showed that while in the CF, the microbes were transported horizontally and that coarse sand lenses above the WT served as preferred paths for microbial transport that facilitated the relatively early arrival of the bacteria at the outflow boundary.

While it had been demonstrated that soluble solutes and microbes can be transported horizontally in the CF in the presence of horizontal GW flow, no study has been conducted evaluating the influence of hydrology on the extent of horizontal transport of contaminants in the CF. Moreover, because the WT is never static under field conditions, it its imperative to examine the fates of solutes and microbes in the CF as the WT fluctuates. This study was conducted to: a) visually assess the effect of horizontal pore-water velocity on the horizontal

transport of solutes and microbes in a CF-GW continuum, and b) evaluate the effect of WT fluctuation on the fate of solutes and microbes in the subsurface.

2. Materials and Methods

2.1. Experimental Set-up

Laboratory simulations of solute and microbial transport were performed in a 90-cm long, 50-cm high and 3.5-cm wide flow cell packed with medium sand (Fig. 1). The front side of the flow cell was covered with 0.64 cm-thick tempered glass that was not ultraviolet (UV) protected and the other sides were made of flat polyvinylchloride (PVC) sheets. Two 2.5 cm-wide chambers, with perforated inner walls were constructed on the two sides of the flow cell (see Fig. 1). The middle 85 cm of the flow cell (located between the two chambers with perforated walls) was packed with commercially available medium sand material at a bulk density of 1.7 g cm^{-3}. The outlet chamber was connected to a plastic tubing with its open end fixed at 12 cm above the bottom of the flow cell. The inlet chamber was connected by plastic tubing to a 25-L (Marriotte bottle) reservoir with the tip of the air inlet tube also set at 12 cm above the bottom of the flow cell. A simulated WT, at 12 cm above the bottom of the flow cell, was then established by introducing water (or broth solution in the case of the microbial simulation) from the reservoir.

A desired slope of the WT that translated to a particular rate of horizontal flow velocity across the flow cell was achieved by manipulating the elevation of the air inlet tube in the Marriotte bottle reservoir. Before any solute or microbial transport simulation was initiated, trial runs were conducted to determine the horizontal pore-water velocities as a function of the slopes of the WT for the experiment.

2.2. Dye Solution and Microbial Suspension

A 0.5 g L^{-1} acid red dye (azophloxine) solution was used for visual evaluation of solute transport at various hydrologic conditions in the simulated vadose zone and shallow GW in the flow cell. The bacteria *Escherichia coli* strain JM109 (Promega Corporation, Madison, WI) was used as the model microorganism. To be able to visually observe the transport of *E. coli*, the bacteria was transformed using the plasmid pGFPuv (Clontech Laboratories, Mountain View, CA.) using the standard transformation protocol (Promega, 2000) to make the bacteria fluoresce under UV light. One hundred µL of the transformed bacterial stock was inoculated into 125 ml of Luria Bertani (LB) broth solution (Difco Laboratories, Detroit, MI) in a 250 ml Erlenmeyer flask. The LB broth solution (25 g LB broth powder per L distilled water) was added with ampicillin at 100 mg L^{-1}. The culture was incubated in a water bath at a constant temperature of 37 ^{o}C and agitated at 100 revolutions min^{-1}. A 2-mL sample was taken from the culture every 4 hours and tested for fluorescence under a 365 nm UV lamp (UVP, Upland, CA.). When a bright green fluorescence (under UV light) of the bacterial suspension was achieved, several stock suspensions were prepared by adding 100 µL suspension to 400 µL of sterile glycerol and stored at -80^{o}C until use. Serial dilution in sterile water and plating on LB agar revealed that bacterial suspension concentration was at 10^{8} cells per mL when a bright green suspension was achieved.

Thirty-six hours before a scheduled microbial transport simulation, the fluorescent bacterial suspension was mass-produced by inoculating 100 µL of stock suspension into each

250 ml Erlenmeyer flask with 125 mL sterile LB broth solution (with ampicillin) and incubated for 36 hours at a 37^{o}C water bath agitated at 100 revolutions min^{-1}.

Two sets of simulation were conducted:

1) subsurface transport of surface-applied dye solution and microbial suspension at three horizontal pore water velocities; and
2) solute (dye) and microbial fate in a simulated rising and falling WT.

2.3. Horizontal Transport of Dye and Microbes

Evaluation of horizontal transport of dye solution and microbial suspension in a simulated vadose zone and shallow groundwater continuum was conducted under three hydrologic conditions:

a) No horizontal flow (flat WT)
b) WT slope of 1.5% - resulting in a horizontal pore-water velocity of ~ 82 cm d^{-1}
c) WT slope of 3.0 % - resulting in a horizontal pore-water velocity of ~160 cm d^{-1}

2.3.1. Solute Transport

Under no flow condition, distilled water was introduced to the flow cell to establish a flat WT at 12 cm above the bottom of the flow cell. The flow cell was then disconnected from the Marriott bottle reservoir and both the outlet and inlet chambers were connected to separate plastic tubing with their ends fixed at 12 cm above the bottom of the flow cell. This allowed water to drain through both sides of the flow cell to maintain the level of the simulated WT even during dye application. The acid red dye solution was applied on the

surface at application spot B (shown in Fig. 1) by pumping the dye solution at a constant rate of 2.4 L d^{-1}. Time-lapse photographs were then taken every 30 minutes for 10 hours.

For the simulation involving a flowing shallow GW, the tubing connected to the inlet chamber was connected to the Marriotte bottle reservoir (see Fig. 1). The air-inlet tube in the reservoir was then raised by 1.3 cm above the flat WT level. This resulted in a 1.5% slope of the WT that resulted in a horizontal pore water velocity of 82 cm d^{-1}. Outlet discharge rate was monitored for four hours (4 hour-long trials) to check whether constant water flow was achieved. Acid red dye solution was then applied at application spot A shown in Figure 1 at a rate of 2.4 L d^{-1}. Time lapse photographs were taken at 30-minute intervals. A similar case but with a WT slope of 3.0% (horizontal pore water velocity of approximately 160 cm d^{-1}) was conducted and time-lapse photographs were taken every 30 minutes for 10 hours.

2.3.2. Microbial Transport

A similar approach used in the solute transport experiment was adopted for the microbial transport simulation except that instead of using distilled water, half-strength LB-broth suspension (with ampicillin) was used to flood the flow cell to achieve the desired WT level. Bacterial suspension was added at the same rate as in the solute transport simulations at spots A or B (depending upon the simulation). Time-lapse photographs were taken every 30 minutes under illumination by a 365 nm UV lamp.

2.4. Solute and Microbial Fate at Rising and Falling WT

The simulation started with a static WT at 12 cm above the bottom of the flow cell. The outlet and inlet chambers were closed (no water coming in and going out). The surface

of the packed soil was covered with four layers of cheese cloth to encourage uniform distribution of the applied dye solution or bacterial suspension.

Two hundred mL of 0.5 g L^{-1} dye solution was evenly spread on the surface and allowed to infiltrate the packed material for one minute. To simulate rainfall, water was then pumped onto the surface through seven plastic tubes connected to a multi-channel variable speed peristaltic pump that delivered water equivalent to 5 cm rainfall for 70 minutes. Time-lapse photographs were taken every 5 minutes until the simulated WT rose by 12 cm (i.e., WT reached 24 cm above the bottom of the flow cell). After the WT rose to the desired elevation, the rain simulation was stopped and drainage simulation commenced.

The flow cell was slowly drained by opening the outlet chamber and dropping the level of the outflow end of the tubing (connected to the outflow chamber) by 1 cm every 5 minutes. Time-lapse photographs were taken every 5 minutes.

3. Results and Discussion

3.1. Effect of Horizontal Pore-Water Velocity on Dye and Microbial Transport

Figure 2a shows that under a flat WT condition (no horizontal water flow) surface-applied dye solution generally moved vertically downward in the unsaturated zone and was then observed to pile-up within the CF before it was able to move under the WT by displacing the dye-free water directly under it to the sides resulting in rise in WT. During this processes the water levels in the inlet and outlet chambers were maintained at 12 cm above the bottom of the flow cell allowing drainage from the flow cell. At the scale modeled, a similar behavior was observed where the bacterial suspension was applied at the surface (Fig. 2b). Similar to the observation with the dye solution, the microbial suspension moved generally downward in the vadose zone and accumulated in the CF before it pierced through the WT and into the simulated GW. Based on these observations, it could be said that in the absence of horizontal groundwater flow, a solute or bacteria from a given source (e.g., a septic system drainfield or an animal waste retention pond) moving vertically through the vadose zone can be expected to effectively remain in the CF and eventually move into the shallow groundwater provided that adequate volume of solution/suspension enters the system through the vadose zone.

When horizontal flow was induced by setting a 1.5 % slope of the simulated WT (pore-water velocity of 82 cm d^{-1}), it was observed that the applied solute initially spread radially around the source and then generally moved vertically downward in the vadose zone as initially observed under no flow conditions (Fig. 3a and 3b). However, as soon as the

solute plume reached the top of the CF, it showed indications of moving horizontally in the down-gradient direction (Fig. 3c). The plume was then observed to be transported progressively towards the down-gradient direction within the CF without moving to below the WT (Fig 3d and 3e). These observations were consistent with the results of Amoozegar et al. (2006) and Silliman et al. (2002). Figure 3f shows that although a part of the plume eventually moved below the WT, most of it was transported horizontally within the CF.

When the horizontal GW gradient (i.e., slope of WT) was 3%, similar to the earlier simulations, the dye plume moved generally downward with some radial dispersion while still above the CF (Fig. 4a and 4b). The plume was observed to be transported horizontally in the down-gradient direction as soon it entered the CF (Fig. 4c and 4d). Compared to the condition when the GW pore-water velocity was 82 cm d^{-1}, the horizontal part of the plume in the CF at GW pore-velocity of 160 cm d^{-1} tended to be thinner – flowing only at the upper portion of the CF (Fig. 4e and 4f). Moreover, 3.5 hours after the dye application, the plume fronts for the two flow rates were at approximately the same position (at approximately 35-40 cm from the inlet chamber) in the flow cell (Figs. 3c and 4c). However, after 7.5 hours (Figs. 3f and 4f), the plume front for the 160 cm d^{-1} pore-water velocity was at the outlet while the plume front for the 82 cm d^{-1} had moved half the distance (at approximately 65 cm from the inlet chamber). This indicates that the rate of horizontal water movement in the CF is proportionally related to the GW lateral flow velocity.

The difference in the position and the rate of advancement of the plumes between the two modeled cases can be explained by the hydrology-induced difference in the sizes of the

dye solution flow-paths. The ratio of the water moving laterally below the WT to the rate at which surface-applied solution enters the CF determines the cross sectional area, and hence the rate at which the plume moves within the CF. Horizontal transport through a relatively thinner portion of the CF, as in the case with 3% WT slope, means that solutes are transported across a flow-path with a smaller average cross sectional area. As a result, a given volume of solution entering the CF under relatively high GW flow velocity will travel faster and farther than at low GW flow velocity.

Transport of *E. coli* was also observed to follow the same general trend as the dye solute. When microbes were applied to one small area on the flow cell surface, they were initially transported downward in the unsaturated zone above the CF and horizontally in the down-gradient direction as soon as they reached the CF (Figs. 5 and 6). Moreover, as with the solutes, horizontal transport of microbes in the CF also tended to remain predominantly in the upper portion of the CF and seemed to be transported faster under higher GW horizontal flow rate.

The above discussion could be summarized into four key points: 1) at the scale modeled, the general behaviors of transport of soluble chemicals and microbes in a vadose zone and shallow GW continuum were comparable, 2) under relatively slow to no horizontal GW flow, surface-applied microbes and solute contaminants entered the GW, 3) at higher horizontal pore-water velocity, solute and microbial transport became more limited to the upper portion of the CF, and 4) the rate of solute transport in the CF increased with increasing the horizontal GW velocity. The later point indicates that the isolation of solute

and microbial transport to the upper portion of the CF leads to the early arrival of the plume at the down-gradient outlet.

3.2 Effect of Water Table Fluctuation

Figure 7 shows the fate of surface-applied solute and microbial contaminants in a rising WT resulting from surface recharge simulating rainfall. The faint red line above the WT in Figure 7a indicates the upper boundary of the CF. This red line was established earlier by applying red dye to the inlet chamber. The dye was then transported horizontally both in CF and below the WT by applying distilled water to the inlet leaving only the top of the CF stained with the red dye.

From an original elevation (Fig. 7a), the WT was observed to rise rapidly as soon as the wetting front (location shown by the dye front) approached the pre-event upper boundary of the CF (faint dye line –see Fig 7b). Moreover, in the absence of GW flow, the location of the faint dye line remained relatively stationary as the solute front approached indicating that water originally in the CF (below the faint dye line) remained in place and did not move up with the rise in WT (Fig. 7c). Water applied from the surface in this case filled the few remaining air-filled pores in the CF resulting in its full saturation and the subsequent rapid rise in WT (Gillham, 1984). Similar results were observed with the microbial simulation where the WT moved up as soon as the microbe front reached the CF (Fig. 7d-f).

In summary, Figure 7 showed two things: 1) solute and microbial contaminants in water entering the soil surface rather uniformly, as in rainfall or irrigation, does not necessarily contaminate the saturated zone itself even if surface recharge result in WT rise

(i.e., solute and microbes do not become a part of the original GW), and 2) water in the pre-event saturated and CF zones does not move up during a surface recharge-induced WT rise. These are important points that need to be considered for collecting subsurface water samples for monitoring purposes.

The effect of a receding WT on the fate of solute and microbial contaminants present in the CF during drainage is shown in Figure 8. Starting from a condition where a solute and microbial plume was initially present in the CF (Fig. 8a and 8d, respectively) no appreciable drop in both plumes was observed when the WT was dropped by 4 cm (Fig. 8b and 8e). As shown in Figures 8c and 8f, solute and microbial contaminants that were in the CF prior to drainage remained in the CF after the WT was dropped to pre-recharge levels.

The drop in WT requires the removal of only a small amount of water from the saturated zone. Removal of water equivalent to ~5% of saturated water content from the top 12 cm of the saturated zone in Figures 8a and 8d for example would rapidly make that region unsaturated resulting in a 12-cm drop in the WT. This would mean that despite the 12-cm drop in WT, 95% of the water (with dissolved solutes or suspended microbes) would still remain it that previously-saturated 12-cm zone. This mechanism explains why no appreciable downward movement in the solute and microbial plume was observed despite the WT fluctuations.

The observations shown in Figures 7 and 8 suggest that the non-detection of surface-applied solute and or microbial contaminants through collection and analysis of samples collected from below the WT does not necessarily mean that solute and microbial

contaminants applied in a pulse at the surface are not in a region where they can be transported horizontally in the subsurface. Indeed contaminants may be lodged in the CF where, as demonstrated in this study, they could be transported horizontally.

4. Summary and Conclusions

This study was conducted to evaluate the effect of horizontal pore-water velocity on the extent of horizontal transport of solutes and indicator microbe in the capillary fringe (CF) and ground water (GW), and to evaluate the effect of water table (WT) fluctuation on the fate of solutes and microbes in the subsurface. Subsurface hydrology influenced the location where surface-applied solutes and indicator microorganisms were transported horizontally in the subsurface. When surface-applied solutes and microorganisms reached the CF, they tended to be transported horizontally in the presence of horizontal GW flow. In addition to horizontal transport in the CF, contaminants were also transported horizontally below the WT when the GW flow velocity was low. In contrast, horizontal transport of surface-applied contaminants tended to be confined to the CF as horizontal GW flow velocity was increased. Confinement of contaminant transport to the upper portions of the CF at higher pore-water velocities also promoted the early arrival of the plume at the outlet. Surface recharge with water having solute and microbial contaminants resulted in WT rise even if the contaminants had not reached the original WT. Subsequent drainage that resulted in a drop in WT did not appreciably leach solute and microbial contaminants that were in the CF prior to drainage. Because solutes and microbes in the CF can be transported horizontally in the presence of horizontal flow of water, the non-detection of these contaminants below the WT despite its fluctuation does not indicate that the surface-applied chemicals and microbes cannot persist and be transported horizontally in the subsurface. These results suggest that

monitoring/sampling the vadose zone, particularly the CF, should be considered when monitoring the horizontal transport of soluble chemicals and microbes in the subsurface.

5. References Cited

Abit, S. M., A. Amoozegar, M. J. Vepraskas and C. P. Niewoehner. 2008a. Solute transport in the capillary fringe and shallow groundwater: Field evaluation. Vadose Zone J. 7:890-898.

Abit, S.M., A. Amoozegar, M. J. Vepraskas and C.P. Niewoehner. 2002b. Fate of nitrate in the capillary fringe and shallow groundwater in a drained sandy soil. Geoderma. 146:209-215.

Amoozegar, A., C.P. Niewoehner and D.L. Lindbo. 2006. Lateral movement of water in the capillary fringe under drain fields. In Proc. 2006 Tech. Educ. Conf., Denver Co. 27-31 Aug. 2006. Natl. Onsite Wastewater Recycling Assoc. Sta. Cruz, CA.

Bedient, P. B., H. S. Rifai and C. J. Newell. 1997. Groundwater Contamination: Transport and Remediation. Prentice Hall PTR. Upper Saddle River, NJ.

Correll, D. 1998. The role of phosphorus in the eutrophication of receiving waters: A review. J. Environ. Qual. 27:261–266.

Coyne, M. 1999. Soil Microbiology: An Exploratory Approach. Delmar Publishers. Albany, NY.

Dunn, A. M., S. E. Silliman, S. Dhamwichukorn and C. F. Kulpa. 2004. Demonstration of microbial transport into the capillary fringe via advection from below the water table. J. Hydrol. 306:50-58.

Frind, E. O. and G. E. Hokkanen. 1987. Simulation of the Borden plume using the alternating direction Galerkin Technique. Water Resour. Res. 23(5):918-930.

Gerba, C.P. 1996. Principles of toxicology. In: Pollution Science. Pepper, I.L, C.P. Gerba and M.L. Brusseau (eds). Academic Press. San Diego CA, pp: 323-343.

Gillham, R. W. 1984. The capillary fringe and its effect on water table rise. J. Hydrol. 67: 307-324.

Ginn, T. R., B. D. Wood, K. E. Nelson, T. D. Scheibe, E. M. Murphy and T. P. Clement. 2002. Process in microbial transport in the natural subsurface. Adv. Water Resour. 25(8-12): 1017-1042.

Henry, E. J. and J. E. Smith. 2002. The effect of surface-active solutes on water flow and contaminant transport in variably saturated porous media with capillary fringe effects. J. Contam. Hydrol. 56:247-270.

LeBlanc, D. R. 1984. Sewage plume in a sand and gravel aquifer, Cape Cod, Massachusetts. USGS Water Supply Paper 2218.

Lee, M. D., J. M. Thomas, R. C. Borden, P. B. Bedient, J. T. Wilson, and C.H. Ward. 1988. Biorestoration of aquifers contaminated with organic compounds. Crit. Rev. Environ. Control. 18:29-89.

Lovley, D. R. 1995. Bioremediation of organic and metal contaminants with dissimilatory metal reduction. Journal of Industrial Microbiology. 14:85-93.

Jawitz, J. W., M. D. Annable and P. S. C. Rao. 1998. Miscible fluid displacement stability in unconfined porous media: Two-dimensional flow experiments and simulations. J. Contam. Hydrol. 31(3-4):211-230.

Martin, J.P. and R.M. Koerner. 1984. The influence of vadose zone conditions on groundwater pollution. Part II: Fluid Movement. J. Hazardous Materials 9:181-207.

Promega. 2000. Technical Bulletin No. 095: *E. coli* Competent Cells. Madison, WI.

Scow, K. M. and K. A. Hicks. 2005. Natural attenuation and enhanced bioremediation of organic contaminants in groundwater. Curr. Opin. Biotech. 16:246-253.

Silliman, S. E., B. Berkowitz, J. Simunek, and M. Th. Van Genuchten. 2002. Fluid flow and solute migration within the capillary fringe. Ground Water. 40(1): 76-84.

USEPA. 2004. Monitoring and Assessing Water Quality. National Water Quality Inventory: Report to Congress, 2004 Reporting Cycle.
At: http://www.epa.gov/owow/305b/2004report/. Accessed: April 2009.

USEPA. 2006. Drinking Water Contaminants. Basic Information About *E. coli* in Drinking Water. At:http://www.epa.gov/safewater/contaminants/ecoli.html. Accessed: April 2009.

6. Figures

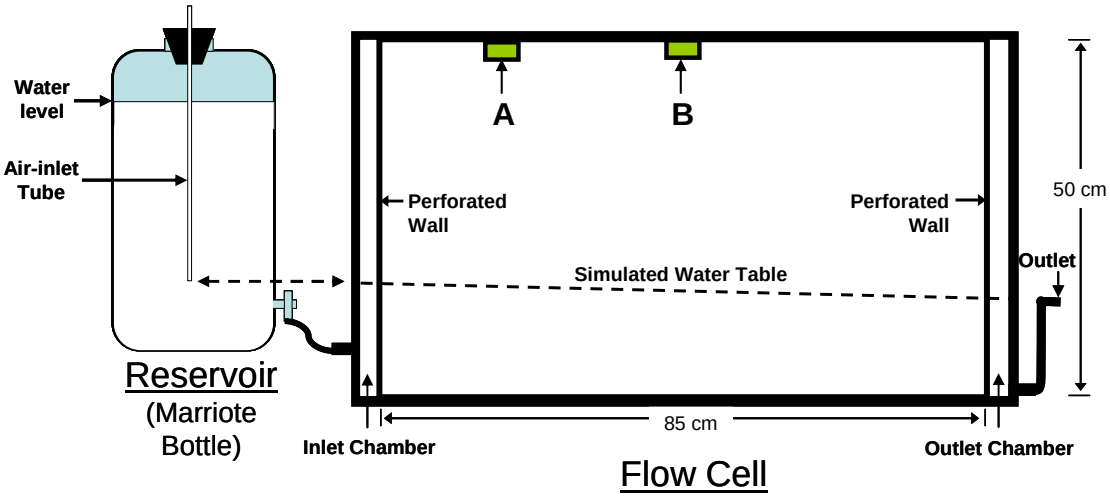

Figure 1. Two-dimensional illustration of the flow cell and the water reservoir used in the modeling of solute and microbial transport. The flow cell was 3.5 cm thick. Note: Illustration is not to scale.

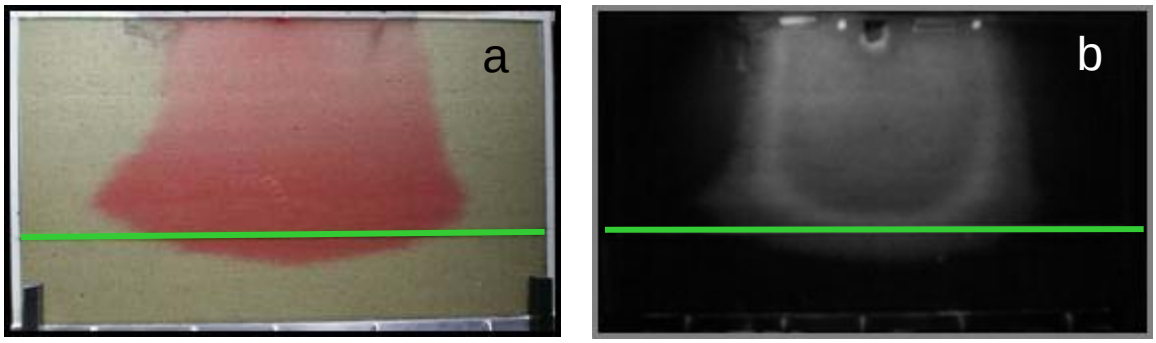

Figure 2. Dye solution (a) and microbial (b) plume in the flow cell under no horizontal water flow after 8 hours of continuous application. Photograph on microbe was taken under 365 nm UV light.

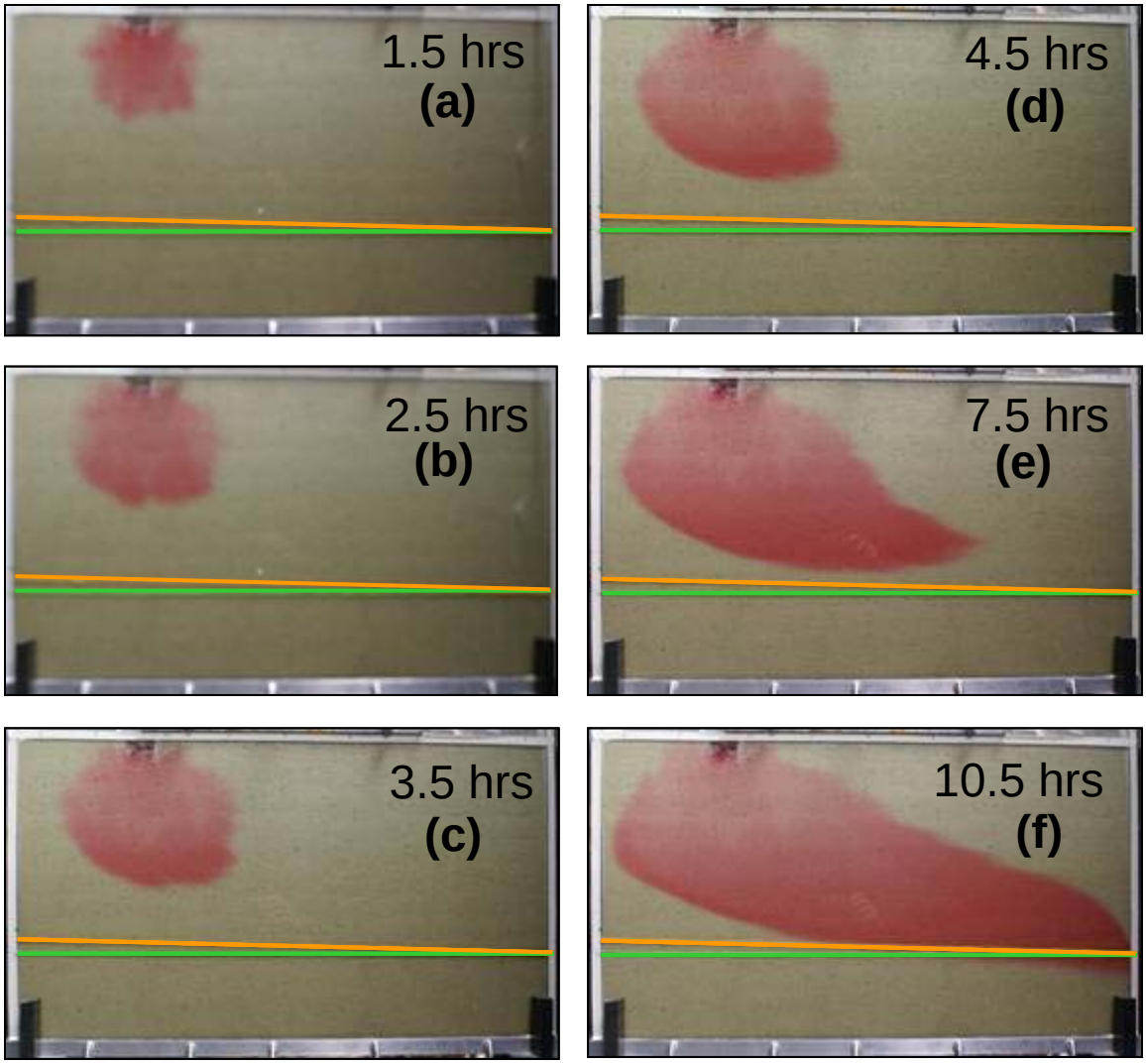

Figure 3. Time-lapse photographs showing the area traveled by the surface-applied dye under a simulated water table (WT) slope of 1.5 %. The orange line represents the WT during simulated left-to-right ground water flow; and the green line represents the WT during static condition.

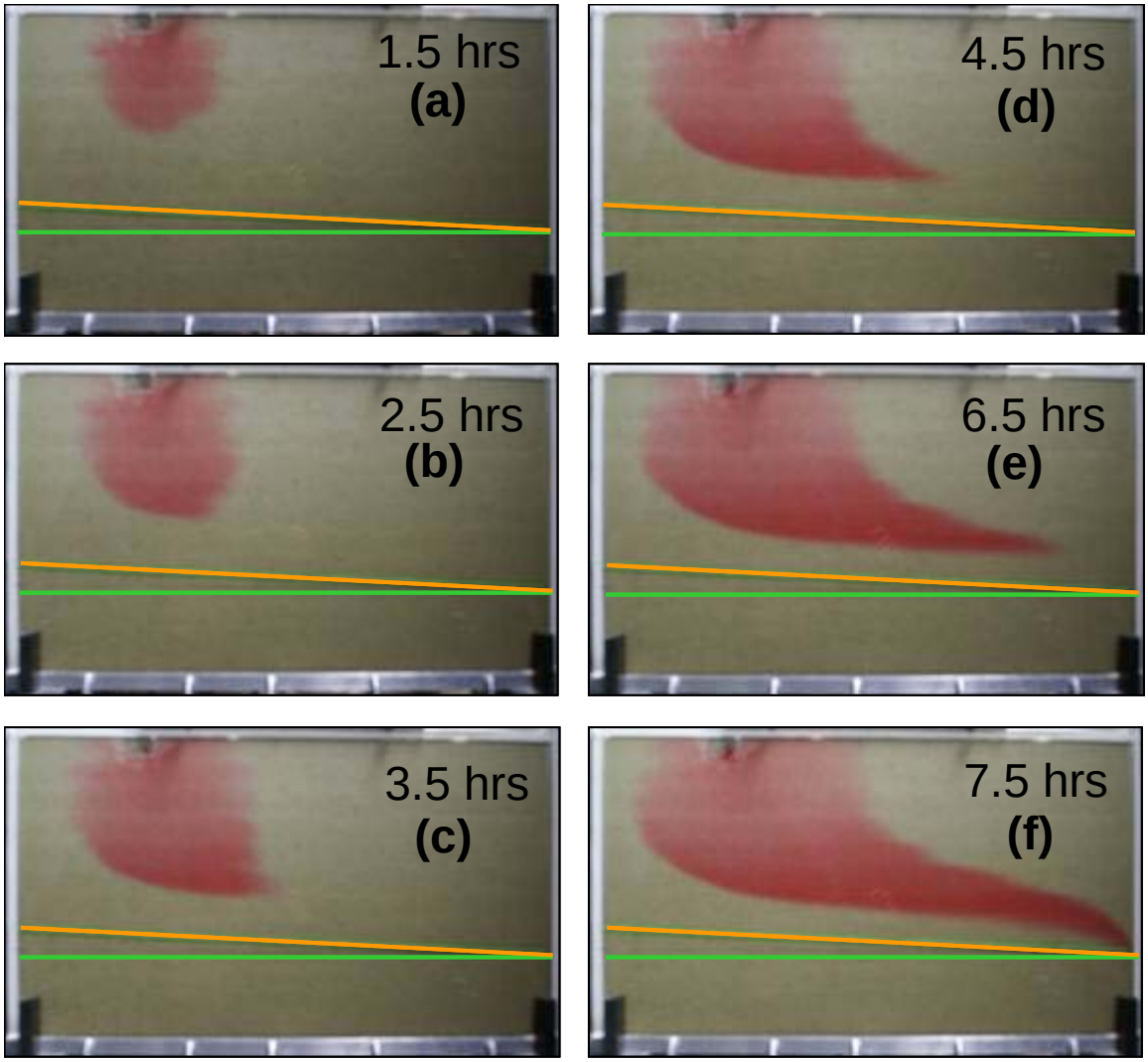

Figure 4. Time-lapse photographs showing the area traveled by the applied dye under a simulated water table (WT) slope of 3.0 %. The orange line represents the WT during simulated left-to-right ground water flow; and the green line represents the WT during static condition.

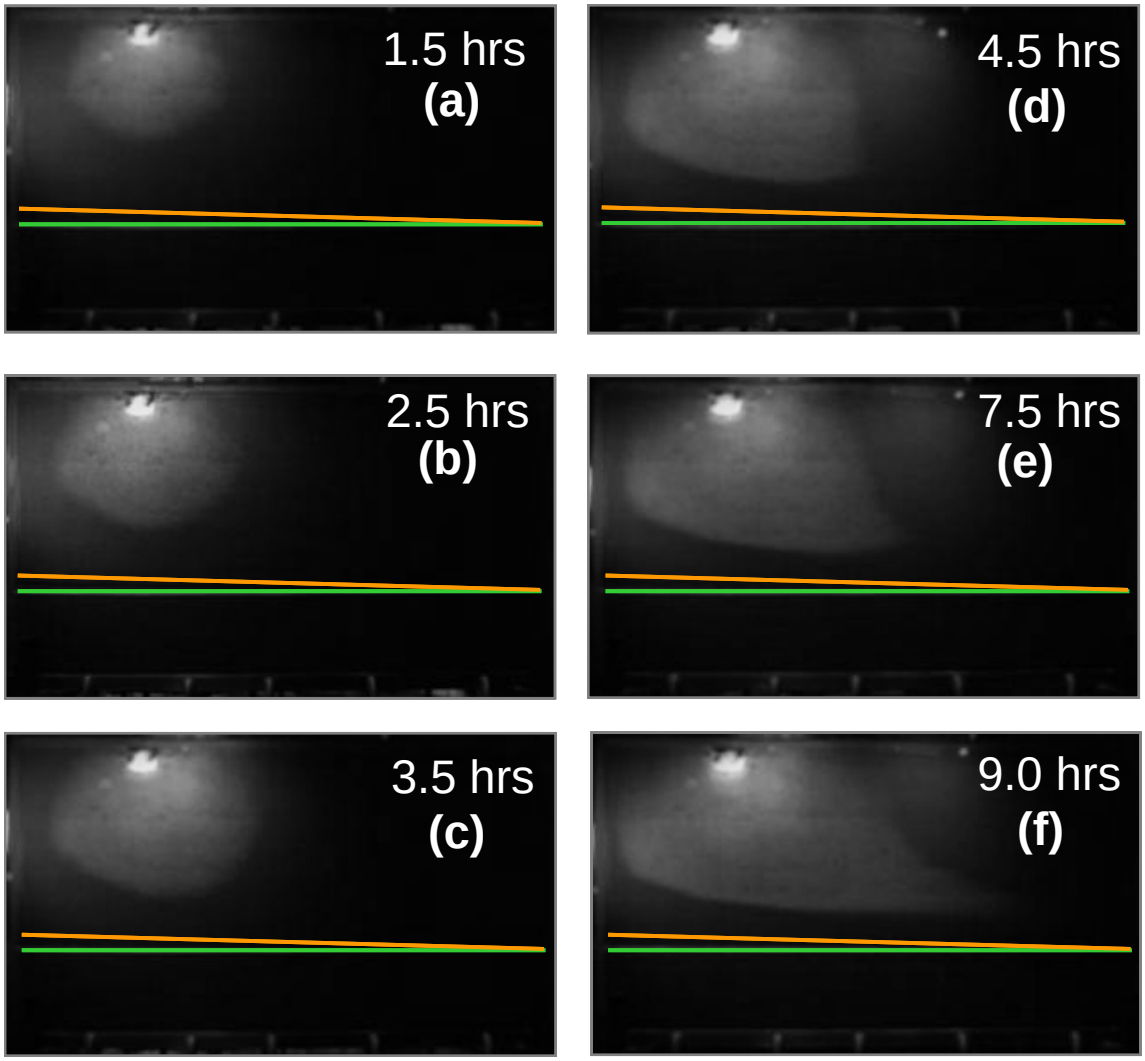

Figure 5. Time-lapse photographs under 365 nm UV light showing the area traveled by the surface-applied *E. coli* under a simulated water table (WT) slope of 1.5 %. The orange line represents the WT during simulated left-to-right ground water flow; and the green line represents the WT during static condition.

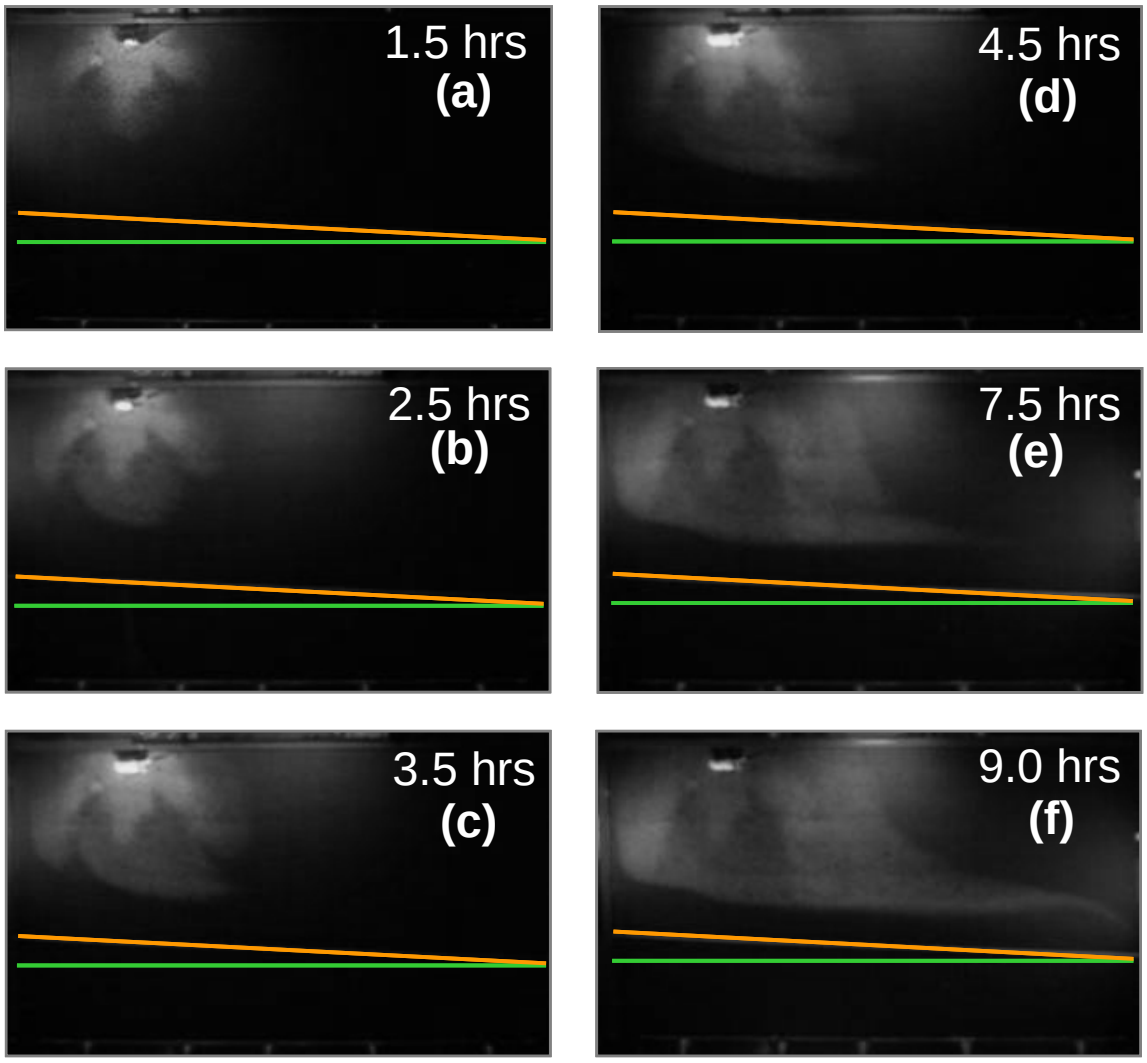

Figure 6. Time-lapse photographs under 365 nm UV light showing the area traveled by the surface-applied *E. coli* under a simulated water table (WT) slope of 3.0 %. The orange line represents the WT during simulated left-to-right ground water flow; and the green line represents the WT during static condition.

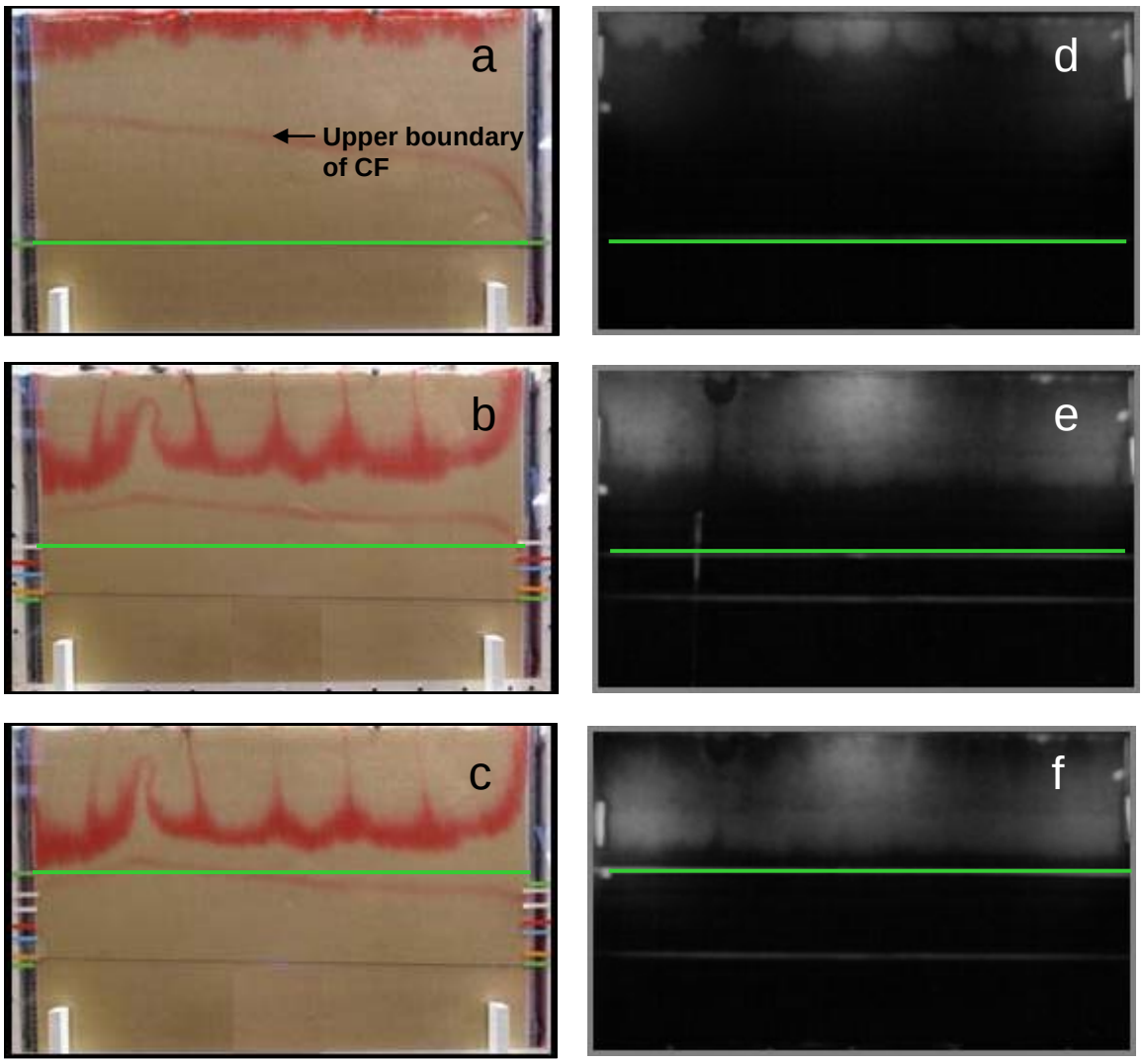

Figure 7. Time-lapse photographs showing the front of a surface-applied dye solution (a-c) and *E. coli* suspension (d-f) leached by a simulated rainfall of approximately 5 cm d^{-1}. The green line indicates the location of the water table.

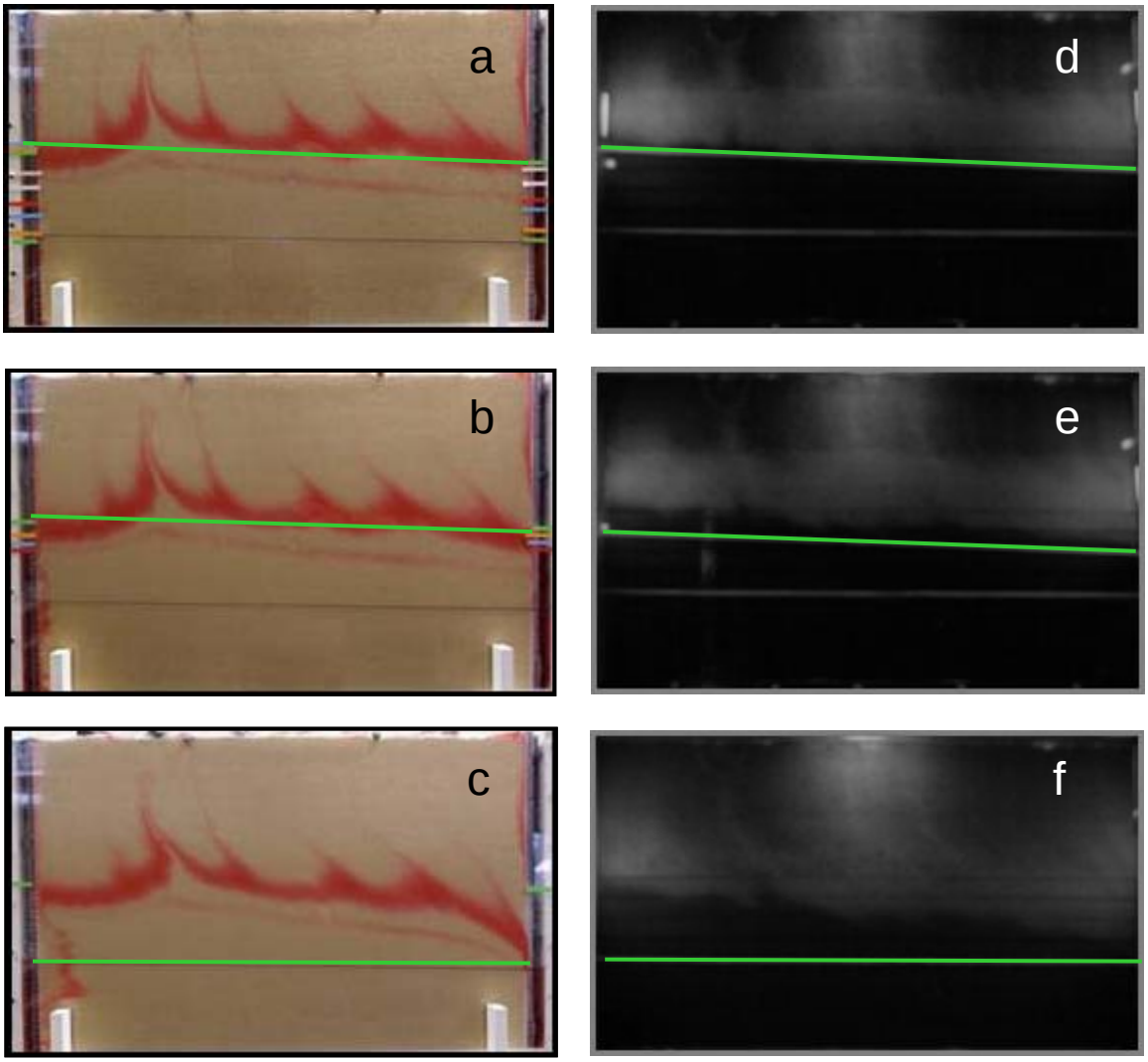

Figure 8. Time-lapse photographs showing the front of a surface-applied dye solution (a-c) and *E. coli* suspension (d-f) as carried by simulated drainage after the simulated rainfall event shown in Fig. 7. The green line indicates the location of the water table.

CHAPTER 2

Hydrologic Effects on the Extent and Rate of Reduction in a Vadoze Zone-Shallow Ground Water Continuum

Abstract

Soil aeration status influences various properties of the soil. This study was conducted to evaluate the effect of pore-water velocity on the development of reduced conditions in a vadose zone-shallow ground water continuum. Two sets of experiments were conducted using 90 × 50 × 8 cm flow cells packed with soil materials collected from drained wetland areas that had different organic carbon (OC) contents. The flow cells were instrumented with platinum-tipped redox electrodes to measure reduction potential (Eh) at various locations above and below a simulated water table (WT) in the flow cells. For the first experiment, Eh measurements were recorded at 15 minute-intervals using a data logger while distilled water was passed through the flow cells at a pore-water velocity of 14 cm d^{-1} for 14 days. For the second experiment, dedicated flow cells were subjected to no flow condition, as well as 7, 14 and 28 cm d^{-1} pore-water velocities across the flow cells. Reduction potential measurements were recorded while the flow cells were subjected to two saturation periods of at least 3 days to evaluate the development of reducing conditions above and below the WT under various pore-water velocities. In the first experiment, reducing conditions were observed at locations below and just above the WT before the end of 14 days regardless of the OC content of the soil material while the upper parts of the capillary fringe in the vadose zone were consistently oxic. The second experiment showed that an increase in

pore-water velocity tended to keep conditions more oxic for extended periods of time. Such effect of pore-water velocity was more pronounced in systems with lower OC content (12.4 g kg^{-1}). These results suggest that managing lateral ground water flow rate could be important in achieving a desired level of reducing conditions in the subsurface especially in soils with lower OC content.

1. Introduction

The aeration status in soils can affect a multitude of biochemical processes that are important to water quality, plant growth, and hydropedology. It is commonly described by reduction potential (Eh) – an electrochemical parameter related to electron transfer between oxidized and reduced chemical species (Gambrell and Patrick, 1980). Reduction potential is an important parameter in assessing water quality because it provides an indication of the likely biochemical reactions that could ultimately determine the speciation and mobility of reducible chemicals (Ponnamperuma, 1972). For example, reduction potentials above a certain value indicate that the conditions are oxidizing so that nitrate (NO_3^-) in ground water would not be denitrified (Patrick and Jugsujinda, 1992), and instead may reach surface water bodies and trigger environmental problems (Anderson et al., 2002; Horrigan et al., 2002). Also, redox-mediated transformation of iron (Fe) compounds play an important role in regulating the concentration of phosphorus (P) in flooded soils that may potentially be exported to adjacent water bodies (Sah and Mikkelsen, 1986; Halford and Patrick, 1979). The degree of reduction also affects the distribution of vegetation by limiting plant communities to those physiologically adapted to certain redox conditions, such as plants with aerencymatic tissues in roots that dominate submerged areas with reducing conditions (Mitsch and Gosselink, 2000). Redox reactions, particularly those involving transformations of Fe and manganese (Mn) compounds leading to formation of redoximorphic features, are important in determining the depths to the seasonal high water table (SHWT) (Vepraskas and

Richardson, 2000). Determination of SHWT is one of the key benchmarks in coming up with proper land-use decisions.

The factors influencing the development of reducing conditions include: a) temperature - which affects microbial activity and solubility of oxygen (Kadlec and Reddy, 2001; Dušek et al., 2008); b) plant activity - which is mainly related to root exudation of oxygen (Armstrong et al., 2000; Flessa, 1994); c) soil organic matter quantity and quality - which impacts microbial activity (Kadlec and Knight, 1996; Whisler et al., 1974); and d) hydrology - which includes precipitation frequency, degree of saturation and frequency of saturation-drainage cycles (Niedermeier and Robinson, 2007).

Much of the studies addressing the impact of hydrology on development of reduced conditions are focused on the effects of duration of saturation (Smith, 2004; Zelasko, 2007), water content and surface recharge via precipitation (Niedermeier and Robinson, 2007; Dušek et al., 2008), and saturation-drainage cycles (Niedermeier and Robinson, 2007; Whisler et al., 1974; Ratering and Condrad, 1998).

Subsurface hydraulic gradient and conductivity control flow rates, and both change across a landscape in a watershed. The effect of flow rate on the development of reduced conditions has not been well-studied. Dušek et al. (2008) evaluated redox dynamics as impacted by horizontal subsurface flow in constructed wetlands and reported a correlation between Eh and flow rate. This correlation was especially true at depths below the root zone where microbial activity was expected to be low. The findings of Dušek et al. (2008) imply

that pore-water velocity may be an important hydrologic parameter that influences the development of reduced conditions.

This study was designed to isolate the effect of pore-water velocity on the development of reduced conditions in a given soil material under controlled conditions both below the WT and also in the vadose zone above it. We compared the relative effect of pore-water velocity on the reduction in two soils of different organic carbon (OC) content (high and low OC content). The specific objective of the study was to evaluate the effect of pore-water velocity on the development of reduced conditions in a vadose zone-shallow groundwater continuum.

2. Materials and Methods

2.1. Soil

The soil materials used in this study were collected from drained wetland areas. Soil classification and site properties of the areas where the soil materials were collected are outlined in Table 1.

The soil materials were air-dried and passed through a 2-mm mesh sieve. Representative air-dried bulk sub-samples were analyzed for physical and chemical properties. Soil texture was determined by the hydrometer method (Gee and Or, 2002) where the samples were pre-treated with 30% hydrogen peroxide prior to dispersion and sedimentation. Saturated hydraulic conductivity (K_{sat}) of each soil material packed uniformly in aluminum cylinders (7.6 cm in diameter and 7.6 cm long) was measured by the constant head procedure (Amoozegar and Wilson, 1999). Using the same cores used in K_{sat} measurements, soil water retention between 0 and 400 cm pressure was measured by the pressure cell procedure (Dane and Hopmans, 2002), and bulk density was measured by the core method (Grossman and Reinsch, 2002). The pH was determined using a 1:1 soil to water mass ratio. Organic carbon and total nitrogen were determined through dry combustion with a Perkin-Elmer PE2400 CHN Elemental Analyzer (Culmo, 1988).

2.2. Experimental Set-up

Ninety-cm long, 50-cm tall, and 8-cm thick flow cells were used in this study (Fig. 1). The front side of each flow cell was constructed using 0.64-cm thick transparent polycarbonate sheet while the bottom and other sides were made of flat polyvinylchloride

(PVC) sheets (Fig. 1; see photographs in Figure A1 in Appendix). Two 2.5-cm wide chambers, with perforated inner walls, were constructed on the two sides of the flow cell. The left and the right chambers were used as inlet and outlet chambers, respectively (see Fig. A1a in Appendix). Four adapters were also installed at the bottom of each flow cell for applying water or draining the flow cell. Each soil material was packed in the middle 85 cm of a flow cell (between the perforated flat PVC sheets isolating the inlet and outlet chambers).

Each flow cell was packed with sieved (2-mm mesh) air-dried soil. The soil was poured incrementally into the flow cell and tamped uniformly with a flat-ended piece of wooden dowel. To minimize layering, the surface of the tamped soil was stirred before more air-dried soil was added on top of it. Packing was done at approximately 5 cm-thick sections at a time.

The platinum-tipped redox electrodes (Pt electrodes) used in this experiment were built according to the specifications in Wafer et al. (2004) and their tips were blackened using a platinizing solution (chloroplatinic acid hexahydrate and lead acetate trihydrate – Ricca Chemicals, Arlington, TX). Blackened electrodes had been recommended for use in measuring reduction potential in soils where aeration would be present part of the time (Whisler et al., 1974; Quispel, 1947) which was the case in Experiment 2 of this study. As the packing progressed, three sets of blackened platinum-tip redox electrodes (Pt electrodes) were installed at 20 cm, 42.5 cm (middle) and 65 cm from the inlet chamber. Each set had Pt electrodes installed at 7, 17, 27 and 37 cm above the bottom of the flow cell (see Fig. 1). The

top 5 cm of the flow cell was packed with commercially-available coarse sand (coarser material than the soil packed in the flow cell) to create a capillary barrier that prevented the flow cell from becoming fully wet to the surface via capillary action. The top of the flow cell was also covered with aluminum foil (with a few pinholes) to further discourage evaporative losses that may encourage upward flux of water in the flow cell. The front (transparent) side was also covered with aluminum foil to prevent light-induced biochemical activities.

As will be described later, a water table (WT) was established at 12 cm above the bottom of each flow cell. Using this arrangement, three Eh measurements were taken frequently from 5 cm below the WT and at 5, 15 and 25 cm above the WT (a total of 12 Pt electrode measurements in each flow cell at each time). Locations in the soil with Pt electrodes are hereafter called "monitoring locations". Each Pt electrode was connected to a CRX10 data logger (Campbell Scientific, Logan, Utah) that was programmed to measure and record redox measurements every 15 minutes.

2.3. Calibration of Electrodes and Data Loggers

To ensure that the Pt electrodes were functioning properly, they were calibrated by submerging the electrodes' platinum tips together with a gel-filled Calomel reference electrode (ID No. 13-620-258, Fisher Scientific, Pittsburgh, PA) in a standard ferrous-ferric iron or Light's solution (Light, 1972) (Fisher Scientific, Pittsburgh, PA). Voltage between each Pt electrode and the reference electrode was measured every 30 minutes for 6 hours using a multi-meter (Radioshack, Fort Worth, TX -- accurate to 0.001V). Electrodes that consistently yielded voltage readings of 420 $\pm$10 mV readings were considered properly

functioning. The well-functioning electrodes were identified, rinsed with distilled water and submerged in distilled water (the tips) until use.

To ensure that voltage readings using different reference electrodes can rightfully be compared with one another, six reference electrodes were submerged in Light's solution together with a single Pt electrode. Voltage between each reference electrode and the Pt electrode was manually measured using a multi-meter every 30 minutes for 6 hours. Four reference electrodes that consistently yielded voltage measurements that were within 10 mV were chosen for use in the experiment.

Data loggers were tested to ensure they were recording voltage measurements accurately. All data loggers were tested using the same set of 12 Pt electrodes and a reference electrode. The tips of the Pt and reference electrodes were submerged in Light's solution while the electrodes were attached to dedicated ports on the data logger (programmed to collect voltage measurements every 15 minutes). Voltage readings using a multi-meter were manually taken immediately after each scheduled data collection by the data logger (every 15 minutes). Voltage measurements collected by the data loggers and those manually measured were within $\pm$ 10 mV. Voltage measurements gathered by different data loggers using the same set of Pt and reference electrodes were also within $\pm$ 10 mV suggesting that voltage measured and recorded by the different data loggers were comparable.

2.3 Experiment 1 -- Extent of Reduction

Four soil materials were used in this experiment: Ponzer Oap, Leon Ap, Leon Bh and Lynchburg A. Before introducing distilled water into each soil-packed flow cell, the outlet

chamber was connected to a plastic tubing with an open end fixed at 12 cm above the bottom of the flow cell. The four ports at the bottom of the flow cell and the inlet and outlet chambers were connected via a plastic tubing manifold to an aeration reservoir (see Figure A1d in Appendix for photograph of manifold). The aeration reservoir was connected to a 25-L distilled water reservoir (Marriotte bottle). The tip of the air inlet tube in the water reservoir was also set at 12 cm above the bottom of the flow cell. A gel-filled Calomel reference electrode (ID No. 13-620-258, Fisher Scientific, Pittsburgh, PA) and the 12 Pt electrodes installed in each flow cell were connected to a dedicated CRX10 data logger (Campbell Scientific, Logan, Utah).

Distilled water from the Marriotte bottle reservoir was initially supplied to the aeration reservoir while clamping the tubing that connected the aeration reservoir to the flow cell. Using an aerator, air was bubbled through the distilled water in the aeration reservoir to keep it uniformly aerated. Once a static water level in the aeration reservoir was established, the tubing connecting the aeration reservoir to the flow cell was unclamped allowing delivery of water through the manifold to the bottom and sides of the flow cell to establish a simulated WT. The soil material in the flow cell was saturated from the bottom to prevent air entrapment as the flow cell was flooded to the desired elevation. As soon as water started to flow into the outlet chamber, the reference electrode was immediately installed in the outlet chamber (tip of reference electrode submerged in water). The data loggers were programmed to collect voltage measurements (between reference and Pt electrodes) every 15 minutes.

Four hours after a static WT was established at 12 cm above the bottom of the flow cell, all the tubes that connected the aeration reservoir to the bottom and sides of the flow cell were clamped. Distilled water from the aeration reservoir was immediately applied to the inlet chamber through a separate tube using a small peristaltic pump (Fig 1). The peristaltic pump continuously supplied distilled water to the inlet chamber at a rate that resulted in a pore-water velocity of approximately 14 cm d^{-1} across the flow cell.

The experiment was run for two weeks by continuously applying distilled water to the inlet chamber and draining the outlet chamber at 12 cm above the bottom of the flow cell. Outlet samples were collected daily and analyzed for pH and dissolved organic carbon (DOC) concentration. Analysis of DOC was carried out using the Total Organic Carbon Auto-analyzer (Shimadzu Corp., Columbia, MD). Two replicates of Experiment 1 were conducted. Temperature in the laboratory was monitored to ensure that the room temperature was at 23 $\pm$ 1^{o}C for all treatments and replications.

2.4. Experiment 2 -- Hydrologic Effects on Reduction Rate

Soil materials used in Experiment 2 included Leon Ap and Leon Bh. Four flow cells were packed with each soil material, with each flow cell devoted to one of the following hydrologic treatments:

a) Treatment 1: no flow

b) Treatment 2: horizontal pore-water velocity of approximately 7 cm d^{-1}

c) Treatment 3: horizontal pore-water velocity of approximately 14 cm d^{-1}

d) Treatment 4: horizontal pore-water velocity of approximately 24 cm d^{-1}

Packing of soil materials, instrumentation and method of establishing a WT in the flow cells were similar to ones described earlier (see Sections 2.2 and 2.3).

A WT was initially established at 12 cm above the bottom of each flow cell. After one day, the flow cells were initially drained by connecting the manifold connected to the bottom of each flow cell to a vacuum trap. Air in the vacuum trap was evacuated to create 300 cm of tension for five minutes facilitating the removal of water from the flow cell. After five minutes, tension in the vacuum trap was increased to 400 cm to further drain the flow cell for another five minutes.

The system was initially saturated for a day and later drained before the actual reduction rate experiment was conducted for: (1) pre-wetting the system, and (2) obtaining a fairly uniform starting condition (in terms of water content) between the two saturation periods conducted in the experiment. Starting from an air-dried soil in the flow cell, up to 10 hours were required to establish a flat WT and for capillary action to wet-up all locations in the vadose zone where Pt electrodes were installed. Pre-wetting the system shortened the lag-time between the instant that water was introduced to the flow cell in the first saturation period of the experiment (as will be discussed later) and the time that the Pt electrode started to detect a change in Eh due to change in water content, thus allowing all the Pt electrodes to respond to changes in conditions within an hour from re-flooding. The pre-wetting allowed a more accurate determination of the time when the reduction process in a monitoring location commenced.

Eighteen hours after initial drainage, each flow cell was re-connected to the vacuum pump and was drained at 400-cm tension for five minutes. The manifold was then reconnected to the aeration reservoir to supply distilled water to the flow cells and re-establish the WT. Four hours after the WT was re-established at 12 cm above the bottom of the flow cell, the clamps on the manifold connected to the flow cell (see Fig. 1 for location of clamps) were closed. Distilled water was then introduced into dedicated inlet chambers to bring about horizontal flow across the packed soil (none applied to the no-flow designated flow cell). A pre-determined number of different sizes (inner diameters) of pump tubings were installed in a variable rate peristaltic pump. These tubes supplied distilled water from the aeration reservoir to the inlet chambers at rates equivalent to horizontal pore-water flow velocities of 7, 14 or 28 cm d^{-1} across the respective (dedicated) flow cell. Outlet samples were collected daily and analyzed for pH and DOC, and Eh within the soil was measured every 15 minutes for the duration of water flow through the flow cells.

Flow cells packed with Leon Ap were continuously run for three days before being drained and re-saturated after 18 hours of drainage as described earlier. Two saturation periods were conducted after the initial drainage. The saturation period for the Leon Ap extended a relatively short 3-day period because the daily manual monitoring of the reduction potentials revealed that the environment below the WT and some of the locations above the WT were reduced after three days allowing collection of enough data to provide information for evaluation of the rate of reduction.

For the flow cells packed with Leon Bh, however, the WT was maintained for up to a week after re-saturation. Daily monitoring of the reduction potentials within the flow cells for this soil material revealed that more than 3 days were required for developing reduced conditions in the flow cell. This was particularly true for the second saturation cycle.

3. Results and Discussion

Soil properties are summarized in Table 2. It should be noted that the soil materials used in this study had a wide range of organic carbon (OC) contents. The Ponzer soil material had the most amount of OC at 195 g kg^{-1}, the Leon Bh material had the least amount with only 12.4 g kg^{-1}, while Leon Ap and Lynchburg soil material each had around 35 g kg^{-1}.

"Reducing conditions" were defined for this study using the Eh-pH line developed for the identification of hydric soils (USDA, 2007). The equation for the Eh-pH line is: hydric reduction standard Eh = 595 – (60 × pH). For a given pH, when the Eh is below the hydric reduction standard, the soil is considered "anaerobic" and meets the reduction requirement for hydric soils. The following are the calculated hydric reduction standard Eh for the different soils: Ponzer: 313 mV; Lynchburg: 326 mV; Leon Ap: 258 mV; and Leon Bh: 268 mV. The pH values used in the above equation are the average pH of outflow solutions collected from the flow cells packed with the respective soils. Conditions were considered oxidizing if the reduction potential in each soil material was above the respective hydric reduction standard Eh and reducing if it reached below it.

Moisture release curves of evenly packed soil materials indicated that all of them remained very close to saturation even after application of 40 cm of pressure suggesting that the CF above the simulated WT was at least 30 cm thick (Fig. A2 in Appendix). This showed that the locations above the WT that had been equipped with Pt electrodes were well within the CF.

3.1. Extent of Reduction in a Vadose Zone-Shallow Ground Water Continuum

Figure 2 shows the average Eh detected at various monitoring locations below and above the WT during the course of the 14-day experiment. Regardless of the soil OC content, the locations 5 cm below and above the WT became reduced before the end of the 14-day experiment. Locations 15 cm and more above the WT remained aerobic from the start through the end of the experiment.

The following are needed for reducing conditions to develop: the movement of atmospheric oxygen into the soil must be stopped; there must be enough organic carbon ready for assimilation; and an active microbial population has to be present (Vepraskas and Richardson, 2000). We expect reducing conditions to develop below the WT and even in the CF just above the WT where water content is at or very close to saturation. The upper locations of the CF, however, may be very close to saturation but may have enough air-filled pores to allow the regular re-supply of oxygen, thus keeping such locations oxic. Oxygen can also be transported to the upper part of the CF by diffusion and perhaps convection from the vadose zone above, while such transport to the lower parts of the CF near the WT could be limited.

These findings have important implications in subsurface fates of contaminants. It has been documented in a limited number of studies that solutes applied to the vadose zone could be transported horizontally in the capillary fringe (CF) (Abit et al., 2008a, b; Amoozegar et al., 2006; Silliman et al., 2002). Knowing that conditions in a large portion of the CF can be

aerobic, contaminants such as nitrate could persist because of the oxic conditions and remain in mobile form while being transported horizontally above the water table (i.e., within the unsaturated zone above ground water).

3.2 Effect of Pore-water Velocity on Reduction

Figure 3 shows the typical changes in reduction potential at various depths as the flow cell was subjected to saturation, drainage, and re-saturation. Notice that the saturation period in Figure 3 was similar to that shown in Figure 2 where the upper portion of the CF stayed aerobic while monitoring locations at 5 cm above and below the WT responded to saturation by becoming progressively reduced. Figure 3 also shows that Eh instantly increased above the hydric reduction standard line following drainage and stayed aerobic until the flow cell was re-saturated. The following discussions are focused only on the results from the monitoring locations 5 cm below and 5 cm above the CF because these were the only areas where reducing conditions developed. [Note: the blips in the Eh curves at around hour 140 occurred during recharging the batteries connected to the data logger and should be ignored.]

Figures 4 and 5 show representative data measured at 5 cm below the WT at the middle of the flow cell (mean of two replicates). For presenting data, we selected the middle monitoring location to represent the conditions in the flow cell as it was least affected by the external conditions (i.e., was farthest from the inlet and outlet chamber that were open to the atmosphere).

Increasing flow velocity slowed down the development of reducing conditions. This was obvious in flow cells packed with Leon Bh material wherein the degree of reduction was

observed to be distinctly slower at a pore-water velocity of 24 cm d^{-1} compared to those subjected to slower pore-water velocities (Fig. 4). In the case of those packed with Leon Ap material, there were indications that reduction potential dropped more sharply (with time) under no flow than those subjected to water flow (Fig. 5). However, the trends were not as distinct as those observed in flow cells packed with Leon Bh soils. This could be taken as indication that the effect of faster pore-water velocities on slowing-down the development of reducing conditions is less-pronounced in the flow cell packed with Leon Ap soil material which has a relatively higher DOC content than the Leon Bh soil material.

The rate of supply of oxygen (in the aerated water), for microbes to use as electron acceptors in microbial respiration, is higher in systems with faster pore-water velocity. Under such condition, it is expected that system would stay oxic for a relatively extended period. This was believed to be the reason behind the relatively slower rate of reduction in flow cells subjected to faster pore-water velocity as shown in Figures 4.

Draining the flow cell after the first saturation period (using a vacuum pump) not only removes dissolved organic matter but possibly some fine particulate organic matter as well. The Leon Ap soil material had a relative higher TOC (Table 2) and drainage of such soil material only resulted in relatively minimal decrease in DOC between saturation periods (Table 3). Assuming that microbial activity is largely a function of DOC concentration, then microbial activities in the two saturation periods should be comparable. As a result, there was no substantial change in trend of reduction between saturation cycles in the flow cells packed with Leon Ap (i.e., Eh was generally below the hydric reduction line after 72 hours in both

saturation periods) (Fig. 5). Dissolved organic carbon in the second saturation period in the flow cell packed with Leon Bh (which had relatively lower TOC –see Table 2) was observed to be substantially lower than in the first saturation period (Table 3). The potentially lower microbial activity resulting from a lower DOC is believed to be responsible for the distinctly slower development of reducing conditions when the Leon Bh-packed flow cells were subjected to the second saturation period (Figure 4). It is also possible that the organic material left in the Leon Bh-packed flow cells during the second saturation period were largely more recalcitrant types leading to lower degree of microbial activity and hence a slower development of reducing conditions.

There was no strong relationship indicating that Eh tended to he higher at the end of the 1st saturation period when flow cells packed with Leon Ap soil material were subjected to faster pore-water velocities (r^2 of only 0.26 and 0.24 for 5 cm above and 5 cm below the WT, respectively) (Fig. 6). There was also no relationship observed in the 2nd saturation period (data no shown).

In contrast, there was a relatively stronger relationship indicating that the Eh in flow cells packed with Leon Bh soil material tended to be higher after 72 hours of saturation (1st saturation period) when subjected to faster pore-water velocities (Fig. 7). The plot showing the Eh at the end of the 2nd saturation period showed an even stronger relationship between Eh and pore-water velocity. It should be noted that outflow DOC from flow cells packed with Leon Bh soil material was consistently lower than those from flow cells packed with Leon Ap material and that outflow DOC was lower during the 2nd saturation period (Table 3).

These known, it could then be deduced that the tendency of a faster pore-water velocity to slow-down the development of reducing conditions is more-pronounced in systems with lower OC content. Said differently, the results indicate that faster pore-water velocities tended to slow-down the development of reducing conditions especially in systems with low OC content. The absence of a similar effect in flow cells packed with Leon Ap soil material indicate that the tendency of a higher pore-water velocity to slow-down the development of reducing conditions was negated by the tendency of the relatively higher OC content to enhance microbial activity and promote reduction.

The coupled effects of higher rate of oxygen re-supply and lower microbial activity in systems with lower soil OC contents is believed to be the reason for the relatively slower development of reducing conditions in Leon Bh-packed flow cells subjected to faster pore-water velocities.

4. Summary and Conclusion

This study was conducted to evaluate the effect of pore-water velocity on the development of reduced conditions in a vadose zone-shallow groundwater continuum. Reduction potentials (Eh) below the water table (WT) and at 5 cm above the WT were already below the standard hydric reduction line within 14 days from initial saturation. In contrast, locations at 15 and 25 cm above the WT remained oxic. This was observed to be true under conditions where the soil total organic carbon content ranged from 12.4 to 195 g kg^{-1}. An increase in pore-water velocity was observed to keep conditions more oxic for extended periods of time. Such effect of pore-water velocity was more pronounced in systems with lower organic matter content. These results suggest that management of hydrology; for example, controlled drainage (Skaggs and Gilliam, 1981); is important in achieving a desired level of reducing conditions in the subsurface especially in soils with lower organic matter content.

5. References Cited

Abit, S. M., A. Amoozegar, M. J. Vepraskas and C. P. Niewoehner. 2008a. Solute transport in the capillary fringe and shallow groundwater: Field evaluation. Vadose Zone J. 7: 890-898.

Abit, S.M., A. Amoozegar, M. J. Vepraskas, and C.P. Niewoehner. 2002b. Fate of nitrate in the capillary fringe and shallow ground water in a drained sandy soil. Geoderma. 146:209-215.

Amoozegar, A., C.P. Niewoehner and D.L. Lindbo. 2006. Lateral movement of water in the capillary fringe under drain fields. In Proc. 2006 Tech. Educ. Conf., Denver Co. 27-31 Aug. 2006. Natl. Onsite Wastewater Recycling Assoc. Santa Cruz, CA.

Amoozegar, A. and G. V. Wilson. 1999. Methods for measuring hydraulic conductivity and drainable porosity. In: R.W. Skaggs and J. van Schilfgaarde (eds). Agricultural Drainage. Agronomy Monograph no. 38. SSSA, Madison, Wisconsin.

Armstrong,W., D. Cousinsa, J. Armstrong, D. W. Turnerb and P.M. Beckettc. 2000. Oxygen distribution in wetland plant roots and permeability barriers to gas exchange with the rhizosphere: a microelectrode and modeling study with *Phragmites australis*. Ann. Bot. 86 (3):687-703.

Anderson, D.M., Glibert, P.M. and J.M. Burkholder. 2002. Harmful algal blooms and eutrophication nutrient sources, composition, and consequences. Estuaries and Coasts. 25(4b): 704-726.

Culmo, F.C. 1988. Principle of Operation – The Perkin-Elmer PE2400 CHN Elemental Analyzer. Perkin Elmer Corp., Norwalk, CT.

Dane, J. H., and J. W. Hopmans. 2002. Water retention and storage. In: J. H. Dane, and G. C. Topp (eds). Methods of Soil Analysis Part 4: Physical Methods. No. 5 in Soil Sci. Soc. Am. Book Series. Soil Sci. Soc. Am., Madison, WI.

Dušek, J., T. Picek and H. Čížková. 2008. Redox potential dynamics in a horizontal subsurface flow constructed wetland for wastewater treatment: Diel, seasonal and spatial fluctuations. Ecological Engineering. 34(3):223-232.

Flessa, H. 1994. Plant-induced changes in redox potential of the rhizoshpere of submerged vascular macrophytes *Myriophyllum verticillatum* L. and *Ranunculus circinatus* L. Aquat. Bot. 47:119-129.

Gambrell, R.P., and W.H. Patrick, Jr. 1980. Chemical and microbiological properties of anaerobic soils and sediments. In D.D. Hook et al. (eds) Plant Life in Anaerobic Soils and Sediments. Ann Arbor Science Publ.,Ann Arbor, MI.

Gee, G. W., and D. Or. 2002. Particle-size analysis. In: J. H. Dane, and G. C. Topp (eds). Methods of Soil Analysis Part 4: Physical Methods. No. 5 in Soil Sci. Soc. Am. Book Series. Soil Sc. Soc. Am., Madison, WI.

Grossman, R. B., and T. G. Reinsch. 2002. Bulk density. In: J. H. Dane, and G. C. Topp (eds). Methods of Soil Analysis Part 4: Physical Methods. No. 5 in Soil Sci. Soc. Am. Book Series. Soil Sc. Soc. Am., Madison, WI.

Halford, I.C.R. and W.H. Patrick. 1979. Effects of reduction and pH changes on phosphate sorption and mobility in an acid soil. Soil Sc. Soc. Am J. 43:292-297.

Horrigan, L., R. S. Lawrence and P. Walker. 2002. How sustainable agriculture can address the environmental and human health harms of industrial agriculture. Environmental Health Perspectives. 110: 445-456.

Kadlec, R.H. and K. R. Reddy. 2001. Temperature effects on treatment wetlands. Water Environ. Res. 73(5): 543-557.

Kadlec, R.H. and R.L. Knight. 1996. Treatment Wetlands. CRC Press, Boca Raton, FL.

Light, T.S. 1972. Standard solution for redox potential measurements. Anal. Chem. 44:1038-1039.

Mitsch, W. and J.G. Gosselink. 2000. Wetlands. 3rd ed, Van Nostrand Rendhold. NY.

Niedermeier, A. and J.S. Robinson. 2007. Hydrological controls on soil redox dynamics in peat-based, restored wetland. Geoderma. 137:318-326.

Patrick, W. H. and A. Jugsujinda. 1992 .Sequential reduction and oxidation of inorganic nitrogen, manganese, and iron in flooded soil. Soil Sci. Soc. Am. J. 56:1071-1073.

Ponnamperuma, F.N. 1972. The chemistry of submerged soils. Adv. Agron. 24:29-96.

Quispel, A. 1947. Measurement of oxidation-reduction potentials of normal and inundated soils. Soil Sci. 63:265-275.

Ratering, S. and R. Condrad. 1998. Effect of short-term drainage and aeration on the production of methane in submerged rice soil. Global Change Biology. 4:397-407.

Sah, R.H. and D.S. Mikkelsen. 1986. Transformations of inorganic phosphorus during flooding and drainage cycles of soils. Soil Sc. Soc. Am J. 50:62-67.

Silliman, S. E., B. Berkowitz, J. Simunek, and M. Th. Van Genuchten. 2002. Fluid flow and solute migration within the capillary fringe. Ground Water. 40(1): 76-84.

Skaggs, R.W. and J.W. Gilliam. 1981. Effect of drainage design on nitrate transport. Trans. Am. Soc. Ag. Eng. 24:292-234.

Smith, H.C. 2004. Time required for anaerobic conditions to develop in saturated soils. Masters Thesis. Department of Soil Science. North Caolina State University, Raleigh, NC.

USDA. 2007. Technical standards for hydric soils. Hydric Soils Technical Notes 11. at: http://soils.usda.gov/use/hydric/ntchs/tech_notes/index.html. Accessed: April 2009.

Vepraskas, M.J. and J.L. Richardson. 2000. Wetland Soil: Genesis, Hydrology, Landscapes and Classification. Lewis Publishers, USA.

Wafer, C.C., J. B. Richards, and D.L. Osmond. 2004. Construction of platinum-tipped redox probes for determining soil reduction potential. J. Environ. Qual. 33: 2375-2379.

Whisler, F.D., J.C. Lance, and R.S. Leinebarger. 1974. Redox potentials in soil columns intermittently flooded with sewage water. J. Environ. Qual. 3(1): 68-74.

Zelasko, A. 2007. Soil reduction rates under water saturated conditions in relation to soil properties. Masters Thesis, Department of Soil Science North Carolina State University, Raleigh, NC.

6. Tables and Figures

Table 1. Classification and site properties of areas where the soil materials used in the experiment were collected.

Soil Series	Taxonomic Classification	Drainage Classification	Depth of collection (cm)	Land Use	Location
Ponzer (Horizon Oap)	Loamy, mixed, dysic, thermic, Terric Haplosaprists	Very Poorly Drained	0-10	Drained wetland that was devoted agriculture	Juniper Bay, Robeson County, NC (34°30'30"N 79°01'30"E)
Leon (Horizons Ap and Bh)	Sandy, siliceous, thermic, Aeric Alaquod	Poorly Drained	Ap - 0-10 Bh - 10-20	Drained wetland that was devoted agriculture	Juniper Bay, Robeson County, NC (34°30'30"N 79°01'30"E)
Lynchburg (Horizon A)	Fine-loamy, siliceous, semiactive, thermic, Aeric Paleaquult	Somewhat Poorly Drained	0-10	Cleared and drained wetland area	Frog Level Crossroad, Greenville, NC (35°34' 0" N 77°26'26" E)

Table 2. Selected properties of soil materials used in the experiment.

Soil Material	Texture	pH	TOC ($g\ kg^{-1}$)	Total N ($g\ kg^{-1}$)	Bulk Density ($Mg\ m^{-3}$)	Porosity ($cm^3\ cm^{-3}$)	Ksat ($m\ d^{-1}$)
Ponzer	Muck	5.5	195.3	5.7	0.62	0.64	1.2
Lynchburg	LS	4.5	35.8	1.2	1.05	0.54	0.3
Leon Ap	LS	5.3	35.4	1.3	1.32	0.48	3.0
Leon Bh	LS	4.9	12.4	0.3	1.43	0.45	4.6

Table 3. Summary of mean dissolved organic carbon at the start and end of two saturation periods in flow cells packed with Leon Ap and Leon Bh soil materials.

Soil	Power –water velocity (cm d^{-1})	Dissolved Organic Carbon (mg L^{-1})			
		Saturation Period 1		Saturation Period 2	
		Start	End	Start	End
Leon Ap	7	138.0	132.5	122.0	114.0
	14	130.0	115.0	96.0	83.0
	28	121.0	102.5	91.5	81.0
Leon Bh	7	96.5	79.5	60.0	23.5
	14	83.5	70.5	46.5	18.0
	28	90.0	71.5	48.0	13.5

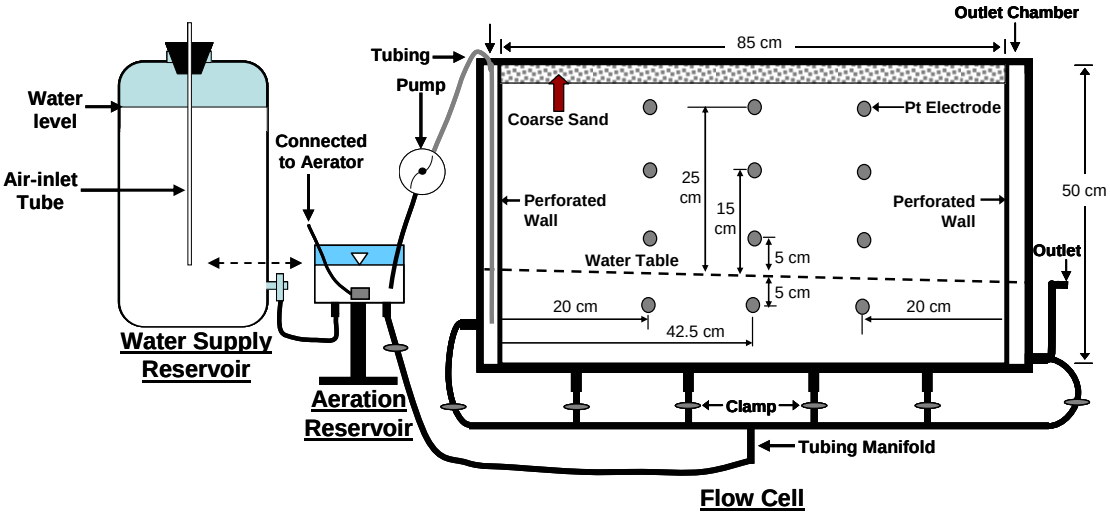

Figure 1. Two-dimensional diagram of the experimental set up. Thickness of the flow cell was 8 cm.

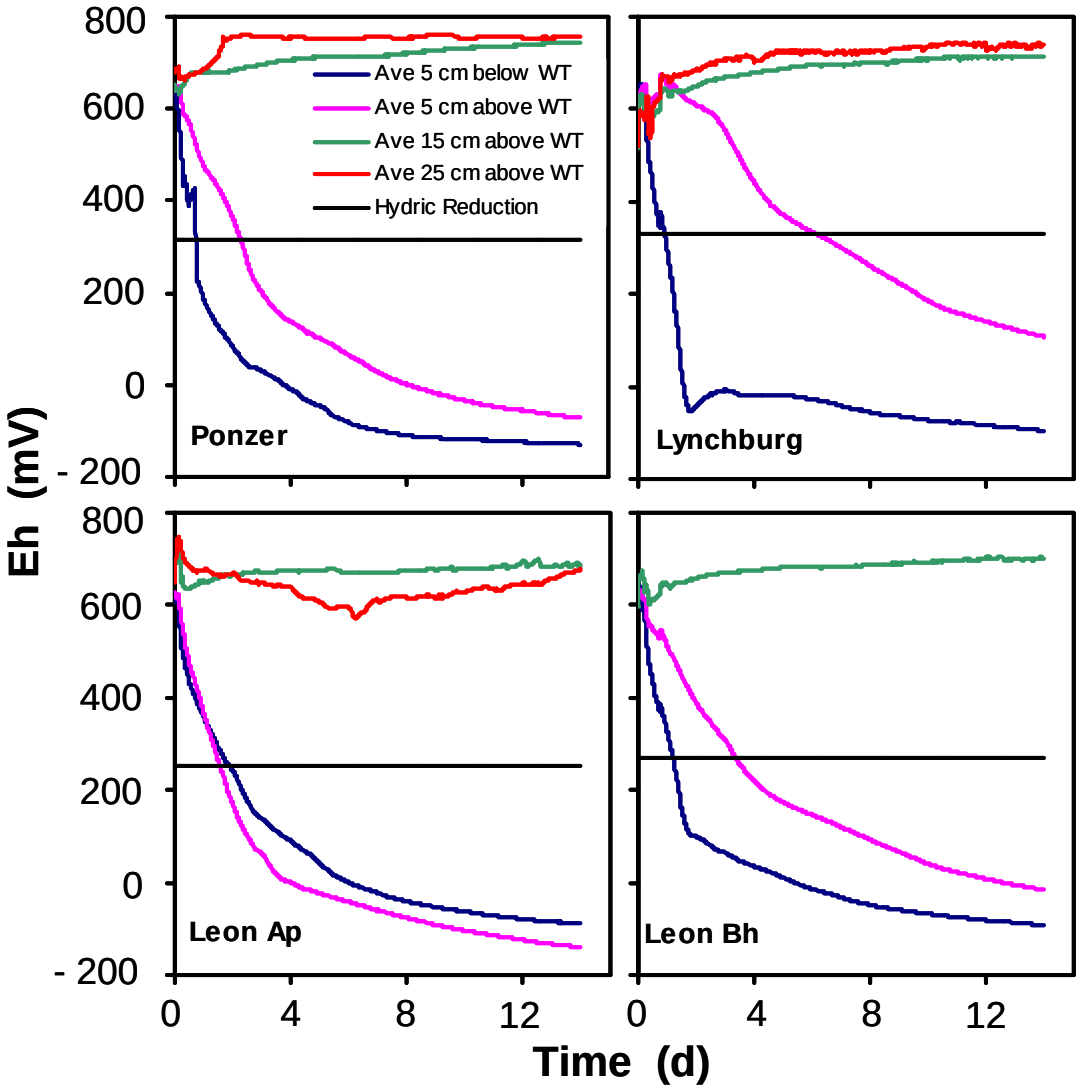

Figure 2. Mean reduction potentials (Eh) at monitoring locations below and above the water table of flow cells packed with different soil materials when distilled water flowed across the flow cell at a pore-water velocity of 14 cm d^{-1} for 14 days. Mean Eh for a monitoring location/depth were computed from two replicates, each with three Pt electrodes installed at a particular depth.

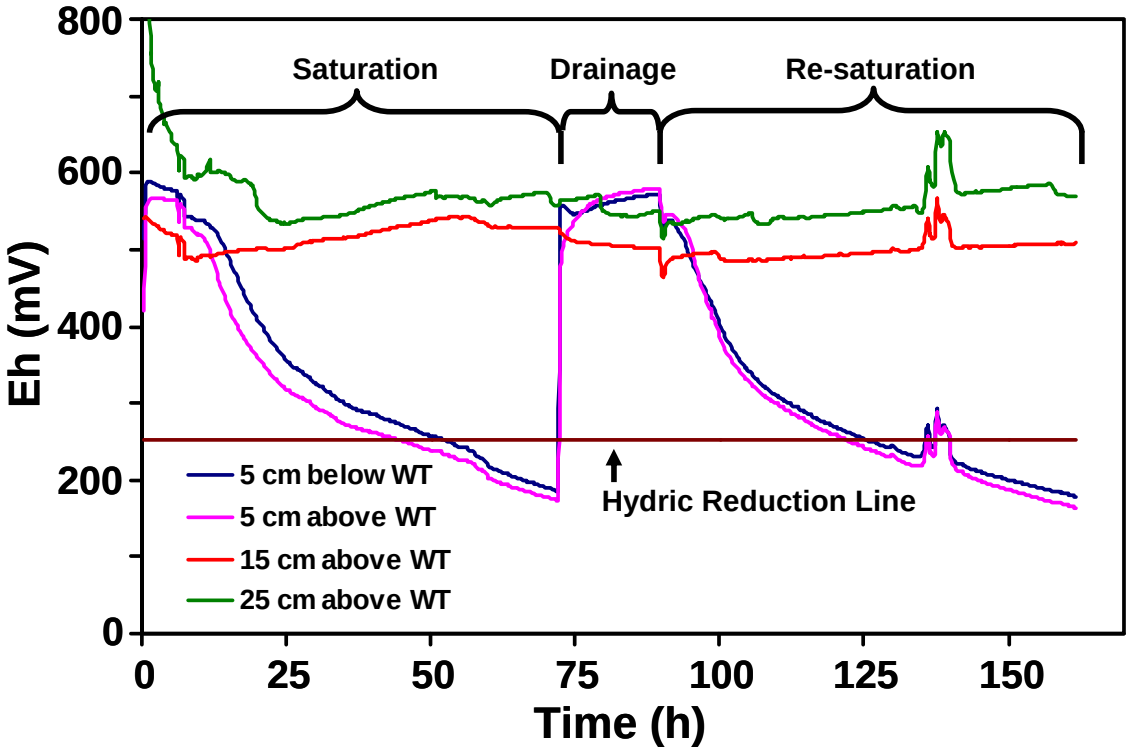

Figure 3. Typical trends in reduction potential (Eh) measured at a monitoring point in a Leon Ap-packed flow cell subjected to saturation, drainage and re-saturation. Representative data shown were measured at the middle of the flow cell under no-flow condition.

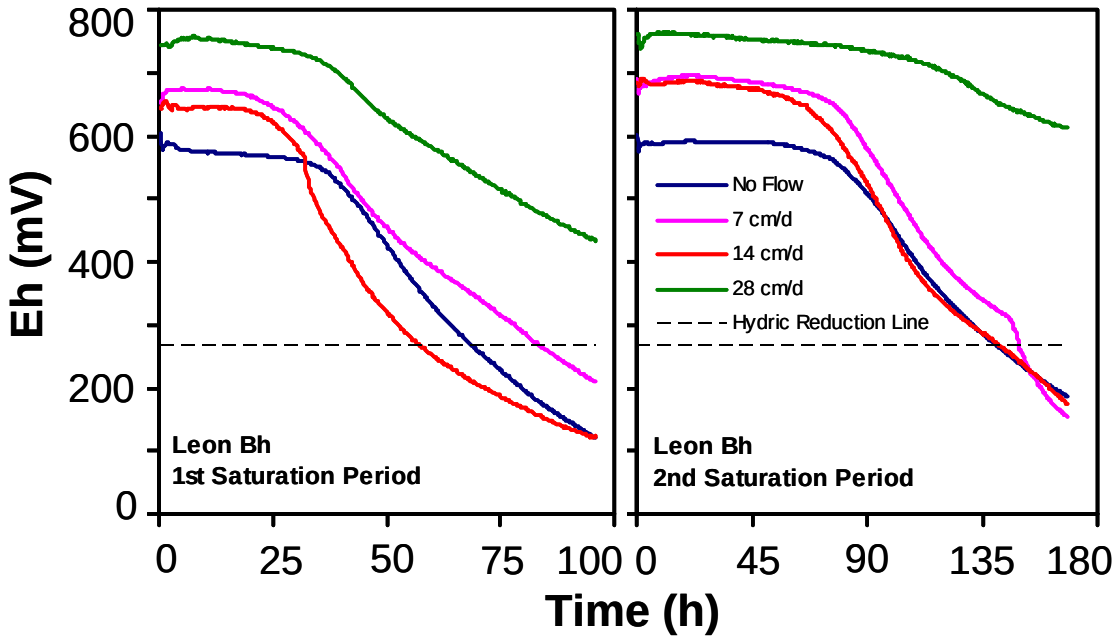

Figure 4. Reduction potential (Eh) at 5 cm below the water table at the middle of the soil column in flow cells packed with Leon Bh soil materials subjected to various pore-water velocities for two successive saturation periods.

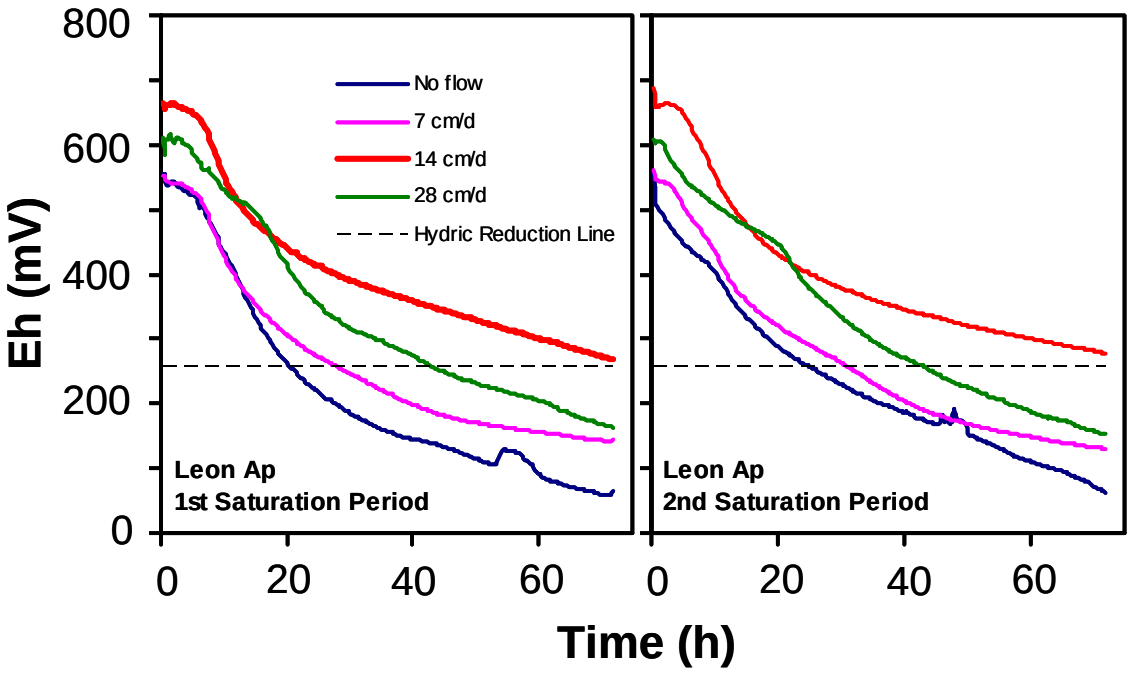

Figure 5. Reduction potential (Eh) at 5 cm below the water table at the middle of soil column in flow cells packed with Leon Ap soil materials subjected to various pore-water velocities for two successive saturation periods.

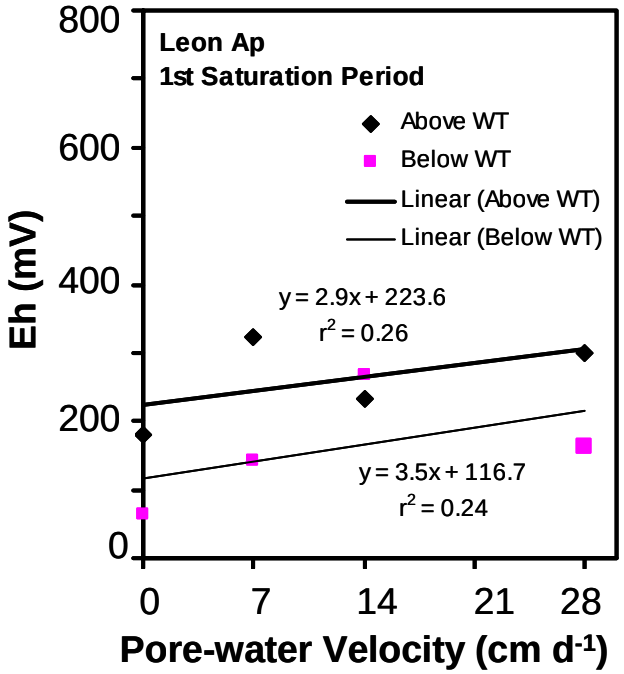

Figure 6. Average reduction potential (Eh) at 5 cm below and above the water table in the middle of the flow cell measured 72 hours from the onset of the 1st saturation period where flow cells packed with Leon Ap soil materials were subjected to various pore-water velocities.

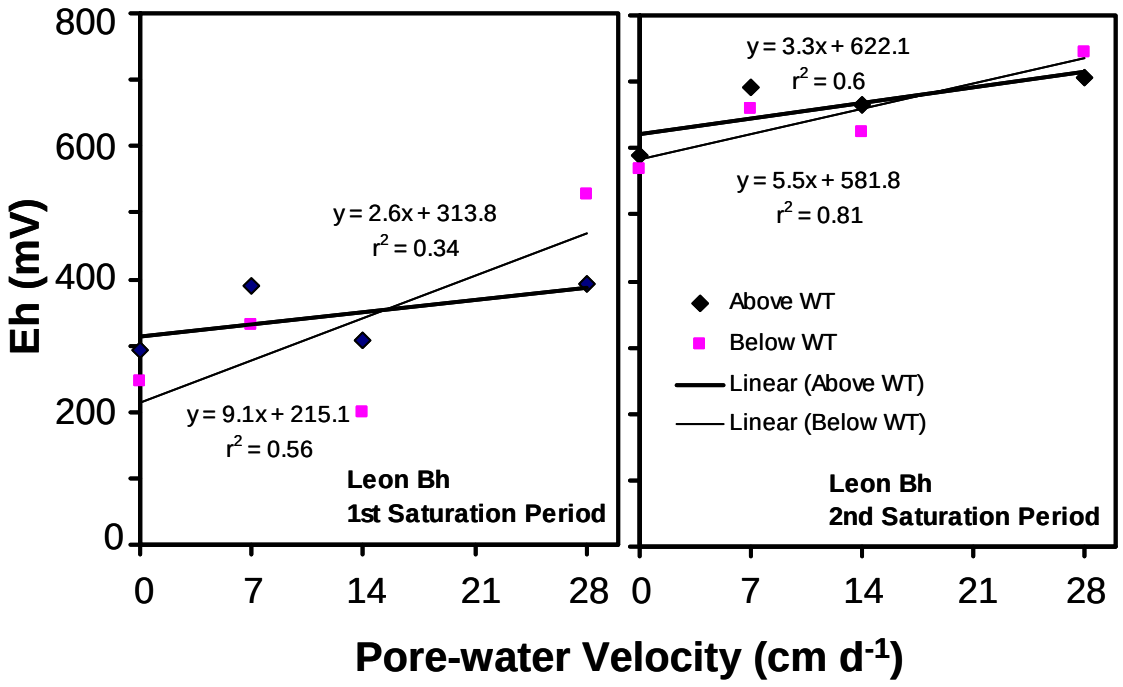

Figure 7. Average reduction potential (Eh) at 5 cm below and above the water table in the middle of the flow cell measured 72 hours from the onset of the 1st and 2nd saturation periods where flow cells packed with Leon Bh soil materials were subjected to various pore-water velocities.

7. Appendix

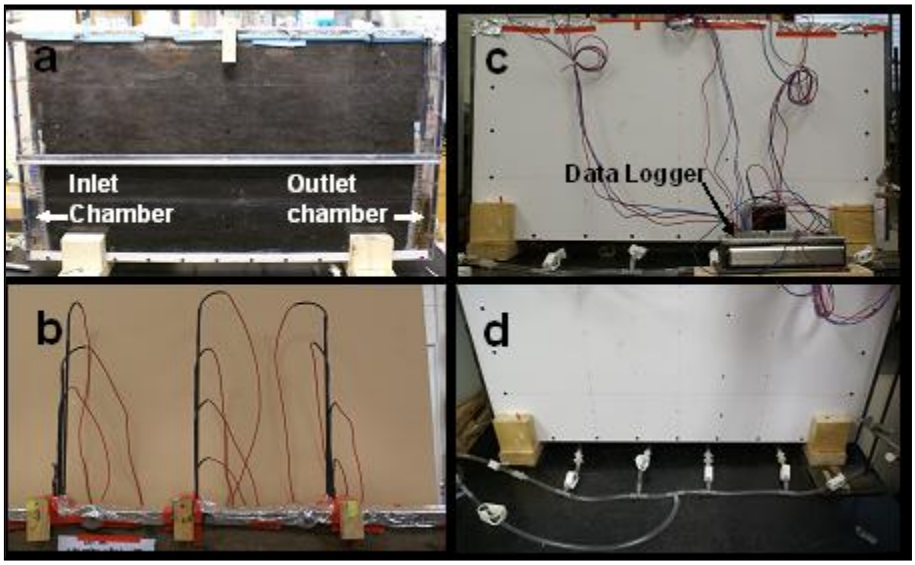

Figure A1. Photographs showing the front view of the flow cell (a), the back view of the flow cell with Pt electrode connected to the data logger (b), the Pt electrodes protruding at the top of the flow cells (c), and the plastic tubing manifold connected to sides and bottom of the flow cell (d).

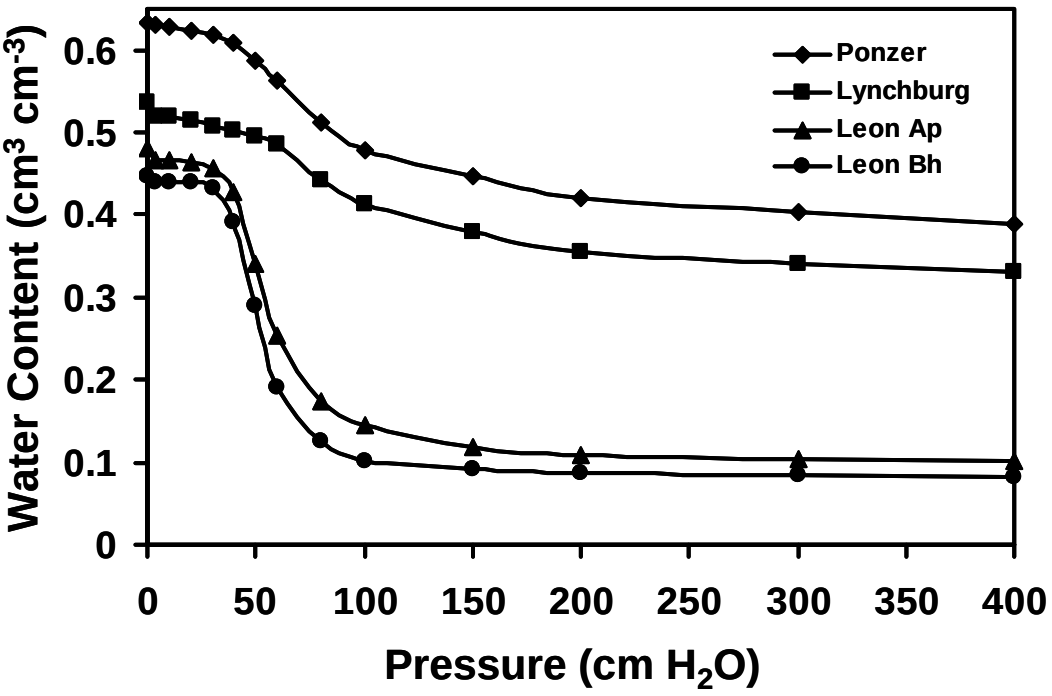

Figure A2. Moisture release curves of the soil materials used in the experiment.

CHAPTER 3

Evaluation of Fate of Nitrate in a Simulated Vadose Zone-Shallow Ground Water Continuum

Abstract

The persistence of health and ecological issues arising from excessive nitrate (NO_3^-) in surface and ground waters emphasizes the need for further study of subsurface NO_3^- fate and transport. This study was conducted to evaluate the effect of pore-water velocity on the fate and transport of NO_3^- in a simulated vadose zone-shallow ground water continuum. A simulated water table (WT) was established in a 90 × 50 × 8 cm flow cell packed with soil material having 36 g kg^{-1} organic carbon (OC). A solution with 100 mg L^{-1} NO_3-N and bromide (Br^-) was continuously passed through the flow cell horizontally at various pore-water velocities. Outlet NO_3-N and Br^- concentrations were monitored with time. In another experiment, two 240 × 60 × 25 cm flow cells were separately packed with soils of different OC content and a NO_3^- and Br^- solution was passed through the flow cell horizontally at various pore-water velocities while maintaining a WT within the flow cell. Nitrate-N and Br^- concentrations at the outlet and at certain locations above and below the WT were routinely monitored in these flow cells. Extended residence time of a NO_3^--containing solution in the flow cell resulting from a very slow pore-water velocity yielded a more effective removal of NO_3^- from solution. The degree by which NO_3^- persisted while it was transported in the subsurface was determined by the redox potential along its flow path. While NO_3^- was essentially lost in anaerobic regions below the WT, it persisted while in transport in the

aerobic regions within the CF. The persistence of aerobic condition allowed some NO_3^- to be transported farther horizontally in the CF with minimal NO_3^- loss. The results suggest that NO_3^- removal by the soil could be improved by managing the hydrology and the non-detection of NO_3^- below the WT does not always indicate that NO_3^- is not transported horizontally in the subsurface.

1. Introduction

Excessive NO_3^- in ground water and surface water bodies could have harmful environmental and health consequences. It can instigate environmental disasters such as eutrophication which may lead to algal blooms (Anderson et al., 2002) and reduced ecological biodiversity (Horrigan et al., 2002). In addition, excessive NO_3^- in drinking water could pose human health problems (Gupta et al., 2007). Long-term monitoring programs reveal an increasing trend in NO_3^- contamination in groundwater (Nolan and Stoner, 2000; Spalding and Exner, 1993) and it remains a key nutrient contaminant in surface waters (USEPA, 2004).

Nitrate is efficiently transported in the subsurface because it is relatively soluble and is not prone to extensive adsorption by soil particles (Stumm and Morgan, 1996). Besides removal from solution due to plant uptake and microbial immobilization, loss of NO_3^- is primarily accomplished by microbially-mediated biochemical processes such as denitrification and dissimilatory nitrate reduction to ammonia (DNRA) (Coyne, 1999; Tiedje, 1988).

Denitrification is mediated both by heterotrophic and autotrophic bacteria that are capable of reducing NO_3^- to N_2 via the intermediates NO_2^-, NO, and/or N_2O (Tiedje, 1988). Dissimilatory nitrate reduction to ammonia, on the other hand, involves the conversion of NO_3^- to ammonium (NH_4^+) and requires the same set of conditions needed for denitrification (Coyne, 1999). It specifically occurs when labile organic carbon concentration exceeds that of NO_3^- (D'Angelo and Reddy, 1993; Korom, 1992) and at lower Eh values than that

required for denitrification (Appelo and Postma, 1994). Denitrification is primarily performed by facultative anaerobic microorganisms that can utilize NO_3^- as electron acceptors in the absence of O_2, making it a more important NO_3^--loss mechanism under moderately anoxic conditions (as when there is some O_2 release from roots) (Matheson et al., 2002). In contrast, DNRA is performed by anaerobic, fermentive microorganisms that are prevalent under highly reduced soil environments (Caskey and Tiedje, 1979).

Nitrate losses via denitrification and DNRA are expected to occur below the water table (WT) (i.e., groundwater) where reducing conditions are more likely to develop due to lack or absence of oxygen re-supply. This has been observed in the field where up to 100% of the applied NO_3^- was lost when it reached the shallow ground water (Abit et al., 2008a). In contrast, NO_3^- could be transported in the vadose zone with minimal losses (Abit et al., 2008a; Green, et al., 2008).

Horizontal fate and transport of NO_3^- in the ground water have been extensively documented (Karr et al., 2001; Schuh et al., 1997; Starr et al., 1996). Horizontal transport of solutes in the vadose zone; specifically in the capillary fringe (CF), however, has only been examined by a few studies (Abit et al., 2008b; Amoozegar et al., 2006; Silliman et al., 2002). Furthermore, no study has been conducted to quantify the relative contribution of the vadose zone (including the CF) and the shallow ground water to the overall subsurface horizontal transport of NO_3^-.

In general, we expect denitrification and DNRA to occur when active microorganisms and sufficient assimilable organic substrates are present under a hydrology that encourages

development and persistence of anoxic conditions (Tiedge, 1988). Persistence of NO_3^- in the vadose zone and ground water systems with abundant organic matter and active microorganisms, in effect, could largely be a function of hydrologic factors, such as the pore-water velocity of NO_3^--containing solution as it flows through the soil. The objective of this study was to evaluate the effects of pore-water velocity on the fate and transport of NO_3^- in a simulated vadose zone-shallow ground water continuum.

2. Materials and Methods

2.1. Soil

Two soil materials were used in the experiment. One was commercially-available sand (hereafter called "sand") and the other was collected from the surface horizon of the sand rim of Juniper Bay – a wetland restoration site at Robeson County, NC (34^{o}30'30"N 79^{o}01'30"E) classified under the Leon Series (Aeric Alaquod, hereafter called "Leon soil"). Soil materials were air-dried and passed through a 2-mm sieve prior to packing in flow cells as well as chemical and physical analysis.

Texture of each soil material was determined by the hydrometer method (Gee and Or, 2002) where soil samples were pre-treated with 30% hydrogen peroxide prior to dispersion and sedimentation. Saturated hydraulic conductivity (K_{sat}) of the soil materials packed uniformly in cylindrical cores (7.6 cm diameter and length) was measured by the constant head procedure (Amoozegar and Wilson, 1999). Using the same intact cores used for K_{sat} measurements, soil water retention between 0 and 400 cm pressure was measured by the pressure cell procedure (Dane and Hopmans, 2002). Soil pH was measured from a 1:1 soil-to-distilled water suspension (weight basis) while total organic carbon and total nitrogen were determined by dry combustion with a Perkin-Elmer PE2400 CHN Elemental Analyzer (Culmo, 1988).

2.2. Experiment I. Hydrologic Effects on NO_3^- Loss

The flow cell used in this study was 90-cm long, 50-cm wide and 8-cm thick. The front side of the flow cell was constructed using 0.64 cm-thick transparent polycarbonate

sheet while the bottom and other sides were made of flat polyvinylchloride (PVC) sheets (Fig. 1). Four adapters were installed at the bottom of the flow cell for applying water or draining the flow cell. Two 2.5 cm-wide chambers, with perforated inner walls, were constructed on the two sides of the flow cell. The middle 85 cm of the flow cell (standing on its length) that was enclosed by perforated, flat PVC sheets was packed with the Leon soil material. Packing was done by adding previously sieved (2-mm mesh) air-dried soil in the flow cell and tamping uniformly with a flat-ended piece of wooden dowel. To minimize layering, the surface of the tamped soil was stirred before more air-dried soil was added on top of it. Packing was done at approximately 5 cm-thick sections at a time. The top 5 cm of the flow cell was packed with commercially-available coarse sand (coarser than the Leon soil). The coarse sand served as a capillary barrier that kept the packed flow cell from becoming wet (via capillary action) all the way to the top. Having the capillary barrier also reduced the likelihood of evaporative losses. The top of the flow cell was then covered with aluminum foil (with a few pinholes) to further discourage evaporative losses that may encourage upward flux of water in the flow cell. The front (transparent) side was covered with aluminum foil to prevent any impact that light could have on chemical reactions or microbial activities.

To the left and right of the soil-packed region were the inlet and outlet chambers, respectively (see Fig. 1). The outlet chamber was connected to a plastic tubing with an open end fixed at 12 cm above the bottom of the flow cell. At the bottom of the flow cell were four inlet/outlet ports that were connected via a plastic tubing manifold to an aeration reservoir.

The aeration reservoir was connected to a 25-L solution reservoir (Marriotte bottle). The tip of the air inlet tube in the solution reservoir was also set at 12 cm above the bottom of the flow cell.

A solution of 100 mg L^{-1} each of nitrate-N (NO_3-N) and Br^- (hereafter called "inlet solution"; prepared using KNO_3 and KBr), placed in the solution reservoir was initially supplied to the aeration reservoir while clamping the tubing that connected the aeration reservoir to the flow cell. Using an aerator, air was bubbled through the solution in the aeration reservoir to maintain aerobic condition. Once a static water level in the aeration reservoir was established, the tubing connecting the aeration reservoir to the flow cell was unclamped allowing delivery of the inlet solution through the manifold to the bottom and sides of the flow cell to establish a simulated WT. The soil material in the flow cell was saturated from the bottom to prevent air entrapment as the flow cell was flooded to the desired elevation. Four hours after a static WT was established at 12 cm above the bottom of the flow cell, all the tubings connecting the aeration reservoir to the bottom and sides of the flow cell were clamped and the solution from the aeration reservoir was applied only to the inlet chamber through a separate tube using a peristaltic pump (see Fig 1).

A total of four flow cells were similarly prepared and each one was dedicated to a constant horizontal pore-water velocity of 3.5, 7, 14 or 28 cm d^{-1}. To achieve these different horizontal pore-water velocities, a pre-determined number of pump manifold tubes with different diameters were installed in a variable-rate peristaltic pump. These tubes supplied the inlet solution from the aeration reservoir to the inlet chamber of each flow cell to achieve

the dedicated horizontal pore-water flow velocities. Inflow solution was continuously pumped into the flow cells for 7 days while maintaining the water level in the outflow chamber at 12 cm above the bottom of the flow cell. Outlet samples of 30 mL were collected daily and flow rates were monitored every three days. Collected outlet samples were analyzed for pH, NO_3-N, Br^-, and dissolved organic carbon (DOC). Nitrate-N and Br^- were analyzed using a Lachat Quickechem 8000 slow injection auto analyzer and DOC was analyzed using the Total Organic Carbon Auto-analyzer (Shimadzu Corp., Columbia, MD) (Greenberg et al., 1992). After seven days, the supply of NO_3-N and Br^- solution was stopped and the flow cells were drained.

The flow cells were drained by connecting the manifold (connected to the bottom of the flow cell) to a vacuum trap. Air in the vacuum trap was evacuated to create 300 cm of tension for five minutes facilitating the removal of water from each flow cell. After five minutes, tension in the vacuum trap was increased to 400 cm to further drain the flow cell for another five minutes. Eighteen hours after drainage, each flow cell was re-connected to the vacuum pump and was drained at 400-cm tension for another five minutes. The manifold was then reconnected to the aeration reservoir to supply inlet solution to the flow cell and re-establish the WT. Four hours after the WT was re-established at 12 cm above the bottom, the tubing manifold connecting the aeration reservoir and the flow cell was again clamped and the inflow solution was pumped into the inlet reservoir of each flow cell at the appropriate rate to achieve the desired pore-water velocity (i.e., 3.5, 7, 14 or 28 cm d^{-1}) assigned to that flow cell. Three saturated flow-drainage cycles were run for each replicate. At the end of the

three saturation-drainage cycles, the flow cells were emptied, cleaned and re-packed with the same soil. The three saturation-drainage cycles were then repeated to duplicate the experiment.

Single-factor analysis of variance of mean equilibrium concentrations detected at the outlet was conducted using the Windows Excel Analysis Tool Package (Microsoft Corp. Redmond, WA). The Duncan Multiple Range Test was used to determine significant differences between specific treatments (Gomez and Gomez, 1984).

2.3. Experiment II. Fate and Horizontal Transport of NO_3^- in a Simulated Vadose Zone-Shallow Ground Water Continuum

2.3.1. Set-up

Evaluation of NO_3^- fate and transport was conducted using two 240-cm long by 60-cm high and 25-cm thick flow cells (hereafter referred to as “large flow cell” - Fig. 2). The front side of each flow cell was constructed using 1.25-cm thick transparent polycarbonate sheet while the rest of the sides and bottom were constructed using 1.9 cm-thick flat PVC sheets. Similar to the smaller flow cells described in Section 2.2, to the left and right of the flow cells were the inlet chamber and outlet chamber, respectively (see Fig. A1 in Appendix). Four adapters were installed at the bottom for applying water or draining the flow cell. The inner 220 cm of the flow cell (standing on its length) between the inflow and outflow chambers inscribed by two perforated walls (to allow water to pass through effectively) was packed with either sand or Leon soil material depending upon the simulation.

There were four sampling stations in each flow cell designated as stations 1, 2, 3 and 4 that were located 25 cm, 65 cm, 110 cm and 195 cm from the inlet chamber, respectively (Fig. 2). Each sampling station had four tension samplers installed to collect soil solution samples at 7.5, 12.5, 27.5 and 32.5 cm above the bottom of the flow cell. As will be discussed later, a WT was established at 20 cm above the bottom of the flow cell allowing to have a tension sampler at 7.5 and 12.5 cm below the WT and at 7.5 and 15 cm above the WT at each location. For a photograph of the flow cell and the sampler diagram, see Figures A2 and A3 in the Appendix). Each sampling station had a platinum-tipped redox electrode (Pt electrode) installed at the same depth where the porous cup of the tension sampler was installed (Fig. A2c in Appendix). Locations in the flow cell where redox potential (Eh) and solution samples were collected are hereafter referred to as "monitoring locations". Placement of redox electrodes and tension samplers enabled simultaneous monitoring of the Eh and the concentrations of non-conservative NO_3^- relative to that of the conservative Br^- along the flow path. The information gained would provide some insight into the fate of NO_3^- as it was potentially transported horizontally through the flow cell both below and above the WT.

2.3.2. Horizontal Transport Simulations

One of the two large flow cells used in the horizontal transport simulation experiment was packed with sand and the other with Leon soil material. A manifold constructed of plastic tubing was connected to four inlet/outlet adaptors at the bottom and the inlet and outlet chambers (see Fig. 2). Distilled water was introduced to each flow cell by connecting a

25-L Marriotte bottle reservoir to the manifold. The tip of the air-entry tube in the reservoir and the open end of the drainage tube connected in the outlet were set at an elevation that corresponded to 20 cm above the bottom of the flow cell. This allowed the establishment of a simulated WT inside the flow cell at the desired elevation. When the water level in the inlet and outlet chambers and in the piezometers (see Fig. 2 for locations of piezometers) indicated that a flat WT had been established, a gel-filled Calomel reference electrode (Fisher Scientific, Pittsburgh, PA; ID No. 13-620-258) was installed at the inlet chamber (tip of the electrode was submerged in water in the inlet chamber). Initial redox potential (Eh) readings were taken by measuring voltage between the Pt and reference electrodes using a multi-meter (Radioshack, Fort Worth, TX - accurate to 0.001V). The multi-meter readings were added to 0.25 V (or 250 mV) to convert them into Eh values. In addition, 30 mL background water samples were collected from all tension samplers as well as from inlet and outlet chambers of each flow cell.

To collect samples, each tension sampler was connected to a designated vacuum trap (similar to system of Hendrickx et al., 2002) (Fig. A3 in Appendix). Each sampler (with vent open) was initially purged by evacuating air from the dedicated vacuum trap using a pump. After purging, the vent of the tension sampler was closed, and a 60 mL sample bottle was placed inside the vacuum trap (see Fig. A3B in Appendix for a photograph of vacuum trap with sample bottle). The trap was then re-connected to the vacuum pump to apply a tension of 400 cm. This allowed extraction and delivery of soil solution from the surroundings of the

sampler to the sample bottle inside the vacuum trap. Thirty mL of sample were collected using each tension sampler for each sampling.

Samples were also collected from the inlet and outlet chambers using a dedicated plastic syringe with its tip connected to the plastic tubing that extended 10 cm below the water level inside each chamber. Thirty-mL samples were collected from the inlet and outlet chambers every time soil solution samples were collected using the tension samplers. All samples were frozen prior to analysis of solution pH as well as NO_3-N, Br^-, and DOC concentrations.

After collection of the background samples, the WT was allowed to recover to the 20-cm level in both flow cells. The tubings in the manifold connecting the outlet and inlet chambers and the bottom inlets to the reservoir were clamped and disconnected from the reservoir. The outflow end of the plastic tubing connected to the outlet chambers was then fixed at 20 cm above the bottom of the respective flow cells.

2.3.2.a. Horizontal Flow Simulation in Sand

The plastic tubing directly connecting the inlet chamber to the reservoir was clamped, detached from the distilled water-filled Marriotte bottle reservoir and connected to another 25-L Marriotte bottle reservoir with a solution of 15 mg L^{-1} each of NO_3-N and Br^- dissolved in distilled water (no organic material). Water was then rapidly pumped out of the inlet chamber using an electric vacuum pump. When the chamber was emptied, the plastic tubing connected to the solution reservoir was immediately unclamped thereby introducing the NO_3-N and Br^- solution into the inlet chamber. The tip of the air-entry tube in the NO_3^- and Br^--

containing reservoir was raised to an elevation of 21 cm. This resulted in a sloping WT that translated to a horizontal flow rate of approximately 10 cm d^{-1} across the flow cell. Outlet discharge rate was monitored hourly for 6 hours after the inflow solution change to determine whether the desired flow rate was achieved.

Soil solution samples from all monitoring locations (including inlet and outlet chambers) were then collected and redox potential readings were taken daily for the next 21 days. After collecting samples on the 21st day, the tubing supplying the inlet solution was clamped (no flow) for seven days. Samples were collected on the 3rd and 6th days from the start of the no-flow condition to determine if there was any effect of zero pore-water velocity on the fate of NO_3^-.

After seven days under no-flow conditions, the tubing connected to the inlet chamber (still clamped) was disconnected from the reservoir containing the solution of NO_3-N and Br^- in distilled water and connected to another 25-L reservoir with 15 mg L^{-1} NO_3-N and Br^- dissolved in ground water. The ground water used as carrier for the NO_3^- and Br^- in this part of the experiment was collected from the wetland restoration site where the Leon soil material was collected. This groundwater had an average DOC concentration of 83 mg L^{-1} with NO_3^- content below the detection limit. The inlet chamber was then drained by pumping out the original solution (NO_3^- and Br^- in distilled water) rapidly. When drained, the solution of NO_3^- and Br^- in ground water was immediately introduced to the inlet chamber. The tip of the air-entry tube in the new reservoir was set to maintain the horizontal pore water velocity of 10 cm d^{-1}. The solution in the reservoir was manually stirred for 5 minutes

twice daily to prevent the development of anoxic conditions in the reservoir. Soil solution samples were collected and Eh at every monitoring location was measured at least every 4 days. After 28 days of running at a pore-water velocity of 10 cm d^{-1}, the air-entry tube in the reservoir was raised to the elevation of 21.5 cm above the bottom of the flow cell. This increased the horizontal pore-water velocity to 20 cm d^{-1}. Sampling and measurements of Eh were continued as before. After another 28 days, the pore-water velocity was further increased to 40 cm d^{-1} while continuing the same soil solution sampling and Eh measurement regimes without interruption. After 28 days of passing the solution at a pore-water velocity of 40 cm d^{-1}, flow was stopped for 14 days. Soil solution samples and Eh data were gathered on the 14^{th} day after flow was stopped. The flow cells were then drained and three sets of intact core samples from the 4 to 12 cm, 23 to 31 cm and 40 to 48 cm depth intervals were collected for bulk density determination using the core method (Grossman and Reinsch, 2002).

2.3.2.b. Horizontal Flow Simulation in Leon Soil

As described earlier, a WT was established at 20 cm above the bottom of the flow cell packed with Leon soil material. After collecting background soil solution samples and allowing the WT to reach to the desired level, the inlet chamber was rapidly drained and then immediately filled with a solution containing 15 mg L^{-1} of NO_3-N and Br^- in distilled water using a Marriotte bottle reservoir. Horizontal flow was then initiated by raising the air-entry tube in the Marriotte bottle reservoir. Soil solution and Eh data were collected daily.

Two problems were encountered early in the experiment using Leon soil material:

1) a constant discharge rate at the outflow was not established even after three weeks from the onset of the experiment, and
2) NO_3^- concentrations detected above the WT through the first three weeks of this experiment were as high as 30 mg L^{-1}, which was twice the inflow solution concentration of 15 mg L^{-1}.

The first problem was probably due to reductions in the hydraulic conductivity of the packed soil material, and the latter problem was mainly due to dissolution/mineralization of NO_3^- from the soil collected from a previously farmed field. These problems prompted the following two changes in how the experiment in the Leon soil-packed flow cell was operated:

1) the inflow solution concentration was increased to 100 mg L^{-1} for both NO_3-N and Br^- in distilled water. Increasing the NO_3^- concentration to 100 mg L^{-1}, which was at least three times the highest detected NO_3^- concentration above the WT in the first three weeks, allowed the assessment of whether the NO_3^- that was applied through the inlet chamber moved from below the WT into the CF and became transported horizontally above the WT.
2) the WT slope was maintained at 2.5 % for the remainder of the experiment. Because achieving a desired constant hydrologic condition within the timeframe of the study proved to be difficult, simulating the four hydrologic conditions imposed on the sand-packed flow cell (10 cm d^{-1}, 20 cm d^{-1} and 40 cm d^{-1} and no flow) was changed to just

simulating two cases: a flowing system at approximately 10 cm d^{-1} and a non-flowing system.

Monitoring of NO_3^- and Br^- concentration in the flow cell with Leon soil continued for 50 days after the change in inflow solution to 100 mg L^{-1} for both NO_3-N and Br^-. Samples from all monitoring locations in the flow cell (including the inlet and outlet chambers) and Eh data were collected at least every four days. Flow was then stopped and samples were collected after 14 days under no-flow conditions. At the end of the experiment, the flow cell was drained and intact core samples were collected for bulk density analysis in the same manner as in the sand-packed flow cell.

3.0 Results and Discussion

3.1. Soil Properties

Properties of the two soils used in the experiment are summarized in Tables A1 and A2 of the Appendix. Saturated hydraulic conductivities of both soil materials were expectedly high at 6.6 and 3.0 m d^{-1} for the commercial medium sand and the loamy sand-textured Leon soil materials, respectively. The Leon soil material had significantly higher total organic carbon and total nitrogen content than the sand. Moisture release curves of the Leon soil revealed that its water content remained very close to saturation despite application of 30 cm of pressure (Figure A4 in Appendix). This suggested that the CF above the simulated WT in the Leon soil-packed flow cell was at least 30 cm thick. The sand, on the other hand, was already drained significantly at pressures greater than 20 cm suggesting that the CF thickness in the sand-packed flow cell was roughly 20 cm.

The large flow cells packed with Leon soil materials had bulk densities of 1.35-1.36 Mg m^{-3}. An increasing bulk density with depth was observed with the sand-packed flow cell where the bulk densities ranged from 1.43 to 1.62 Mg m^{-3}.

3.2. Hydrologic Effects on NO_3^- Loss

Pore-water velocity influenced the degree by which NO_3^- was removed from solution as it passed through the small flow cells packed with Leon soil material. Figure 3 shows that when the NO_3^- and Br^- solution flowed through the Leon soil material at 28 cm d^{-1}, NO_3^- in the outflow solution was reduced to 95% of the inflow concentration. This was significantly a lower degree of NO_3^- removal when compared to around 80% NO_3^- loss when the solution

was only flowing at 3.5 cm d^{-1}. It should be noted that these reductions in NO_3^- concentrations were not due to dilution as evidenced by the essentially similar concentration of Br^- (conservative tracer) detected at the inlet and outlet chambers for all pore-water velocities. Comparison of mean concentrations detected at the outlet chamber of each treatment from day 3 through day 7 (during which outlet normalized NO_3^- concentrations appear to have equilibrated as shown in Fig. 3) reveal statistically different means (Fig 4). This provides statistical validity to the earlier discussion (involving Fig. 3) suggesting that pore-water velocity influenced the degree of NO_3^- removal by the soil. The concentration of DOC detected at the outlet when pore-water velocity was 3.5 cm d^{-1} was also observed to be roughly 4 to 6 times higher than those observed in other treatments (Fig. 5) during the days when outlet NO_3-N concentrations seemed to have stabilized (see Fig. 3).

Difference in the pore-water velocities could also be viewed as a difference in the residence times of the applied solution in the flow cell. A pore-water velocity of 28 cm d^{-1} translates to a residence time of roughly 2.8 days, while a pore-water velocity of 3.5 cm d^{-1} translates to a residence time of 23 days. The longer residence time seemed to have allowed more organic carbon to be dissolved into solution that could have promoted an increase in the rate of biochemical activity leading to NO_3^- loss. The higher rate of biochemical activity coupled by the longer period of time that a solution was subjected to such biochemical processes (i.e., denitrification or DNRA) is believed to be the reason why NO_3^- content at the outlet was observed to be lower at slower pore-water velocities.

3.3. Horizontal Transport Experiment

3.3.a. Sand-Packed Flow Cell

As discussed earlier, hydrology played an important role in NO_3^- removal as the inlet solution flowed horizontally through the Leon soil material. Because it had been demonstrated that solutes are transported horizontally in the subsurface both below and above the WT (Silliman et al., 2002; Abit et al., 2008b), the next concern was to determine whether there is a difference in the degree in NO_3^- loss below and above the WT. There are field data showing that NO_3^- persists in the subsurface while being transported horizontally in the CF (Abit et al., 2008a) indicating that perhaps conditions in the CF favor persistence of NO_3^-. This study was conducted to test the hypothesis that difference in reduction potential above and below the WT leads to a difference in the degree of NO_3^- persistence when it is transported both above and below the WT.

Figure 6 shows solute concentrations detected at all the monitoring locations after 21 days of continuously applying the solution containing NO_3^- and Br^- in distilled water to the inlet chamber of the large flow cell packed with sand. The following could be deduced from Figure 6: a) consistent with the visual simulation of Silliman et al. (2002), NO_3^- and Br^- were transported horizontally both below and above the CF, and b) with very low DOC in all samples (< 2.0 mg L^{-1}), normalized concentrations of both solutes were comparable suggesting the absence of appreciable NO_3^- loss as it is transported horizontally both above and below the WT. A week under no-flow did not result in reduction of NO_3^- concentration

suggesting that despite modification of hydrology to favor NO_3^- loss, it still does not happen perhaps due to the lack organic carbon.

Introducing organic matter into the system, however, changed the concentrations of NO_3^- at the outlet. Figure 7 shows two things: a) there was NO_3^- loss when the inlet solution of NO_3-N and Br^- in ground water had an average of 83 mg L^{-1} of DOC, and b) higher degree of NO_3^- loss was observed at slower flow velocity across the flow cell. It should be noted that the latter observation agrees with the observation earlier discussed in the Hydrologic Effects on NO_3^- Loss experiment.

Lower normalized NO_3^- concentration, relative to normalized concentration of Br^-, at the outlet was indicative of some NO_3^- loss within the flow cell. Figure 8 shows the comparison of normalized NO_3-N and Br^- concentrations at station 3 of the sand-packed flow cell on the same days that the outlet data shown in Figure 7 were collected. Station 3 was chosen as representative location for presenting data because it was at the middle (hence, least affected by outside conditions) and could be taken as the best representative of the conditions in the flow cell. As expected, NO_3^- loss was practically absent when the DOC in solution was <2.0 mg L^{-1} (Fig 8A). When ground water solution was applied, the highest degree of NO_3^- loss in the flow cell was observed under the slowest (10 m d^{-1}) flow velocity used in the study (Fig. 8B). This was consistent with the observation of the relatively lowest normalized NO_3^- concentration at the outlet in Figure 7. Figure 8B also shows that NO_3^- loss was more extensive below the WT. Increasing the pore-water velocity from 10 cm d^{-1} to 20

cm d^{-1} and then 40 cm d^{-1} resulted in lesser NO_3^- losses at station 3 (Figures 8C and 8D, respectively).

The higher overall degree of NO_3^- loss at slower flow velocities can be explained by the concept of residence time. Under slower flow velocity, residence time is longer. An extended duration that the solution stays within the system provides more time for dissolved oxygen to be depleted by aerobic respiration thereby enhancing utilization of NO_3^- as the preferred electron acceptor. In addition, it lengthens the contact time between the solution and microbes lodged on solid surfaces thus increasing likelihood that those microorganisms responsible for NO_3^- loss via denitrification or DNRA will have access to the NO_3^- in solution. Higher NO_3^- loss below the WT could also be explained largely by the development of reducing conditions below the WT.

3.3.b. Leon Soil-Packed Flow Cell

As indicated before, the NO_3-N and Br^- concentrations in the solution applied to the large flow cell packed with Leon soil materials were increased to 100 mg L^{-1}. Comparison of inflow and outflow NO_3-N and Br^- concentrations reveal substantial NO_3^- loss in the flow cell packed with Leon soil. Figure 9 shows that while Br^- concentration steadily increased at the outlet after it broke through the flow cell, the concurrent increase in NO_3-N concentration at the outlet was substantially lower. On the 50^{th} day of running the 100 mg L^{-1} NO_3-N and Br^- solution through the flow cell, outlet Br^- concentration was 90 mg L^{-1} while only 31 mg L^{-1} of NO_3^- was detected (roughly 67% less NO_3^-).

We examine Figure 10 to determine where and to what degree did NO_3^- loss in the flow cell take place. For presenting data, we selected the inner sampling stations (stations 2 and 3) to represent the conditions in the flow cell as it was least affected by the external conditions. This figure shows that as the plume moved through stations 2 and 3 (65 and 110 cm from inlet chamber, respectively), Br^- was detected at all depths, but NO_3^-detection was limited only at 15 cm above the WT throughout the duration of the experiment.

Sampling locations where some NO_3^- was detected were those that remained aerobic for extended periods of time. The NO_3-N and Br^- concentrations and redox potentials for the final day (Fig. 11) shows that in stations 2, 3 and 4, NO_3^- was only detected at monitoring locations that were aerobic (Eh above the arbitrary 250 mV denitrification line as described in Patrick and Jugsujinja, 1992). It should be noted that the non-detection of NO_3^- at some monitoring locations is not due to the physical inability of solutes to reach those locations as Br^- was detected in all of them. Nitrate loss via two pathways, denitrification and DNRA, are favored under anaerobic conditions (Coyne, 1999) and are believed to be responsible for the non-detection of NO_3^- at anaerobic monitoring locations.

Although the detection of NO_3^- at all depths in station 1 (see Fig. 11) may have been partly due to the persistence of aerobic conditions, it could also be due to the fact that it is very close (only 25 cm) to the inlet chamber. In effect, the solution can reach station 1 in a relatively shorter period of time before NO_3^- is effectively removed from solution by denitrification and/or DNRA. In fact, when the supply of NO_3^- solution to the inlet chamber

was cut, NO_3^- concentration at station 1, especially below the WT, dropped appreciably (Figure 12).

Despite the absence of re-supply of NO_3^- (from the inlet), NO_3^- still persisted at 15 cm above the WT where the Eh remained to indicate aerobic conditions (Fig 12). Although the Eh at 15 cm above the WT generally indicated aerobic condition, NO_3^- loss was still observed at that zone and that may be due to the following: i) denitrification in anaerobic micro-sites (even if the Pt electrode indicated aerobic conditions); and ii) diffusion to, and subsequent denitrification of the NO_3^- in deeper depths that were devoid of NO_3^-.

Results from the flow cell supplied with distilled water for 60 days at a flow velocity of 20 cm d^{-1} (Appendix Fig. A5) shows that NO_3^- was only detected at 15 cm above the WT at concentrations that were less than 6 mg L^{-1}. This suggests that NO_3^- detected in the CF of the Leon soil where 100 mg L^{-1} NO_3^- was applied was indeed from the inlet solution. The detection of higher NH_4-N concentrations in anaerobic regions (below WT and at 7.5 cm above WT) suggests that DNRA is likely a contributing NO_3^- loss mechanism at the anaerobic regions.

4. Summary and Conclusions

This study was conducted to evaluate the effect of pore-water velocity on the fate of NO_3^- as it moves through a vadose zone-shallow ground water continuum. Subsurface hydrology influenced the location where NO_3^- was transported (above or below the WT) as well as its persistence while in transport. An extended residence time of a NO_3^--containing solution in the soil resulting from a relatively slow pore-water velocity yielded a more effective removal of NO_3^- from solution. Under conditions with very limited organic carbon (<2.0 mg L^{-1}), NO_3^- persisted while in transport both below and above the WT. An increase in organic carbon in solution (83 mg L^{-1}) enhanced some NO_3^- loss below the WT especially under slow pore-water velocity. Nitrate was essentially lost under conditions when the organic carbon content was sufficient for very reducing conditions (Eh < 250 mV) to develop below the WT. Aerobic conditions that were observed in the CF even in soils with sufficient organic matter content allowed NO_3^- to persist at such zone allowing some NO_3^- to be transported horizontally to a farther horizontal distance in the CF with minimal NO_3^- loss. These results suggests two things: a) NO_3^- treatment-potential of a soil body could be enhanced by managing the subsurface hydrology of the system – specifically reducing subsurface pore-water velocity (e.g., decreasing groundwater gradient by manipulating outlet water levels), and b) the non-detection of NO_3^- below the WT does not definitively imply that no appreciable amount of NO_3^- is transported, because it could be moving in the CF.

The results can also be used to explain spikes in NO_3^- concentration in ditches or rivers close to agricultural fields/feedlots/septic drain fields that may occur following storm

events. The percolation of water following storm events could lead to rapid rise in WT resulting in higher subsurface gradient towards ditches or rivers. The higher gradient translates to faster subsurface water flow both above and below the original WT. Transformation of the original CF into saturated zone following major storm events allows the solutes retained in this zone to be transported laterally under faster subsurface velocities. Due to conditions of short residence time during this process, little or no NO_3^- removal could occur in the soil resulting in a spike in NO_3^- concentrations in the ditches.

5. References Cited

Abit, S.M., A. Amoozegar, M. J. Vepraskas, and C.P. Niewoehner. 2002a. Fate of nitrate in the capillary fringe and shallow groundwater in a drained sandy soil. Geoderma. 146:209-215.

Abit, S. M., A. Amoozegar, M. J. Vepraskas, and C. P. Niewoehner. 2008b. Solute transport in the capillary fringe and shallow groundwater: Field evaluation. Vadose Zone J. 7:890-898.

Amoozegar, A., C.P. Niewoehner, and D.L. Lindbo. 2006. Lateral movement of water in the capillary fringe under drain fields. In: Proc. 2006 Tech. Educ. Conf., Denver Co. 27-31 Aug. 2006. Natl. Onsite Wastewater Recycling Assoc. Sta. Cruz, CA.

Amoozegar, A. and G. V. Wilson. 1999. Methods for measuring hydraulic conductivity and drainable porosity. In: R.W. Skaggs and J. van Schilfgaarde (eds). Agricultural Drainage. Agronomy Monograph no. 38. SSSA, Madison, Wisconsin.

Anderson, D.M., P.M. Glibert, and J.M. Burkholder. 2002. Harmful algal blooms and eutrophication nutrient sources, composition, and consequences. Estuaries and Coasts. 25(4b): 704-726.

Appelo, C.A.J., and D. Postma, D. 1994. Geochemistry, Groundwater and Pollution. Balkema, Rotterdam, 536 pp.

Caskey, W.H., and J.M. Tiedje. 1979. Evidence of *Clostridia* as agents of dissimilatory reduction of nitrate to ammonium in soils. Soil Sci. Soc. Am. J. 43:931-936.

Coyne, M. 1999. Soil Microbiology: An Exploratory Approach. Delmar Publishers. Albany, NY.

Culmo, F.C. 1988. Principle of Operation – The Perkin-Elmer PE2400 CHN Elemental Analyzer. Perkin Elmer Corp., Norwalk, CT.

Dane, J. H., and J. W. Hopmans. 2002. Water retention and storage. In: J. H. Dane, and G. C. Topp (eds). Methods of Soil Analysis Part 4: Physical Methods. No. 5 in Soil Sci. Soc. Am. Book Series. Soil Sci. Soc. Am., Madison, WI.

D'Angelo, E.M. and K.R. Reddy. 1993. Ammonium oxidation and nitrate reduction in sediments of hypereutrophic lakes. Soil Sci. Soc. Am. J. 57:1156-1163.

Gee, G. W., and D. Or. 2002. Particle-size analysis. In: J. H. Dane, and G. C. Topp (eds). Methods of Soil Analysis Part 4: Physical Methods. No. 5 in Soil Sci. Soc. Am. Book Series. Soil Sc. Soc. Am., Madison, WI.

Gomez, K.A., and A.A. Gomez. 1984. Statistical Procedures for Agricultural Research. John Wiley and Sons. NY.

Greenberg, A. E., L. S. Clesceri, and A. D. Eaton. 1992. Standard Methods for Examination of Water and Wastewater. 18th Ed. APHA. Washington, DC.

Green, C. T., L. H. Fisher, and B. A. Bekins. 2008. Nitrogen fluxes through unsaturated zones in five agricultural settings across the United States. J. Environ. Qual. 37: 1073-1085.

Grossman, R. B., and T. G. Reinsch. 2002. Bulk density. In: J. H. Dane, and G. C. Topp (eds). Methods of Soil Analysis Part 4: Physical Methods. No. 5 in Soil Sci. Soc. Am. Book Series. Soil Sc. Soc. Am., Madison, WI.

Gupta, S., R.C. Gupta, and A.B. Gupta. 2007. Nitrate toxicity and human health. In: Abrol, Y. P, N. Raghuram and M.S. Sachdev (eds). Agricultural Nitrogen Use and its Environmental Implications. pp. 517-547. I. K. International Publishing House, New Delhi.

Hendrickx, J. M., J. M. Wraith, D. L. Corwin, and R. G. Kachanoski. 2002. Miscible solute transport. In: J. H. Dane, and G. C. Topp (eds). Methods of Soil Analysis Part 4: Physical Methods. No. 5 in Soil Sci. Soc. Am. Book Series. Soil Sci. Soc. Am., Madison, WI.

Horrigan, L., R. S. Lawrence, and P. Walker. 2002. How sustainable agriculture can address the environmental and human health harms of industrial agriculture. Environmental Health Perspectives. 110:445-456.

Karr, J. D., W. J. Showers, J.W. Gilliam, and A.S. Andres. 2001. Tracing nitrate transport and environmental impact from intensive swine farming using Delta Nitrogen-15. J. Environ. Qual. 30:1163-1175.

Korom, S.F. 1992. Natural denitrification in the saturated zone: a review. Water Resour. Res. 28(6):1657–1668.

Matheson, F.E., M.L. Nguyen, A.B. Cooper, T.P. Burt and D.C. Bull. 2002. Fate of ^{15}N-nitrate in unplanted, planted and harvested riparian wetland soil microcosms. Ecological Engineering. 19:249-264.

Nolan, B.T. and J.D. Stoner . 2000. Nutrients in ground waters of the conterminous United States, 1992–1995. Environ. Sci. Technol. 34:1156–1165.

Patrick, W. H. and A. Jugsujinda. 1992 .Sequential Reduction and Oxidation of Inorganic Nitrogen, Manganese, and Iron in Flooded Soil. Soil Sci. Soc. Am. J. 56:1071-1073.

Schuh, W. M., D. L. Klinkebiel, J. C. Gardner, and R. F. Meyer. 1997. Tracer and nitrate movement to groundwater in the Northern Great Plains. J. Environ. Qual. 26: 1335-1347.

Silliman, S. E., B. Berkowitz, J. Simunek, and M. Th. Van Genuchten. 2002. Fluid flow and solute migration within the capillary fringe. Ground Water. 40(1):76-84.

Spalding, R.F. and Exner, M.E. 1993. Occurrence of nitrate in groundwater – a review. J. Environ. Qual. 22:392-402.

Starr, J. L., A. M. Sadeghi, T. B. Parkin, and J. J. Meisinger. 1996. A tracer test to determine the fate of nitrate in shallow groundwater. J. Environ. Qual. 25:917-923.

Stumm, W., and J.J. Morgan. 1996. Aquatic Chemistry, 3rd edn. Wiley-Interscience, New York, 1022 pp.

Tiedge, J.M. 1988. Ecology of denitrification and disimilatory nitrate reduction to ammonium. In: Zehnder, A.J.B. (Ed). The Biology of Anaerobic Microorganisms. Wiley, NY.

USEPA. 2004. Monitoring and Assessing Water Quality. National Water Quality Inventory: Report to Congress, 2004 Reporting Cycle.
At: http://www.epa.gov/owow/305b/2004report/. Accessed: April 2009.

6. Figures

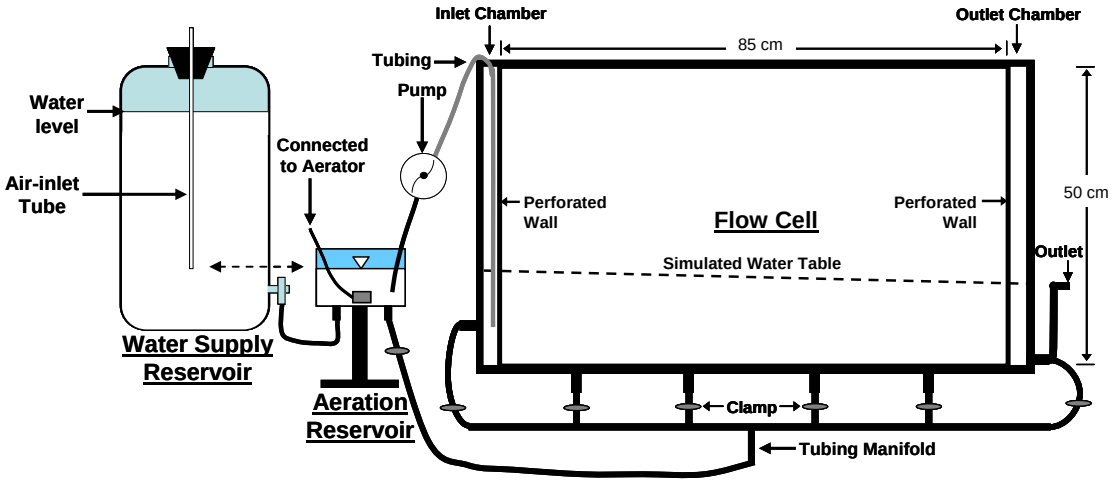

Figure 1. Two-dimensional schematic diagram of the set-up used in Experiment 1. Note: illustration is not to scale and flow cell is 8-cm thick.

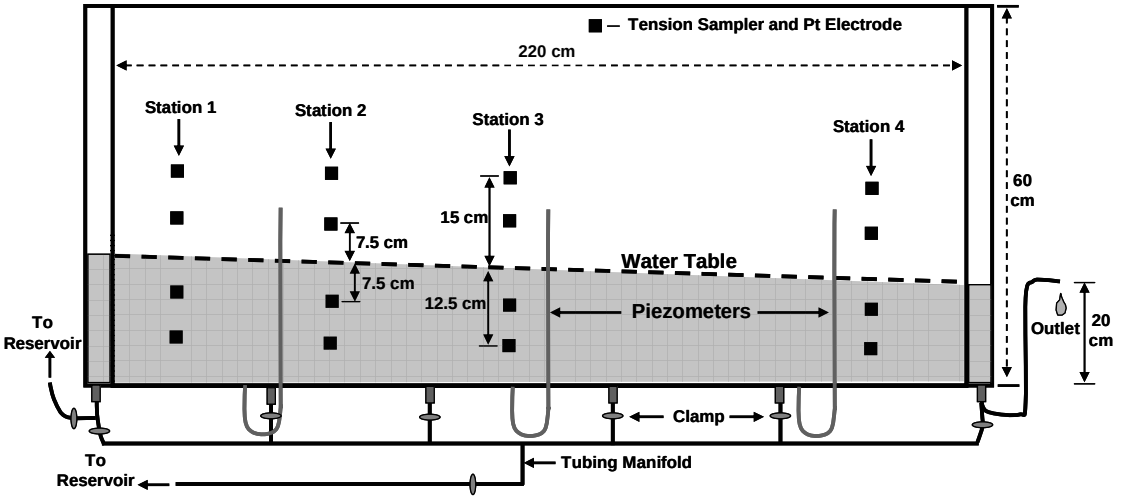

Figure 2. Two-dimensional schematic diagram of flow cell used in Experiment 2. Note: the flow cell is 25-cm wide and this is also referred to as “large flow cell”.

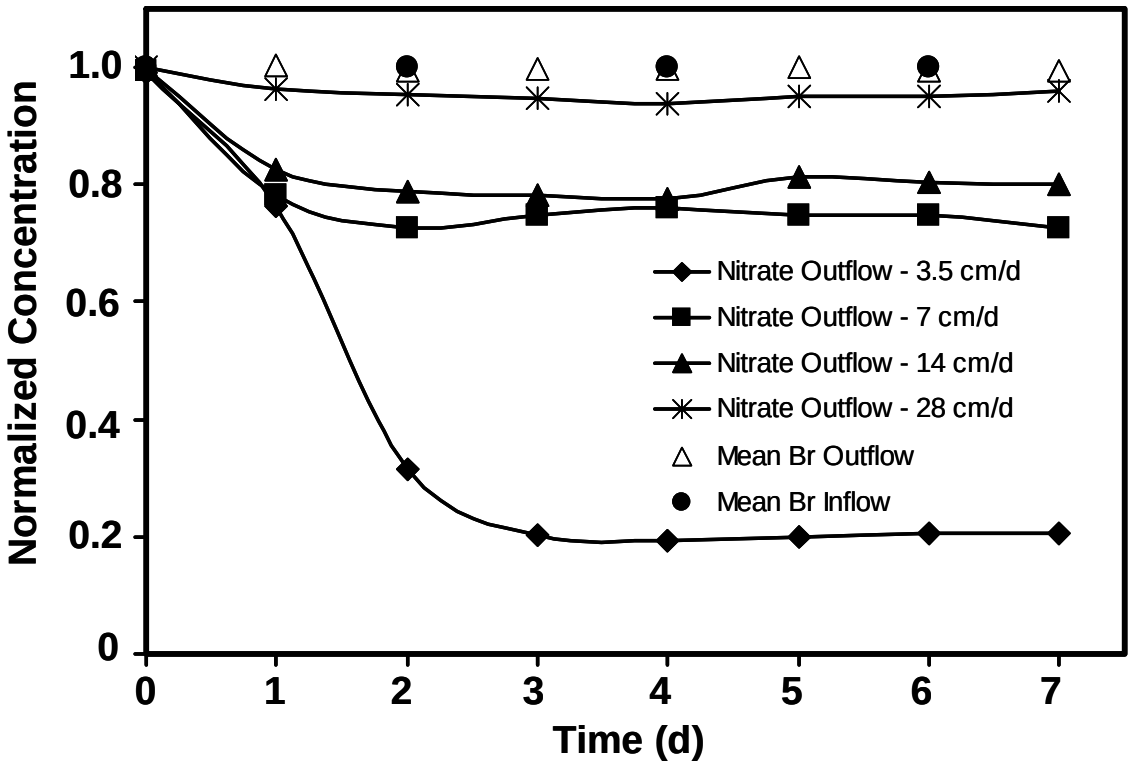

Figure 3. Mean normalized NO_3-N and Br^- concentrations of the solution introduced to the flow cells packed with Leon soil material and in samples collected from the outlet chamber of the flow cells subjected to various horizontal flow velocities. Values are means of detected concentrations from two separated runs with three cycles within each run.

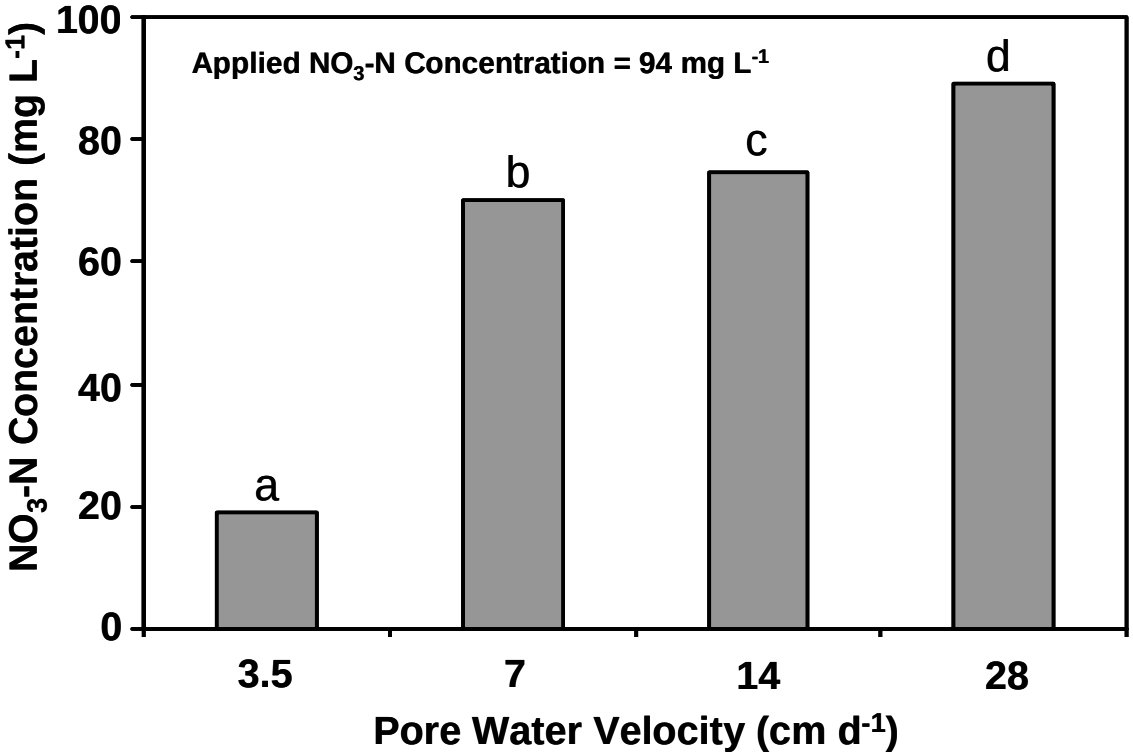

Figure 4. Mean NO_3-N concentrations in samples collected at the outlet chambers of the flow cells packed with Leon soil material and subjected to various flow velocities from day 3 through day 7. Means designated by different letters are statistically different at 5% significant level.

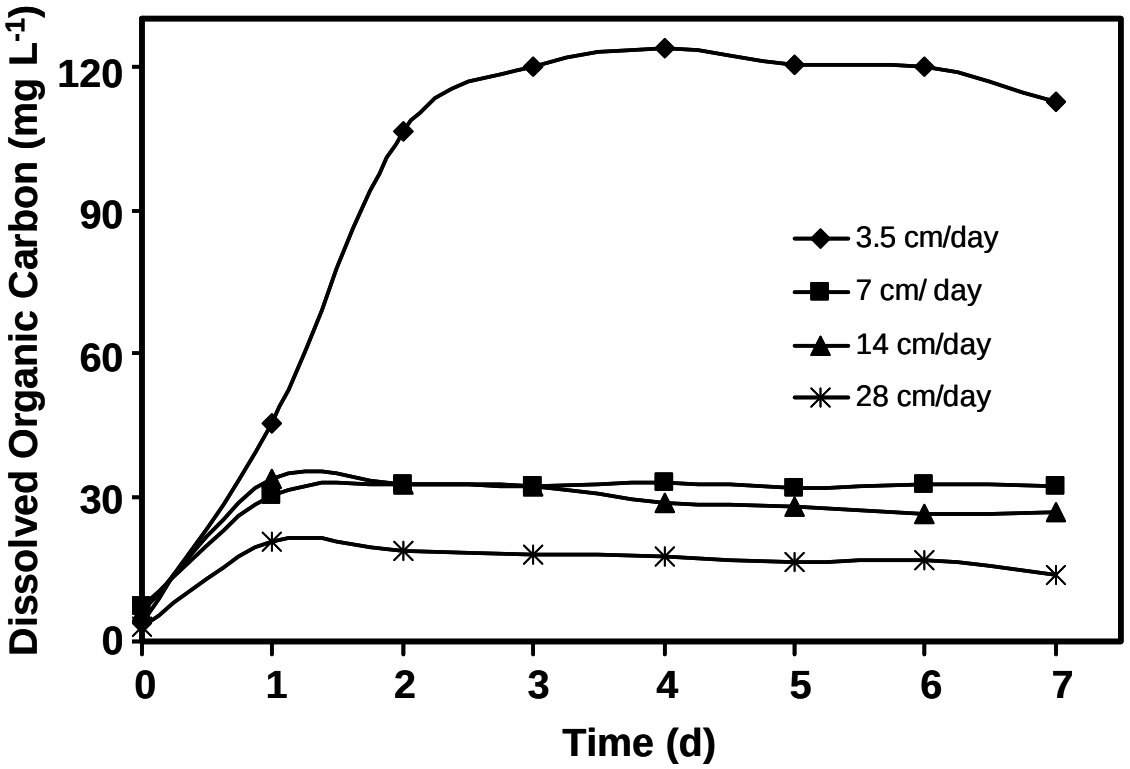

Figure 5. Mean dissolved organic carbon (DOC) concentrations in samples collected at the outlet chambers of the flow cells packed with Leon soil material and subjected to various flow velocities. The DOC in the applied solution was < 0.1 mg L^{-1}.

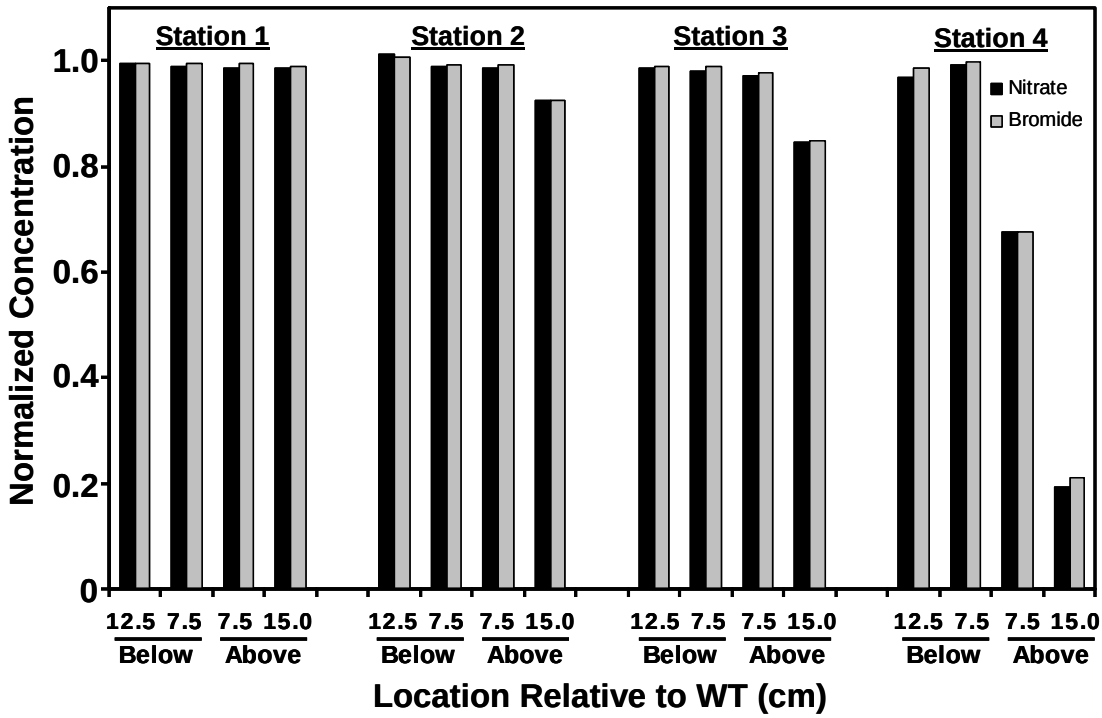

Figure 6. Normalized NO_3-N and Br^- concentrations at all monitoring locations after 21 days of continuously applying a solution containing 15 mg L^{-1} each of NO_3-N and Br^- in distilled water to the inlet chamber of the flow cell packed with sand.

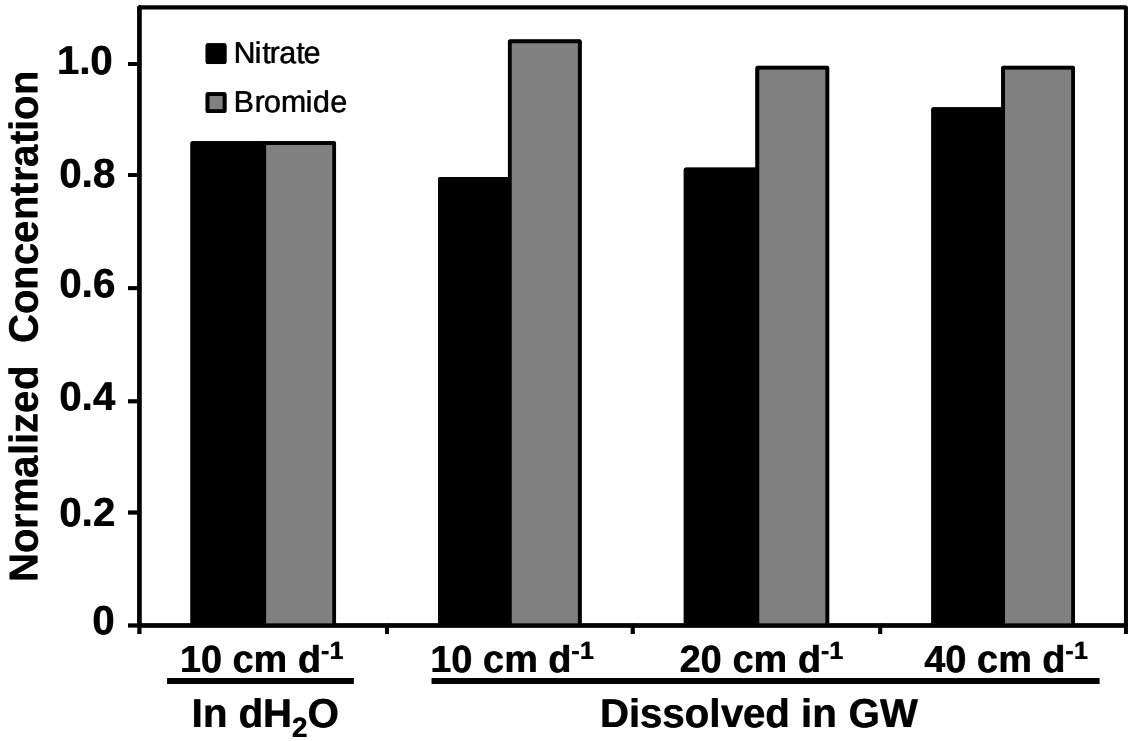

Figure 7. Normalized NO_3-N and Br^- concentrations at the outlet of the flow cell packed with sand at the end of each simulation which were as follows: on the 21st day after start of application of solution of NO_3^- and Br^- in distilled water (dH_2O) and 28th day after start of each simulation with NO_3^- and Br^- dissolved in ground water (GW).

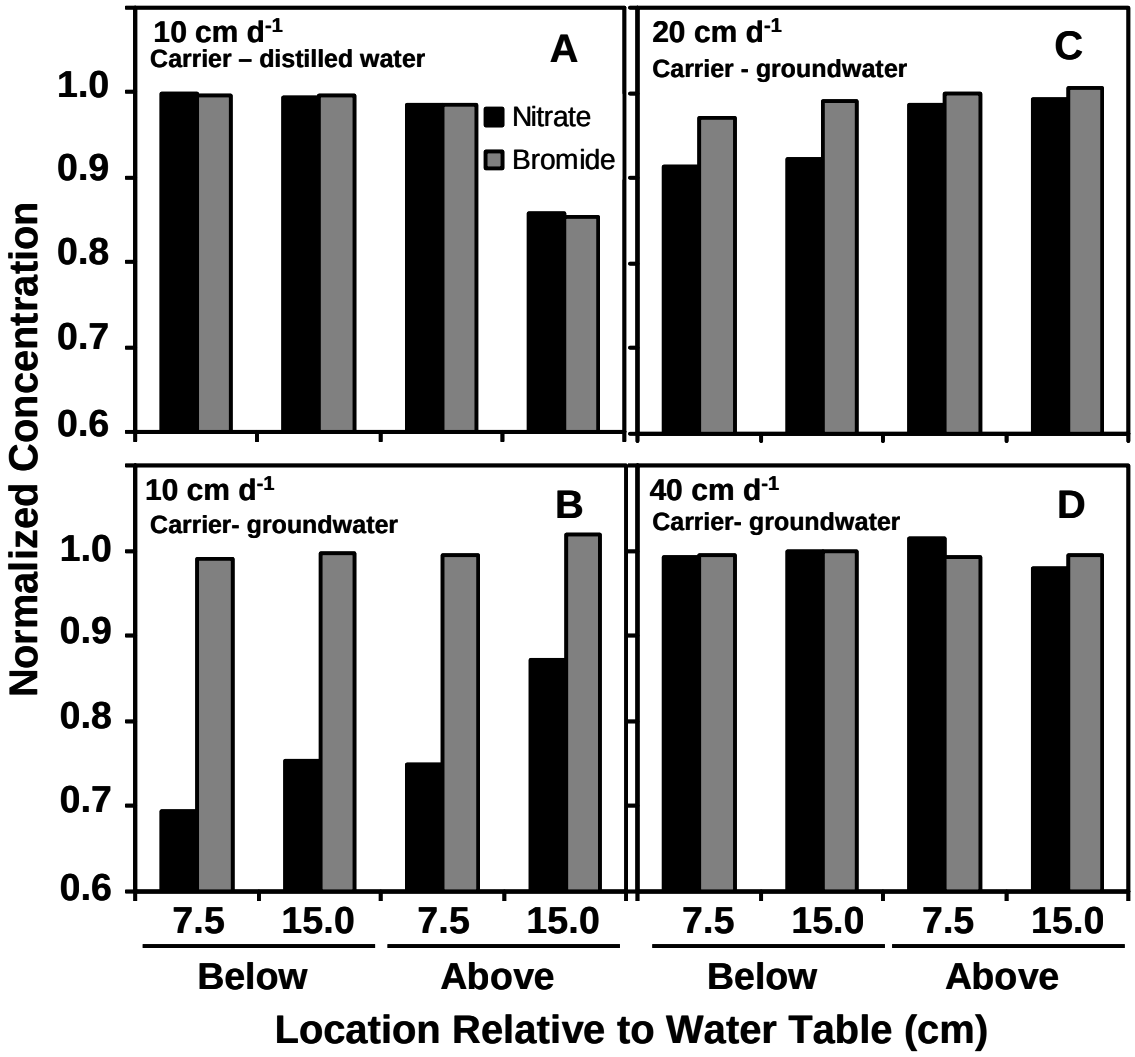

Figure 8. Comparison of normalized NO_3-N and Br^- concentrations detected at station 3 of the large flow cell packed with sand at the end of each respective simulation which were as follows: on the 21st day after start of application of solution of NO_3^- and Br in distilled water (A) and on the 28th day after start of each simulation with NO_3^- and Br in dissolved in ground water (B, C and D).

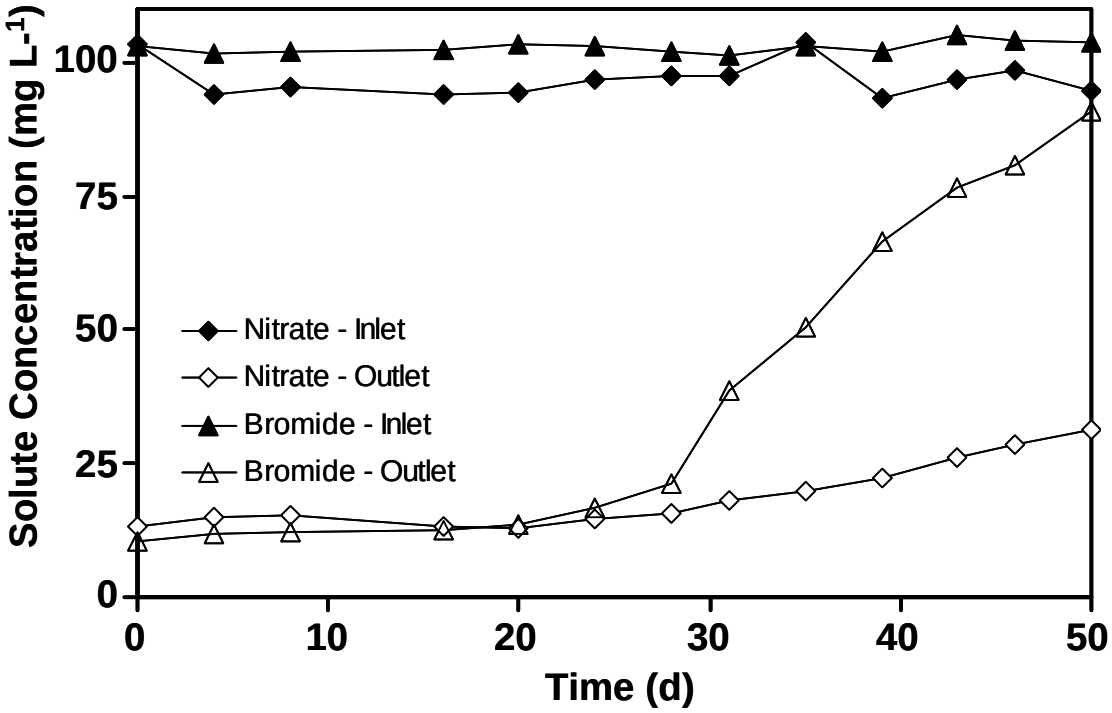

Figure 9. Nitrate-N and Br^- concentrations detected in samples collected at the inlet and outlet chambers of the large flow cell packed with Leon soil material. Day zero is the day the inlet solution was increased from 15 to 100 mg L^{-1} each of NO_3-N and Br^-.

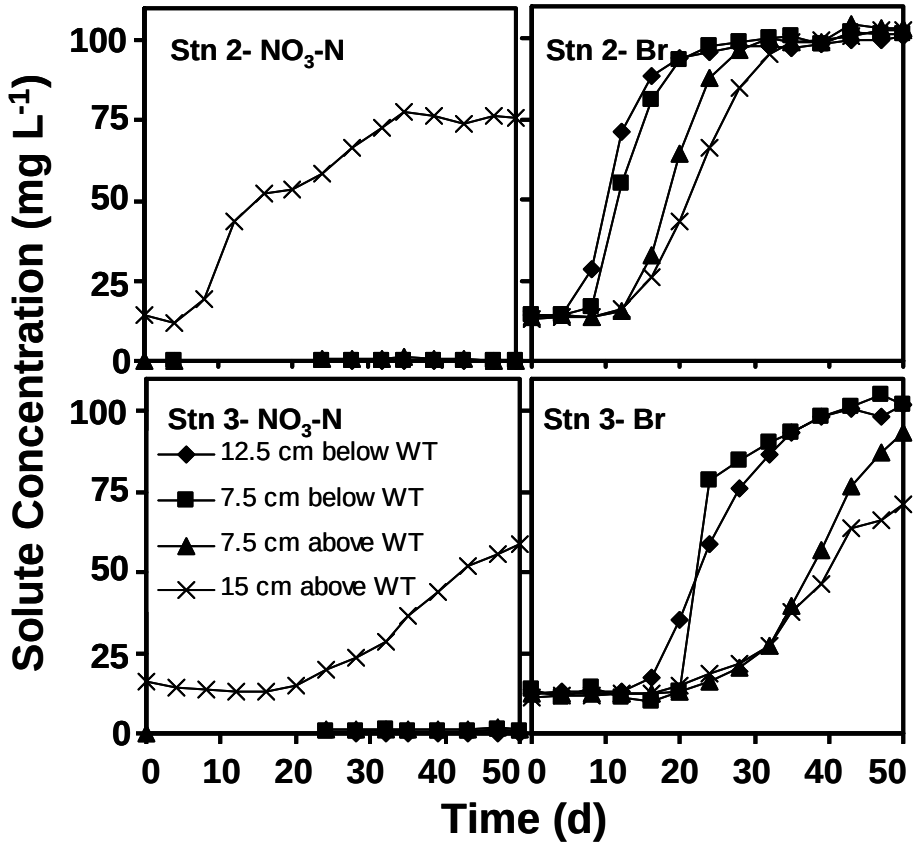

Figure 10. Nitrate-N and Br^- concentrations detected in monitoring locations at stations 2 and 3 in the Leon soil-packed flow cell. Day zero is the day the inlet solution was increased from 15 to 100 mg L^{-1} each of NO_3-N and Br^-. Stations 2 and 3 are located 65 cm and 110 cm from the inlet, respectively.

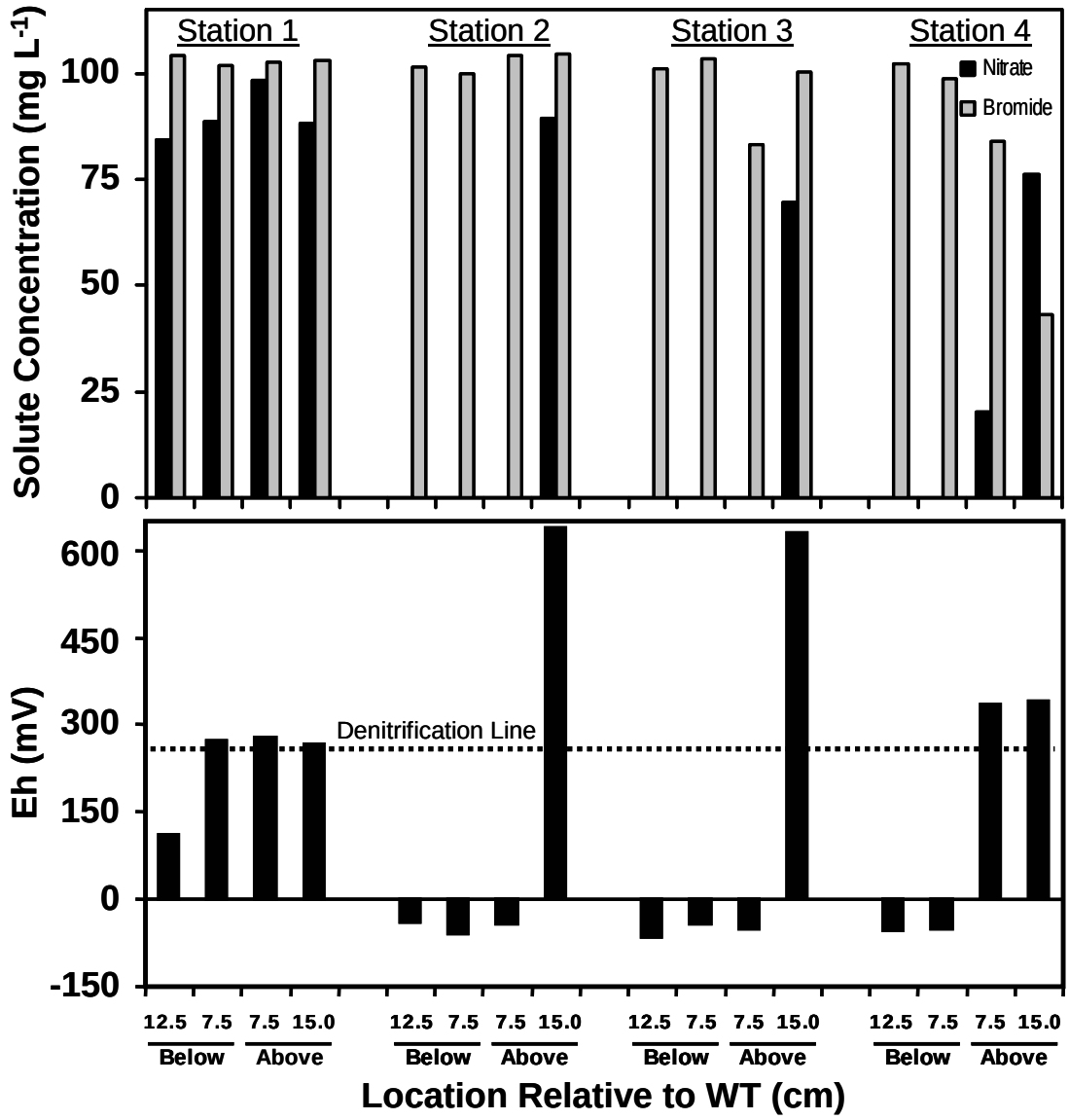

Figure 11. Nitrate-N and Br^- concentrations, and redox potential (Eh) at all monitoring locations in the Leon soil-packed flow cell on the final day of the solute transport simulation. The arbitrary denitrification line is 250 mV—below which nitrate removal via denitrification is expected to be extensive.

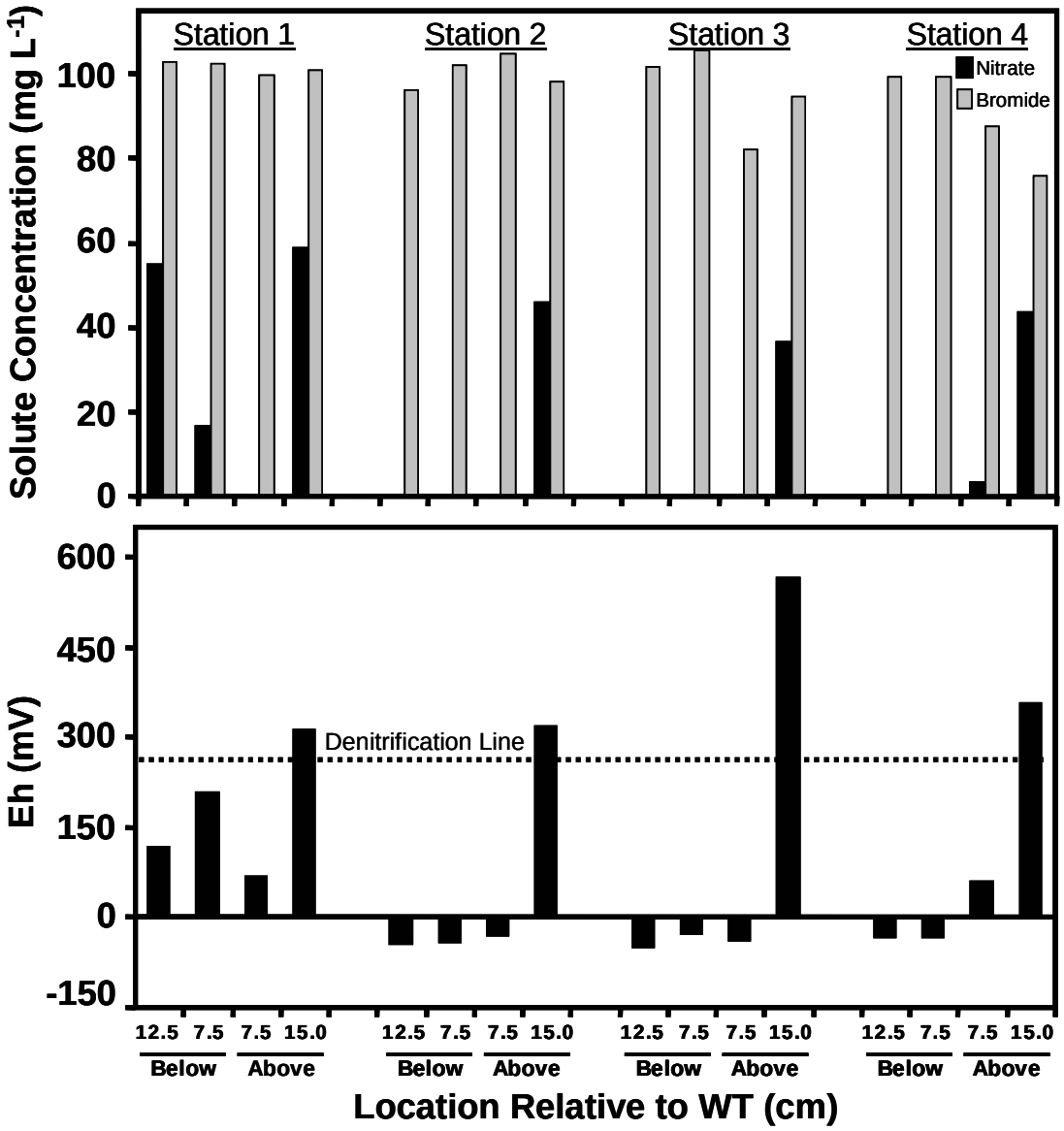

Figure 12. Nitrate-N and Br concentrations, and redox potential (Eh) at all monitoring locations in the Leon soil-packed flow cell 14 days after flow was stopped. The arbitrary denitrification line is 250 mV—below which nitrate removal via denitrification is expected to be extensive.

7. Appendix

Table A1. Properties of soils used in the experiment.

	Texture	K_{sat} (m d^{-1})	Percent OC	Percent N
Leon Ap	Loamy Sand	3.0	3.54	0.12
Commercial Sand	Medium Sand	6.6	0.03	<0.02

Table A2. Bulk density of soils packed in the flow cell.

	Location (depth interval)	Bulk Density (Mg m^{-3})
Leon Ap	Top (4-12 cm)	1.35
	Middle (23-31 cm)	1.36
	Bottom (40-48)	1.36
Commercial Sand	Top (4-12 cm)	1.43
	Middle (23-31 cm)	1.52
	Bottom (40-48)	1.51

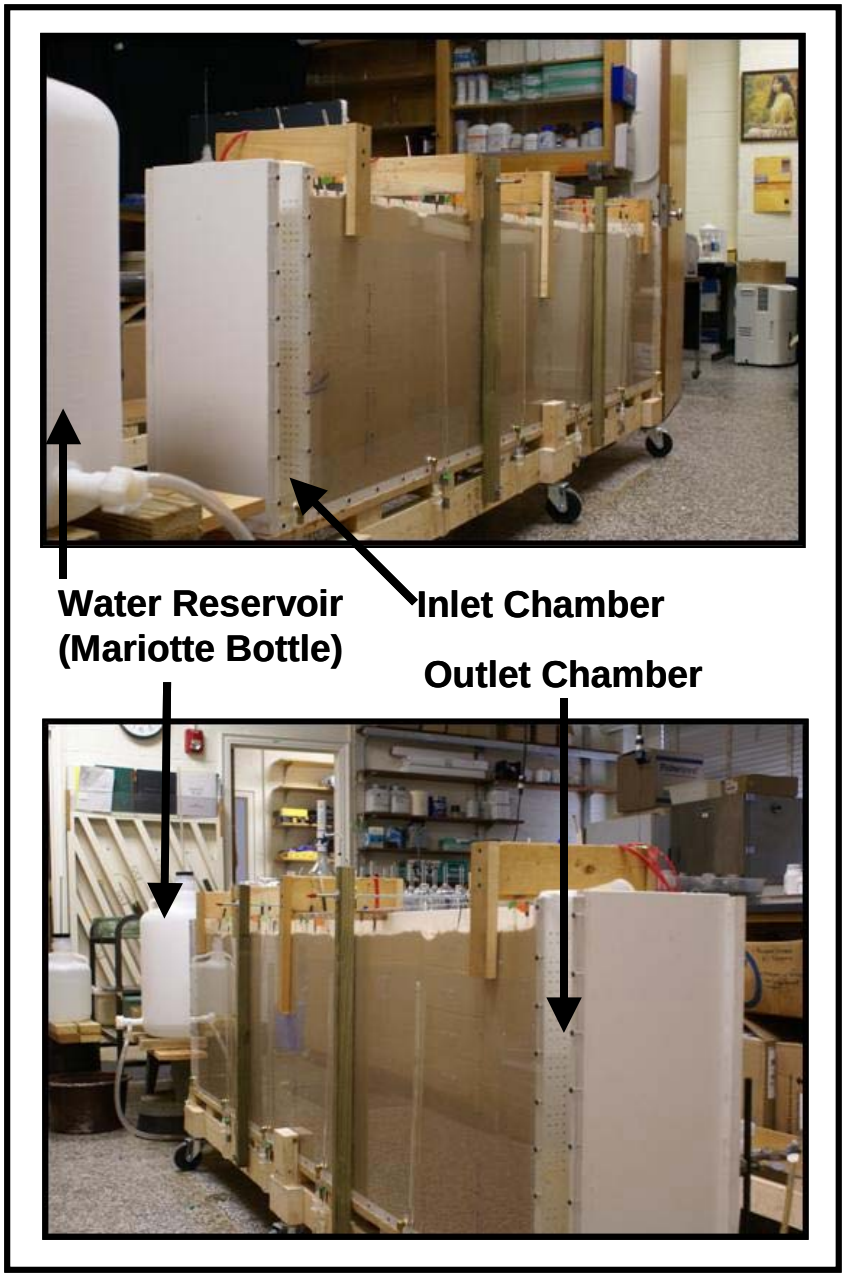

Figure A1. Photographs from two vantage points of the large flow cell used in Experiment 2.

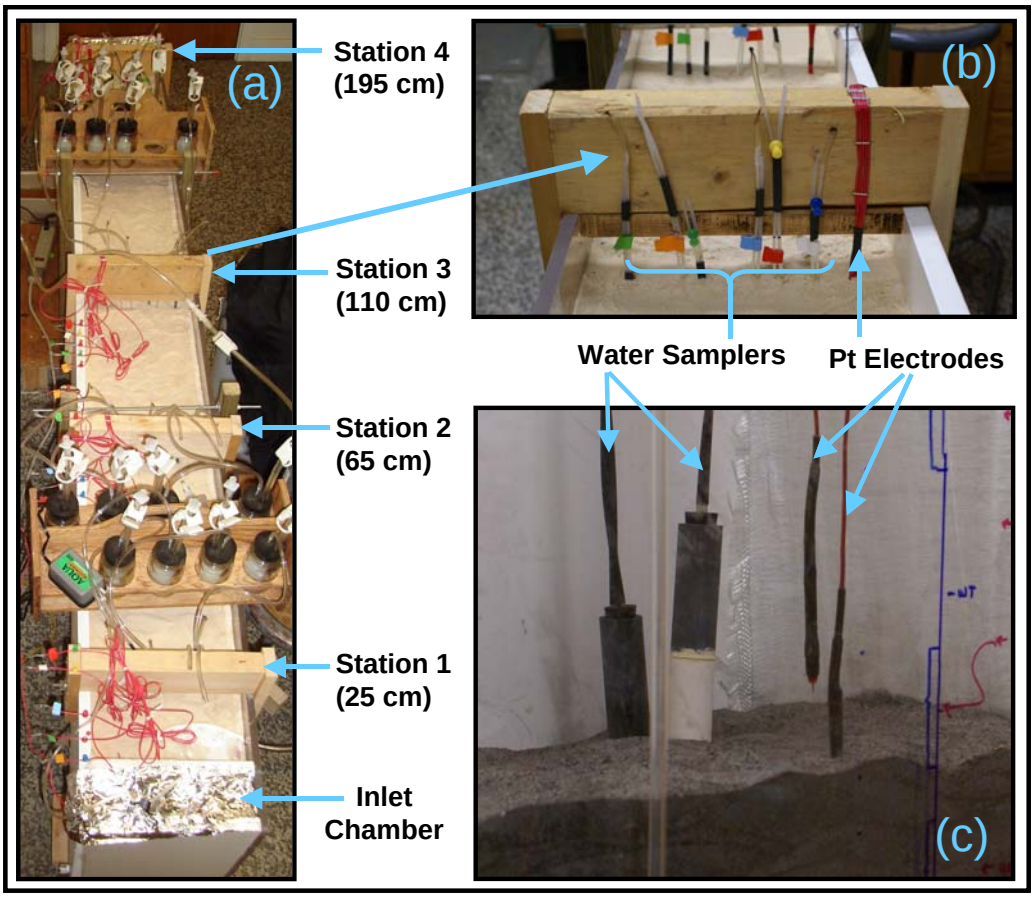

Figure A2. Photographs showing the top-view of the large flow cell (a), a sampling station (b) and water (tension) samplers and Pt electrodes hanging from the sampling station as soil is being packed in the flow cell (c). Note: The top of the flow cell was later covered with aluminum foil.

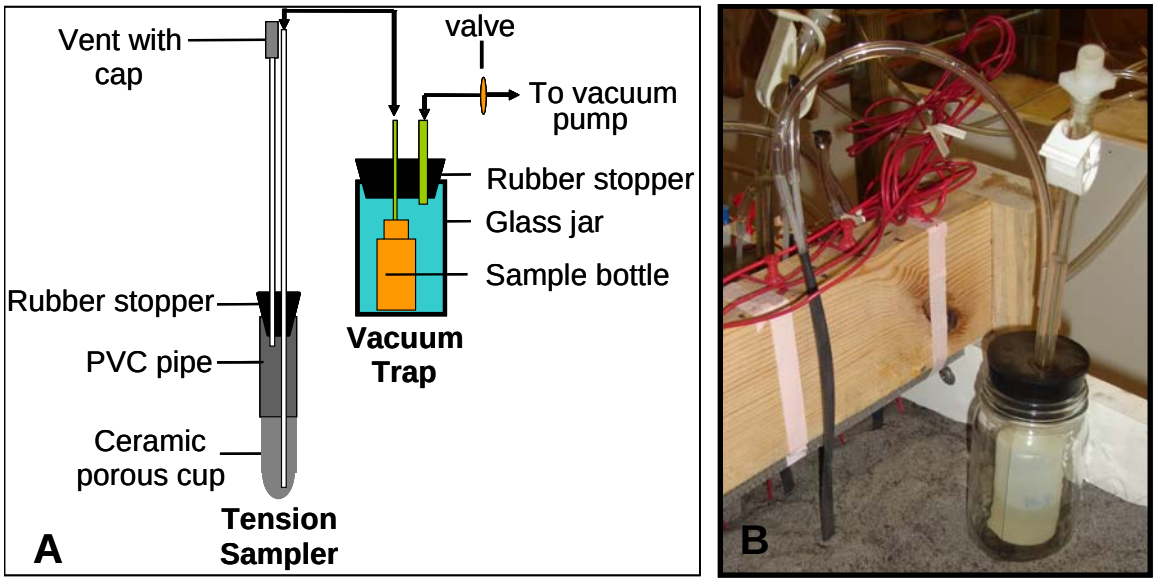

Figure A3. Diagram of the soil collection system (A) and photograph of the vacuum trap connected to a tension sampler.

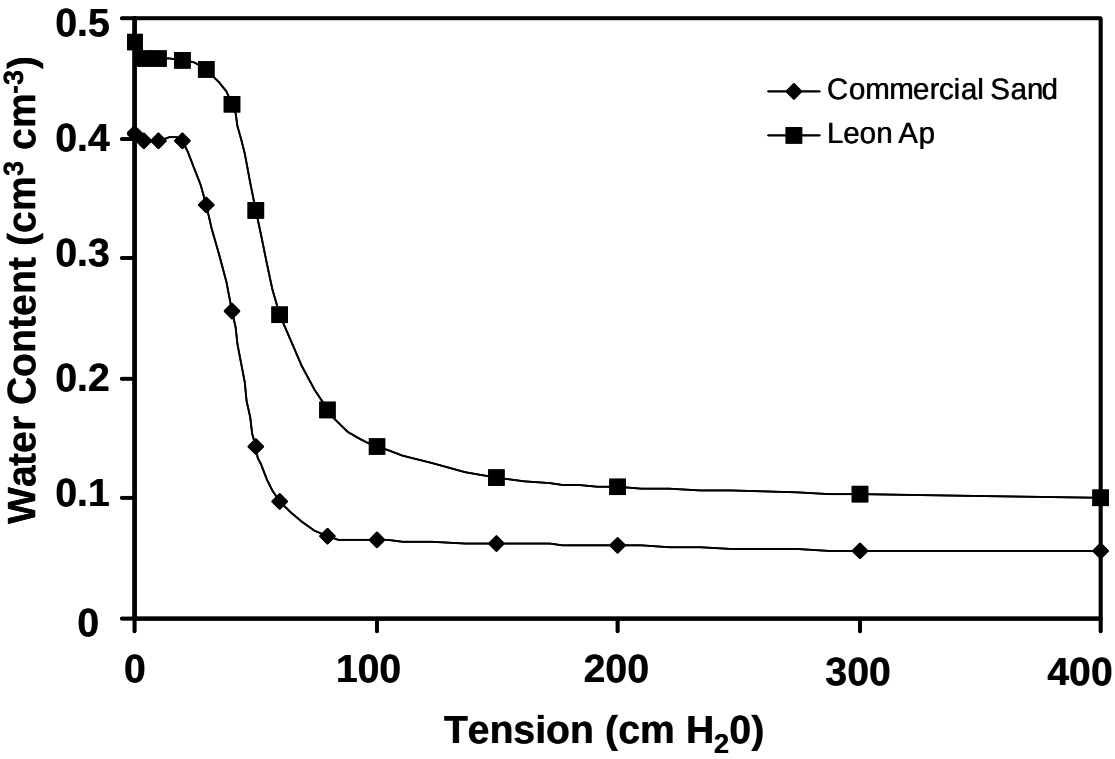

Figure A4. Moisture release curves of the soil materials used in the experiment.

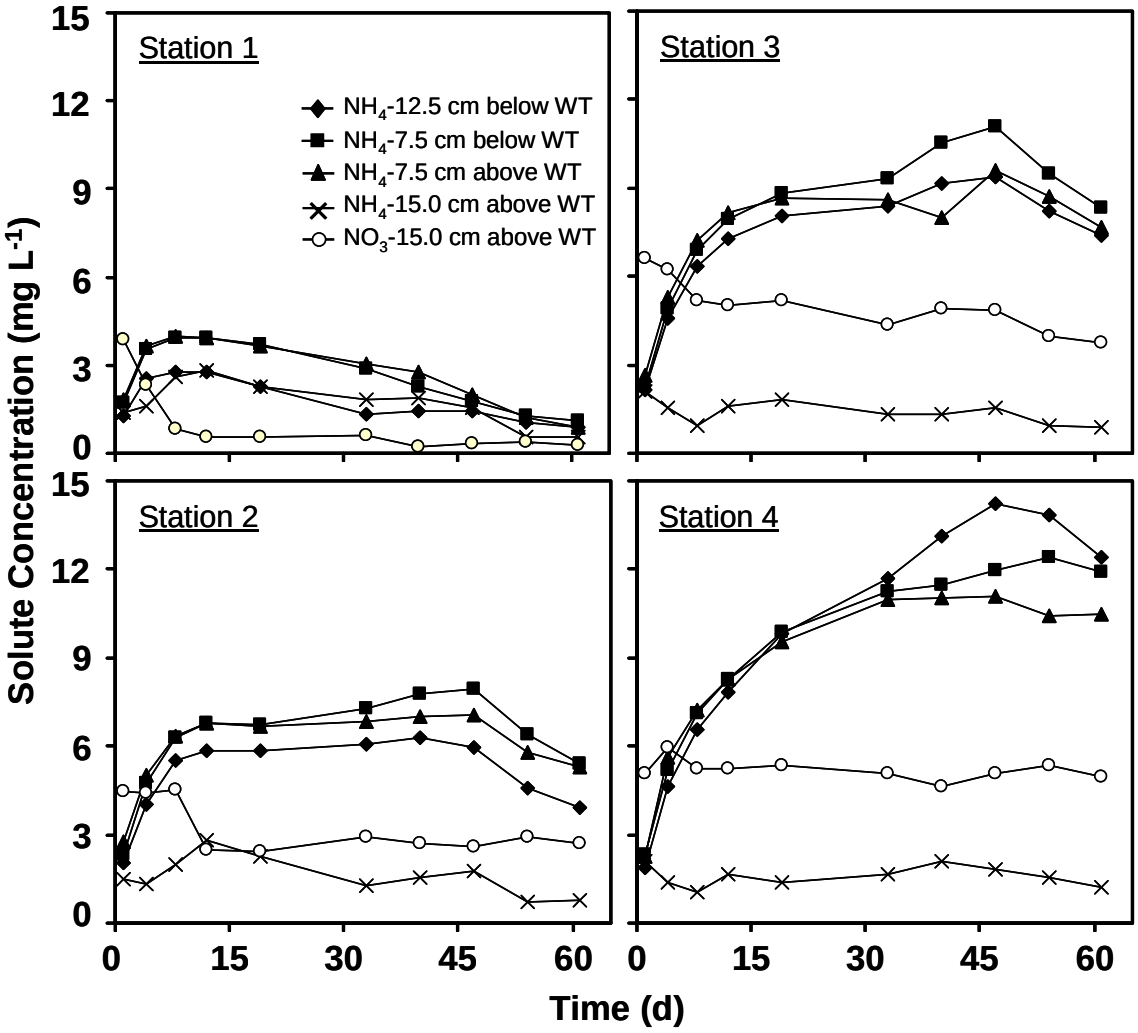

Figure A5. NO_3-N and NH_4-N concentrations, detected in the large flow cell packed with Leon soil applied with distilled water for 60 days. Note: No nitrate was detected at monitoring locations deeper than 15 cm above the WT.

CHAPTER 4

Fate and Horizontal Transport of Surface-Applied Nitrate in the Capillary Fringe above a Shallow Ground Water

Abstract

Substantial horizontal solute transport has been demonstrated to occur in the capillary fringe (CF) above a flowing ground water. This underscores the importance of evaluating fates of contaminants in the CF. This study was conducted to evaluate the fate and horizontal transport of surface-applied nitrate (NO_3^-) in the CF under various simulated hydrologic conditions. Two soils of different organic carbon content were packed in separate 240-cm long, 60-cm high and 25-cm thick flow cells. A simulated water table (WT) was established at 20 cm above the bottom of each flow cell and different pore-water velocities across the flow cell were simulated while a solution of NO_3^- and bromide (Br^-) was continuously applied at a small area on the surface of the soil in the flow cell. Soil solution samples were collected from different depths below and above the simulated WT at different locations along the flow path of the applied NO_3^- and Br^-. Subsurface horizontal transport of surface-applied NO_3^- tended to occur exclusively in the CF as the pore-water velocity was increased. In the flow cell with soil having very limited organic carbon (<0.3 g kg^{-1}), normalized concentration of NO_3-N and Br^- remained very comparable at all monitoring locations above and below the WT. Nitrate loss via denitrification in this case was not observed as conditions were oxidizing. In flow cells with soils having organic carbon content of 35 g kg^{-1}, some Br^- was detected below the water WT while NO_3^- was essentially absent. Conditions below the

WT favored NO_3^- loss via denitrification as reflected by very low reduction potentials. These results suggest that monitoring of subsurface fate and transport of surface-applied NO_3^- in locations with laterally moving shallow ground water should include efforts to collect samples from the CF for monitoring purposes.

1. Introduction

Nitrate (NO_3^-) in contaminated water resources could come from anthropogenic sources such as fertilizer application (Harter et al., 2002), septic systems (Anderson et al., 2002), surface-applied wastewater (Reddy and Dunn, 1984), and concentrated animal feeding operations (Hallberg and Keeney, 1993). Such sources are expected to continue to expand in scale with increasing demand for food as well as housing development. If not managed properly, these sources will continue to contribute to NO_3^- contamination in ground water (Nolan and Stoner, 2000) and surface water bodies (USEPA, 2004).

Monitoring of subsurface NO_3^- contamination is traditionally conducted by collecting ground water samples using monitoring wells or piezometers. Ground water sampling is used to monitor NO_3^- levels around agricultural fields (Jacobs and Gilliam, 1985), near septic system drain fields (Walker et al., 1973) and concentrated animal feeding operations (Kampbell et al., 2003), and abandoned military facilities (LeBlanc, 1984). The extent of NO_3^- transport is usually monitored by installing wells and/or piezometers at various locations in the landscape down-gradient from the source. Downward leaching of NO_3^- in the vadose zone, on the other hand, is monitored by collecting solution samples using porous cup samplers (also known as tension lysimeters) installed at various depths in the vadose zone (Andraski et al., 2000; Gehl et al., 2005; Ridley et al., 2001).

Nitrate is readily transported in the soil because it is soluble and not prone to ion exchange (Macko and Ostrom, 1994**).** In reduced zones in the subsurface, however, NO_3^- can be denitrified and converted to gaseous species. Denitrification is accomplished both by

heterotrophic and autotrophic bacteria that are capable of reducing NO_3^- to N_2 via the intermediates NO_2^-, NO, and/or N_2O (Tiedje, 1988). It generally requires anoxic conditions (Cheneby et al., 1999) and the presence of sufficient assimilable organic substrates as electron donors (Clough et al., 1999, Dodla et al., 2008). The reaction rate is largely determined by the concentration of NO_3^- as the electron acceptor (Elliot and de Jong, 1993; Strong and Fillery, 2002) and the density of denitrifying bacteria (Clough et al., 1999).

In the unsaturated zone, where there is a direct connection of the soil gaseous phase to atmospheric oxygen, NO_3^- could remain in its mobile anionic form. Recent results from studies conducted in arid and semiarid regions indicate that NO_3^- moves conservatively (limited transformation/loss) through the deep unsaturated zone (Walvoord et al., 2003; McMahon et al., 2006). The limited NO_3^- loss in deep unsaturated zones was partly attributed to the very low concentration of dissolved organic carbon and hence reduced microbial activity.

In a field study conducted in an area with a thin vadose zone (shallow water table) and at least 4% soil organic matter, a solution of NO_3^- and Br^- was applied to the unsaturated zone at approximately 20 cm above the water table (WT). Over a course of 83 days, both NO_3^- and Br^- were found to persist in the capillary fringe (CF), the region in the vadose zone with a relatively high degree of saturation, as ground water moved at a rate of approximately 4 cm d^{-1} (Abit et al., 2008a, b). In contrast, NO_3^- was found to be essentially absent at locations below the WT where Br^- was detected over the same distance. Results of Abit et al. (2008a) suggest that even in the presence of sufficient organic carbon for microbial

respiration at zones relatively closer to the surface, the biochemistry in the CF may still favor the persistence of NO_3^- while the underlying ground water may become sufficiently anoxic to promote denitrification.

Results from two-dimensional visual evaluation of miscible solute transport reveal that while surface-applied solutes (e.g., dye) are generally transported vertically in the vadose zone, they could be transported horizontally when they reach the CF on top of horizontally-moving ground water (Amoozegar et al., 2006, Silliman, et al., 2002). In fact, the simulations reveal that up to 100% of the surface-applied solutes can be transported horizontally in the CF without having to reach the WT.

Previous studies have shown that surface-applied solutes can be transported horizontally in the CF and suggested that conditions in the CF may favor NO_3^- persistence. However, a study has yet to be conducted to evaluate the aeration status of the CF and its subsequent effect on the persistence and transport of NO_3^- in the subsurface. This study tested the hypothesis that NO_3^- could be transported horizontally to a farther horizontal distance in the CF than it would below a shallow WT. Also of interest in this study are possible changes in the degree by which horizontal transport of NO_3^- applied to the soil surface becomes limited to the CF due to variations in subsurface hydrology. The specific objective of this study was to evaluate the fate and transport of NO_3^- in the CF under various simulated ground-water hydrology.

2. Materials and Methods

2.1. Experimental Set-up, Soil and Instrumentation

Two 240-cm long by 60-cm high and 25-cm thick flow cells (Fig. 1) were utilized in the experiment. The front of each flow cell was made of 1.25-cm thick transparent polycarbonate sheet while the sides and back were constructed using 1.9-cm thick flat polyvinyl chloride (PVC) sheets. The flow cell was divided into three chambers: two end chambers and a middle chamber. The width of each end chamber was 10 cm and they were separated from the middle chamber by perforated walls (see Figure A1 in Appendix). The middle chamber was 220-cm long and it was packed with soil material. End chambers did not contain soil. Four adapters (hereafter referred to as bottom inlets) were installed at the bottom of each flow cell for water application and drainage

Two soils were used in the experiment. One was commercially-available medium sand (hereafter called "sand") and the other was collected from the surface horizon of the sand rim of Juniper Bay – a wetland restoration site at Robeson County, NC ($34^{o}30'30"$N $79^{o}01'30"$E), classified under the Leon Series (Aeric Alaquod, hereafter referred to as "Leon soil material"). Soil materials were air-dried and passed through a 2-mm sieve.

Packing was done by adding previously sieved (2-mm mesh) air-dried soil in the flow cell and tamping uniformly with a flat-ended piece of wooden dowel. To minimize layering, the surface of the tamped soil was stirred before more air-dried soil was added on top of it. Packing was done at approximately 5 cm-thick sections at a time. Once packed to within 5 cm from the top, the flow cell was covered with aluminum foil (with a few pinholes) to

discourage evaporative losses that may encourage upward flux of water in the flow cell. Porous cup soil solution samplers (2.5 cm in diameter; 1 atm air-entry pressure) and platinum-tipped redox electrodes (Pt electrodes – constructed according to Wafer et al., 2004) were installed in the flow cell as the packing of the soil progressed.

Four sampling stations were installed in each flow cell and designated as stations 1, 2, 3 and 4 at locations that were 25 cm, 65 cm, 110 cm and 195 cm from the inlet chamber, respectively (Fig. 1, see photograph in Appendix Fig. A2a). Each sampling station had four tension samplers (see Fig. A3A in the Appendix for a diagram of the samplers) installed with their cups at 7.5, 12.5, 27.5, and 35 cm from the bottom of the flow cell. As will be discussed later, these depths corresponded to 12.5 and 7.5 cm below the WT and 7.5 and 15 cm above the WT, respectively. At each sampling station, a Pt Electrode was installed at the same depth as the porous cup of the tension sampler (see Fig. A2b and A2c in the Appendix).

Soil materials were air-dried and passed through a 2-mm mesh sieve. Texture of each soil material was determined by the hydrometer method (Gee and Or, 2002). Saturated hydraulic conductivity (K_{sat}) of soil materials packed uniformly in cylindrical cores (7.6 cm diameter and length) was measured by the constant head procedure (Amoozegar and Wilson, 1999). Soil water retention of the intact cores used in K_{sat} measurements was determined between 0 and 400 cm pressure by the pressure cell procedure (Dane and Hopmans, 2002). Soil pH was measured using a 1:1 soil-to-water suspension (weight basis) while total organic carbon and total nitrogen were determined by dry combustion with a Perkin-Elmer PE2400 CHN Elemental Analyzer (Culmo, 1988).

2.2 Experimental Simulations

A plastic manifold was connected to the inlet and outlet chambers and the bottom inlets of each flow cell (see Fig. 1). Distilled water was introduced into each flow cell from the bottom and sides by connecting a 25-L Marriotte bottle reservoir to the manifold. The tip of the air-entry tube in the reservoir and the end of the drainage tube connected to the outlet were set at an elevation that corresponded to 20 cm above the bottom of the flow cell. This arrangement allowed the establishment of a simulated WT inside the flow cells at 20 cm above the bottom of the flow cell. When the water level in the inlet and outlet chambers and in the piezometers for each cell indicated that a flat WT was established, a gel-filled Calomel reference electrode (Fisher Scientific, Pittsburgh, PA; ID No. 13-620-258) was installed in their respective inlet chamber (tip of the electrode was submerged in water in the inlet chamber). Initial reduction potential (Eh) readings were taken and 30 mL background water samples were collected from all tension samplers as well as the inlet and outlet chambers.

A volt-meter (called multi-meter, Radioshack, Fort Worth, TX -- accurate to 0.001V) was used to measure voltage between the Pt and reference electrodes. The multi-meter readings were added to 0.25 V (or 250 mV) to convert them into Eh values.

To collect samples, each tension sampler was connected to a designated vacuum trap (similar to system of Hendrickx et al., 2002) (Appendix Fig. 3). Each sampler (with vent open) was initially purged by evacuating air from the dedicated vacuum trap using a pump. After purging, the vent of the tension sampler was closed and a 60-mL sample bottle was placed inside the vacuum trap (see Fig. A3B in the Appendix for a photograph of trap with

sample bottle). The vacuum trap was then re-connected to the pump to apply a tension of 400 cm. This allowed extraction of soil solution from the surroundings of the cup that were delivered to the sample bottle inside the vacuum trap. Thirty mL of sample were collected using each tension sampler for each sampling. Locations in the flow cell where Eh and solution samples were collected are hereafter referred to as “monitoring locations”.

Samples from the inlet and outlet chambers were also collected using a dedicated plastic syringe with its tip connected to the plastic tubing that extended 10 cm below the water level inside each of the inlet and outlet chambers. Thirty mL of outlet and inlet samples were collected every time soil solution samples were collected using the tension samplers. All samples were frozen prior to analysis for solution pH as well as NO_3-N, Br^-, and dissolved organic carbon (DOC) concentrations. Nitrate-N and Br^- were analyzed using a Lachat Quickechem 8000 slow injection auto analyzer and DOC was analyzed using the Total Organic Carbon Auto-analyzer (Shimadzu Corp., Columbia, MD) (Greenberg et al., 1992).

After collection of the background samples, the WT was allowed to recover to the 20 cm level and the manifold supplying distilled water was disconnected from each flow cell by clamping all the associated tubings attached to the manifold (including the one connected to the reservoir and those connected to the inlet and outlet chambers (see Fig. 1). The outflow end of the tubing connected to the outlet chamber was maintained at 20 cm above the bottom of the respective flow cell. Distilled water was then applied to the inlet chamber using a variable speed peristaltic pump at rates and durations outlined in Table 1.

As soon as distilled water was pumped into the inlet chamber, a solution containing 15 mg L^{-1} each of NO_3-N and Br^- was continuously applied at the surface application area of the sand-packed flow cell (see Fig. 1 for location of surface application spot) at a rate of 3.6 L d^{-1}. A solution containing 100 mg L^{-1} each of NO_3-N and Br^- was supplied to the application spot of the flow cell packed with Leon soil material. The solution containing both Br^- and NO_3^- was surface-applied using three tubes each supplying the solution at a rate of approximately 1.2 L d^{-1} (spread equally throughout the application area). The surface application area was covered with four layers of cheese cloth prior to application of the Br^- and NO_3^- solution to protect the soil surface and encourage even infiltration of the applied solution throughout the enclosed application area. The flow cell was then covered with aluminum foil with a few pinholes to discourage surface evaporation and hence minimizing upward flux of water in the flow cell but still allow air to come in and aerate the vadose zone. To minimize the impact of light on biochemical activity, the front side transparent side was covered with black fabric for the duration of the study.

A particular application rate of distilled water at the inlet chamber was run until at least a roughly stable condition was achieved. Conditions were considered stable when Br^- concentration at the outlet chamber reflected the expected final concentrations for a particular condition. For example, in the simulation where the rate of NO_3^- and Br^- solution application to the surface (3.6 L d^{-1}) was almost equal to the rate (3.5 L d^{-1}) of distilled water supplied to the inlet chamber (total of distilled water and inlet solution applied equal to 7.1 L d^{-1}), stable

condition was considered to be achieved when the Br^- concentration at the outlet was approximately 50% of the concentration of the surface-applied solution.

Reduction potential measurements and 30 mL of soil solution samples were collected from all monitoring points and from the inlet and outlet chambers at least every 4 days. Threshold reduction potential used in deciding whether conditions would favor extensive nitrate loss via denitrification was 250 mV (Patrick and Jugsujinda, 1992). Nitrate loss through denitrification is favored below the threshold, but NO_3^- is expected to persist above it. After the experiment, the flow cells were drained and three sets of intact core samples from the 4 to 12 cm, 23 to 31 cm and 40 to 48 cm depth intervals were collected for bulk density determination using the core method (Grossman and Reinsch, 2002).

2.3. Pore-Water Velocities

Using various rates of water application to the inlet chamber and the constant rate of surface-application of the NO_3^- and Br^- solution, the resulting average pore-water velocities (V_{ave}) in the experiment were computed using the formula:

$$V_{ave} = \text{Flux/Water Filled Porosity},$$

where Flux is the Darcian velocity, which is the total application rate divided by the cross sectional area of the flow. For this study, the total application rate was the rate of distilled water application through the inlet chamber plus the rate of application of the solution to the surface. The cross sectional area of the flow included both the saturated zone and the CF. For both soils the thickness of the saturated zone (below the WT) was 20 cm. The thickness of CF was taken to be 30 cm for Leon soil material and 20 cm for the sand, and water-filled

porosity was equal to 0.48 cm^3 cm^{-3} for Leon soil material and 0.41 cm^3 cm^{-3} for the sand material. Since the CF is nearly saturated, the water filled porosity was taken to be the same as the total porosity for each soil.

The CF was included in the computation of the cross-sectional area through which the applied water passes through because horizontal water flow occurs both in the saturated zone and the CF above it. A summary of the average pore-water velocities that were simulated in the experiment are outlined in Table 1.

3.0 Results and Discussion

3.1. Soil and Solution Properties

Properties of the two soils used in the experiment are summarized in Tables A1 and A2 of the Appendix. Saturated hydraulic conductivities of both soil materials were 6.6 m d^{-1} for the medium sand and 3.0 m d^{-1} for the loamy sand-textured Leon soil. The Leon soil material had considerably more organic carbon than the medium sand (35.4 g kg^{-1} vs. 0.3 g kg^{-1}, respectively). Bulk density of the soil packed in each flow cell slightly increased with depth. The average bulk density for sand was 1.55 g cm^{-3} while the average bulk density for the Leon soil material was 1.34 g cm^{-3}

The moisture release curve for the Leon soil material (Fig. 2) revealed that its water content remained very close to saturation despite application of 30 cm of pressure. This suggested that the CF above the simulated WT in the Leon soil-packed flow cell was at least 30 cm thick. The medium sand on the other hand was already drained significantly at pressures greater than 20 cm suggesting that the flow cells with this material had a CF that was approximately 20 cm thick. The thickness of the CF indicated that the monitoring points above the WT in the flow cells were within the CF for both soils.

Soil solution collected from the sand-packed flow cell had a mean pH of 6.5 and a DOC concentration of 1.46 mg L^{-1}. Mean DOC was higher (108 mg L^{-1}) and pH was observed to be lower (5.6) in solution samples collected from the flow cell with Leon soil. Additional descriptive statistics of soil solution properties are outlined in Table A3 of the Appendix.

3.2. Nitrate, Bromide and Reduction Potential

Only the data from the final day of a particular pore-water velocity run will be presented. We have selected the final day because, with only one exception, the conditions had stabilized such that the reduction potential as well as distributions of NO_3-N and Br^- concentrations were good representatives of the results for each simulated condition.

3.2.a. Medium Sand-Packed Flow Cell

The area traveled by the plume was estimated using monitoring points where Br^- was detected. The surface-applied solutes were largely transported above the WT when the simulated ground water was flowing horizontally at a pore-water velocity of approximately 30 cm d^{-1} (Fig. 3). At this relatively high ground water flow rate, the solutes were detected only in small amounts at 7.5 cm below the WT. Also, note that the conditions both above and below the WT were generally oxic as shown by the Eh values that were generally above the 250 mV denitrification threshold. The very low DOC content (mean DOC = 1.46 mg L^{-1}) in solution may have prohibited the development of reducing conditions for this flow rate. Under these oxidized conditions, surface-applied NO_3^- and Br^- were detected at practically the same normalized concentrations suggesting the absence of NO_3^- loss.

Decreasing the simulated horizontal ground water pore-water velocity to approximately 17 cm d^{-1} had little impact on the reduction potentials as conditions at the monitoring locations remained generally oxic (Fig. 4). Normalized concentrations of NO_3^- and Br^- in the CF and below the WT remained comparable suggesting very minimal to no NO_3^- loss. It should be noted that the normalized concentrations of both solutes at 7.5 cm

below the WT were significantly higher than those under a pore-water velocity of 30 cm d^{-1}. This indicates that at a lower horizontal ground-water velocity, surface-applied solutes have a higher tendency of entering the saturated zone, but their distribution may remain near the WT due to very low to no vertical water movement within the aquifer.

Subsurface horizontal transport of surface-applied solutes was observed to occur only in the CF when the horizontal pore-water velocity was increased to around 43 cm d^{-1} (Fig. 5). As in previous runs, conditions in the CF zone were generally oxidizing with comparable normalized concentrations of NO_3-N and Br^-.

3.2.b. Leon Soil-Packed Flow Cell

Except for the monitoring locations that were 15 cm above the WT, reduction potentials were generally below the 250 mV denitrification threshold suggesting that the saturated zone and part of the CF of the flow cell packed with Leon soil material had reducing conditions (Figs. 6, 7, and 8). Mean solution DOC concentration in the Leon soil-packed flow cell was 108 mg L^{-1}. This higher DOC concentration was apparently enhancing the microbial activity that created reducing conditions.

Under simulated ground-water pore-water velocity of approximately 17 cm d^{-1}, NO_3^- and Br^- were only detected at 7.5 and 15 cm above the WT (Fig. 6), indicating that the solutes moving vertically through the unsaturated zone were stopped within the CF. While normalized concentrations of NO_3-N and Br^- were practically the same at 15 cm above the WT, normalized concentrations of NO_3-N were lower relative to Br^- at 7.5 cm above the WT.

This suggests that NO_3^- loss was favored under reducing conditions near the WT (at 7.5 cm above the WT) within the vadose zone.

Decreasing the pore-water velocity to approximately 12 cm d^{-1} allowed the applied solution to move below the WT (Fig. 7) as shown by the detection of Br^- at 7.5 cm below the WT. However, while Br^- was detected both above and below the WT, NO_3^- was only detected in the vadose zone, with no loss at 15 cm above the WT. At 15 cm above the WT, normalized concentrations of NO_3-N and Br^- were similar under oxidizing conditions (Eh > 250 mV). In contrast, at 7.5 cm above the WT, reducing conditions prevailed and the amount of NO_3^- loss increased with distance along the flow path within the CF with little NO_3^- detected at station 4. No NO_3^- was detected below the WT suggesting that it was transformed/lost under reducing conditions below the WT (where the Eh was < 250 mV).

As in the medium-sand packed flow cell, increasing the pore-water velocity tended to confine horizontal NO_3^- transport only to the CF in the flow cell packed with Leon soil (Fig. 8). The normalized concentrations of both NO_3-N and Br^- at 15 cm above the WT at stations 2, 3 and 4 were 0.7, 0.91 and 1.0, respectively, suggesting the absence of NO_3^- loss within the upper part of the CF. At 7.5 cm above the WT, however, normalized NO_3^- concentrations (compared to Br^- concentrations) decreased significantly at station 3 and little NO_3^- was detected at station 4. It should be noted that the normalized concentrations of both solutes at 15 cm above the WT at station 2 (only 0.7) and at station 3 (0.91) for 29 cm d^{-1} pore-water velocity were lower than their corresponding values for the lower velocities reported earlier. This is most likely due to mixing of fresh water coming from the side with the vertically

moving soil solution containing the two solutes in the unsaturated zone. No Br^- or NO_3^- was detected at 7.5 cm above the WT at station 2 indicating that the bottom of the plume remained well above the WT. Data in Figure 8 are not representative of stable conditions (as described in Section 2.2), and they are from the last set of samples taken before the pump malfunctioned. Despite the premature termination of the experiment, the data in Figure 8 still show the effect of high pore-water velocity on the extent by which NO_3^- was transported in the CF.

Increasing the rate of water application to the inlet chamber reduced the fraction that the surface-applied NO_3^- and Br^- solution contributed to the total amount of water that moved across the flow cell (see Table 1). This means that the surface-applied solution would tend to flow across a smaller fraction of the cross-section of the flow path in the flow cell. Because the solution was surface-applied, its horizontal flow would tend to be isolated in the upper part of the flow path (i.e., top of the CF).

The thickness of the flow path in the sand-packed flow cell was 40 cm (20 cm CF + 20 cm simulated ground water below the WT). When water was applied at the inlet chamber at 3.5 L d^{-1}, the surface-applied solution (applied at 3.6 L d^{-1}) contributed 51% of all the water flowing across the flow cell (Table 1). This translates to around 20.4 cm out of the 40 cm-thick flow path which means that the surface-applied solution would occupy all of the 20-cm CF and even some areas below the WT – which was the case observed in Figure 4. Increasing the rate of water application at the inlet chamber to 14 L d^{-1} reduced the contribution of the surface-applied solution to only 20 % of the total amount of water flowing

across the flow cell. This means that the horizontal transport of the surface-applied NO_3^- and Br^- solution would tend to be isolated to the upper portion of the flow path – or exclusively in the CF as was the case shown in Figure 5.

4. Summary and Conclusions

The objective of this study was to evaluate the fate and transport of nitrate (NO_3^-) entering the capillary fringe (CF) from surface sources under conditions of various simulated ground water flow rates. Subsurface flow rates influenced the location where NO_3^- can be transported as well as its persistence while in transport in the subsurface. Increasing horizontal pore-water velocity increased the tendency for a surface applied NO_3^--containing solution to flow exclusively in the CF. Reduction potential at the upper regions of the CF indicated oxidizing conditions. This resulted in very minimal to practically no NO_3^- loss as it was transported horizontally in the upper regions in CF. There were cases where Br^- was detected below the WT while NO_3^- was absent. This was because conditions below the WT favored NO_3^- loss through denitrification as reflected by the very low reduction potential. As expected, in the absence of sufficient organic carbon, no denitrification was observed above or below the water table. These results showed that oxidizing conditions at the upper portions of CF allow NO_3^- to be transported to greater distances than it would below the WT.

5. References Cited

Abit, S.M., A. Amoozegar, M. J. Vepraskas, and C.P. Niewoehner. 2002a. Fate of nitrate in the capillary fringe and shallow ground water in a drained sandy soil. Geoderma. 146:209-215.

Abit, S. M., A. Amoozegar, M. J. Vepraskas, and C. P. Niewoehner. 2008b. Solute transport in the capillary fringe and shallow groundwater: Field evaluation. Vadose Zone J. 7:890-898.

Amoozegar, A., C.P. Niewoehner, and D.L. Lindbo. 2006. Lateral movement of water in the capillary fringe under drainfields. In Proc. 2006 Tech. Educ. Conf., Denver Co. 27-31 Aug. 2006. Natl. Onsite Wastewater Recycling Assoc. Santa Cruz, CA.

Amoozegar, A., and G. V. Wilson. 1999. Methods for measuring hydraulic conductivity and drainable porosity. In: R.W. Skaggs and J. van Schilfgaarde (eds). Agricultural Drainage. Agronomy Monograph No. 38. Soil Sci. Soc. Am, Madison, Wisconsin.

Anderson, D.M., P.M. Glibert, and J.M. Burkholder. 2002. Harmful algal blooms and eutrophication nutrient sources, composition, and consequences. Estuaries and Coasts. 25(4b):704-726.

Andraski, T. W., L. G. Bundy, and K. R. Brye. 2000. Crop management and corn nitrogen rate effects on nitrate leaching. J. Environ. Qual. 29:1095-1103.

Cheneby, D., A. Hartmann, C. Henault, E. Topp, and J.C. Germon. 1999. Diversity of denitrifying microflora and ability to reduce N_2O in two soils. Biol. Fertil. Soils. 28:16-26.

Clough, T.J., S.C. Jarvis, E.R. Dixon, R.J. Stevens, R.J. Laughlin, and D.J. Hatch. 1999. Carbon induced subsoil denitrification of ^{15}N-labelled nitrate in 1 m deep soil columns. Soil Biol. Biochem. 31:31-41.

Culmo, F.C. 1988. Principle of Operation – The Perkin-Elmer PE2400 CHN Elemental Analyzer. Perkin Elmer Corp., Norwalk, CT.

Dane, J. H., and J. W. Hopmans. 2002. Water retention and storage. In: J. H. Dane, and G. C. Topp (eds). Methods of Soil Analysis Part 4: Physical Methods. No. 5 in Soil Sci. Soc. Am. Book Series. Soil Sci. Soc. Am., Madison, WI.

Dodla, S.K., J.J. Wang, R.D. Delaune, and R.L. Cook. 2008. Denitrification potential and its relation to organic carbon quality in three coastal wetland soils. Sci. Total Environ. 407:471-480.

Elliot, J.A., and E. de Jong. 1993. Prediction of field denitrification rates: a boundary line approach. Soil Sci. Soc. Am. J. 57:82-87.

Gee, G. W., and D. Or. 2002. Particle-size analysis. In: J. H. Dane, and G. C. Topp (eds). Methods of Soil Analysis Part 4: Physical Methods. No. 5 in Soil Sci. Soc. Am. Book Series. Soil Sci. Soc. Am., Madison, WI.

Gehl, R. J., J. P. Schmidt, L. R. Stone, A. J. Schlegel, and G. A. Clark**.** 2005. In situ measurements of nitrate leaching implicate poor nitrogen and irrigation management on sandy soils. J. Environ. Qual. 34:2243-2254.

Greenberg, A. E., L. S. Clesceri, and A. D. Eaton. 1992. Standard Methods for Examination of Water and Wastewater. 18th Ed. American Public Health Association. Washington, DC.

Grossman, R. B., and T. G. Reinsch. 2002. Bulk density. In: J. H. Dane, and G. C. Topp (eds). Methods of Soil Analysis Part 4: Physical Methods. No. 5 in Soil Sci. Soc. Am. Book Series. Soil Sci. Soc. Am., Madison, WI.

Hallberg, G.R., and D.R. Keeney.1993. Nitrate. In: Alley. W. A. (ed). Regional Ground-water Quality. Van Nostrand Reinhold, New York, pp.297-322.

Harter, T., H. Davis, M.C. Mathews, and R.D. Meyer. 2002. Shallow ground water quality on dairy farms with irrigated forage crops. J. Contam. Hydrol. 55:287-315.

Hendrickx, J. M., J. M. Wraith, D. L. Corwin, and R. G. Kachanoski. 2002. Miscible solute transport. In: J. H. Dane, and G. C. Topp (eds). Methods of Soil Analysis Part 4: Physical Methods. No. 5 in Soil Sci. Soc. Am. Book Series. Soil Sci. Soc. Am., Madison, WI.

Jacobs, T.C., and J.W. Gilliam. 1985. Riparian losses of nitrate from agricultural drainage waters. J. Environ. Qual. 4:472-478.

Kampbell, D.H, Y. An, K. P. Jewell, and J.R. Masoner. 2003. Ground water quality surrounding Lake Texoma during short-term drought conditions. Environ. Pollut. 125(2):183-191.

LeBlanc, D. R. 1984. Sewage plume in a sand and gravel aquifer, Cape Cod, Massachusetts. USGS Water Supply Paper 2218.

Macko, S.A., and N.E. Ostrom. 1994. Molecular and pollution studies using stable isotopes. In: Lajtha, K., Michner, R. (Eds.), Stable Isotopes in Ecology and Environmental Science. Blackwell, Oxford, pp. 45–62.

McMahon, P.B., K.F. Dennehy, B.W. Bruce, J.K. Böhlke, R.L. Michel, J.J. Gurdak, and D.B. Hurlbut. 2006. Storage and transit time of chemicals in thick unsaturated zones under rangeland and irrigated cropland, High Plains, United States. Water Resour. Res. 42:W03413.

Nolan, B.T., and J.D. Stoner. 2000. Nutrients in ground waters of the conterminous United States, 1992–1995. Environ. Sci. Technol. 34:1156–1165.

Patrick, W. H. and A. Jugsujinda. 1992 .Sequential Reduction and Oxidation of Inorganic Nitrogen, Manganese, and Iron in Flooded Soil. Soil Sci. Soc. Am. J. 56:1071-1073.

Reddy, M. R., and S. J. Dunn. 1984. Effect of domestic effluents on ground-water quality: A case study. Sci. Total Environ. 40(1):115-124.

Ridley, A.M., R.E. White, K.A. Helyar, G.R. Morrison, L.K. Heng, and R. Fisher. 2001. Nitrate leaching Loss under annual and perennial pastures with an without lime on a duplex (texture contrast) soil in humid southeastern Australia. Euro J. Soil Sci. 52:237-252.

Silliman, S. E., B. Berkowitz, J. Simunek, and M. Th. Van Genuchten. 2002. Fluid flow and solute migration within the capillary fringe. Ground Water. 40(1):76-84.

Strong, D.T., and I.R.P. Fillery. 2002. Denitrification response to nitrate concentration in sandy soils. Soil Biol. and Biochem. 34:945-954.

Tiedge, J.M. 1988. Ecology of denitrification and disimilatory nitrate reduction to ammonium. In: Zehnder, A.J.B. (Ed). The Biology of Anaerobic Microorganisms. Wiley, NY.

USEPA. 2004. Monitoring and Assessing Water Quality. National Water Quality Inventory: Report to Congress, 2004 Reporting Cycle.
At: http://www.epa.gov/owow/305b/2004report/. Accessed: April 2009.

Wafer, C. C., J. B. Richards, and D. L. Osmond. 2004. Construction of platinum-tipped redox probes for determining soil redox potential. J. Environ. Qual. 33:2375-2379.

Walker**,** W. G., J. Bouma, D. R. Keeney, and P. G. Olcott. 1973**.** Nitrogen transformations during subsurface disposal of septic tank effluent in sands: II. Ground water quality. J. Environ. Qual. 2:521-525.

Walvoord, M.A., F.M. Phillips, D.A. Stonestrom, R.D. Evans, P.C. Hartsough, B.D. Newman, and R.G. Striegl. 2003. A reservoir of nitrate beneath desert soils. Science (Washington D.C.). 302:1021–1024.

6. Tables and Figures.

Table 1. Summary of simulations conducted using the flow cells packed with Leon soil and medium sand.

Soil	Duration of run (d)	Cumulative duration (d)	Application rate to inlet chamber ($cm^3\ d^{-1}$)	Total (inlet chamber + surface) application rate ($cm^3\ d^{-1}$)	Cross sectional area of flow path that included the CF at the middle of flow cell * (cm^3)	Estimated pore-water velocity ** (cm d^{-1})	Fraction of surface-applied solution out of the total water applied to the flow cell*** (%)
Leon	24	24	7,000	10,600	1,250	~ 17.3	34
	24	48	3,500	7,100	1,250	~ 11.6	51
	4	52	14,000	17,600	1,250	~ 28.7	20
Sand	14	14	7,000	10,600	1,000	~ 29.9	34
	14	28	3,500	7,100	1,000	~17.3	51
	9	37	14,000	17,600	1,000	~ 42.9	20

Note: Application rate at surface application area was 3,600 $cm^3\ d^{-1}$

* Cross Sectional Area = (CF thickness + groundwater thickness) × width of flow cell

Where: CF thickness = 20 cm in sand; 30 cm in Leon soil material

Thickness of simulated groundwater = 20 cm

Width of flow cell = 25 cm

** Computed as: (Total Application Rate ÷ Cross Sectional Area)/porosity

Where: porosity = 0.48 in Leon soil; 0.41 in sand.

*** Computed as: (3,600 $cm^3\ d^{-1}$ ÷ Total Application Rate) × 100

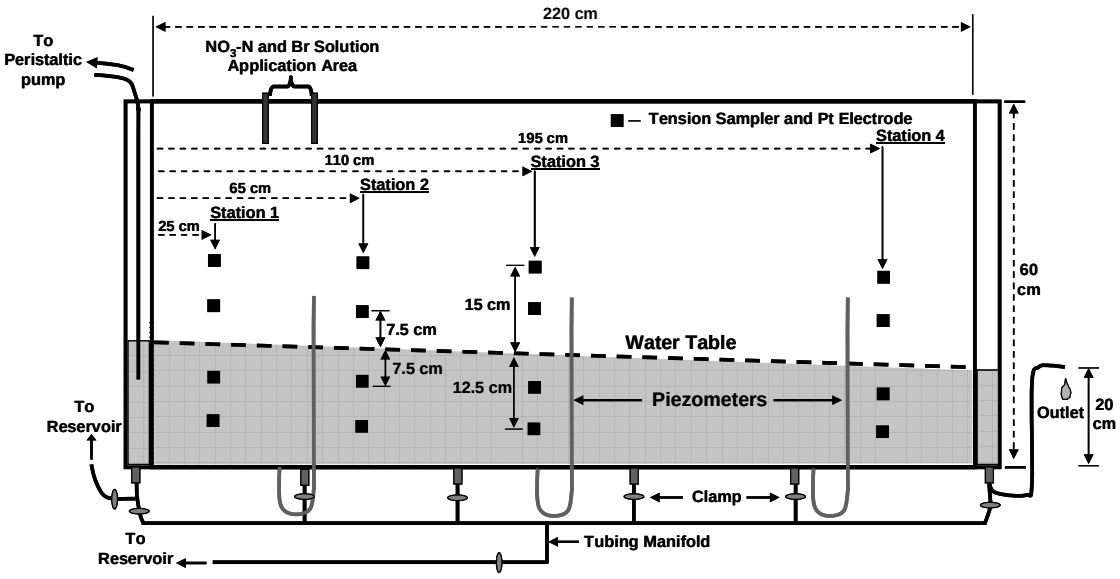

Figure 1. Two-dimensional schematic diagram of the flow cell used in the experiment. The flow cell was 25 cm wide.

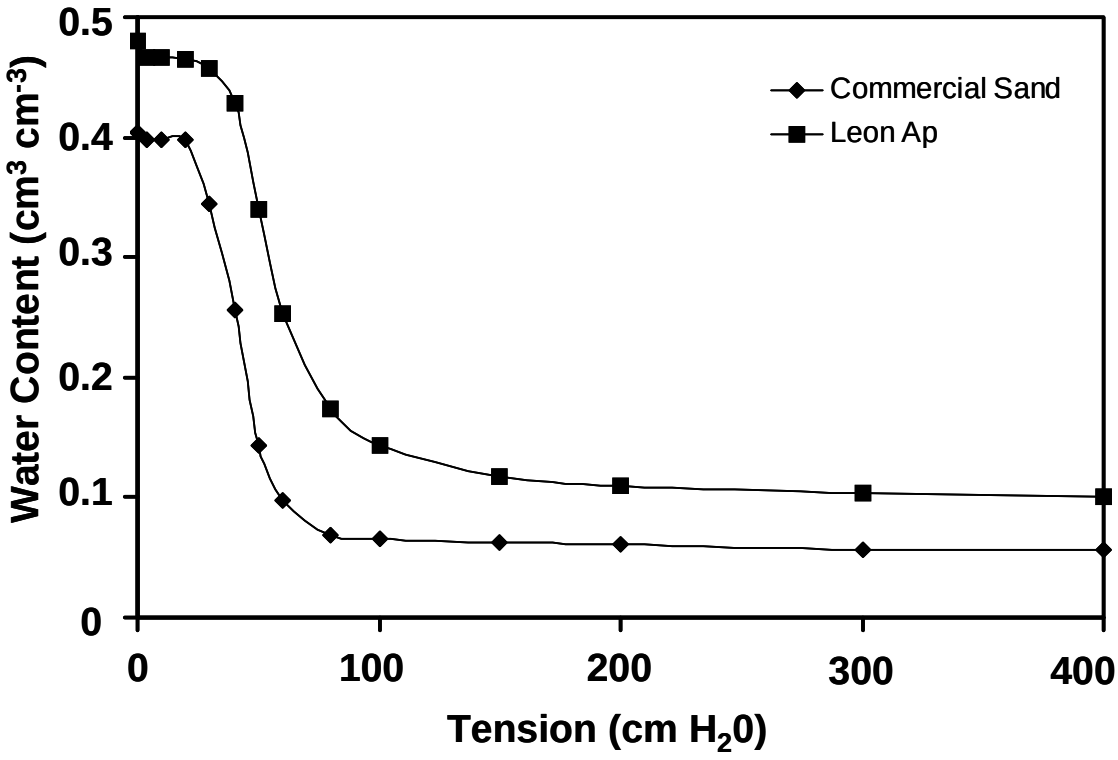

Figure 2. Soil water characteristic curves for the soils used in the experiments.

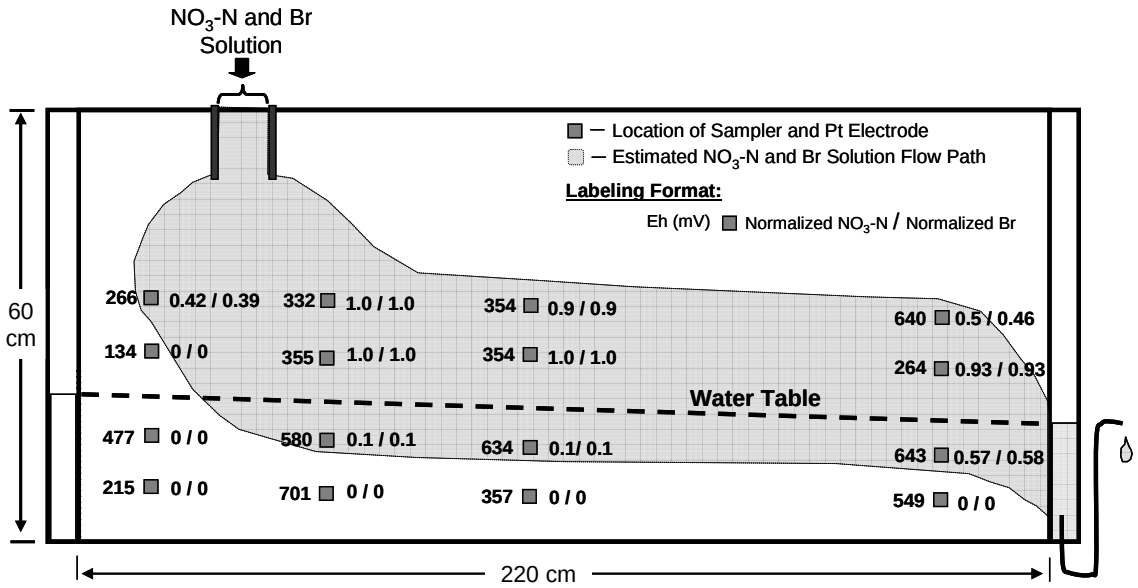

Figure 3. Schematic diagram showing final day reduction potential (Eh) and normalized NO_3-N and Br concentrations at various locations in the medium sand packed flow cell subjected to a horizontal pore-water velocity of ~30 cm d^{-1}. The rate of solute application at the surface was 3.6 L d^{-1} and Eh values above 250 mV indicate oxic conditions.

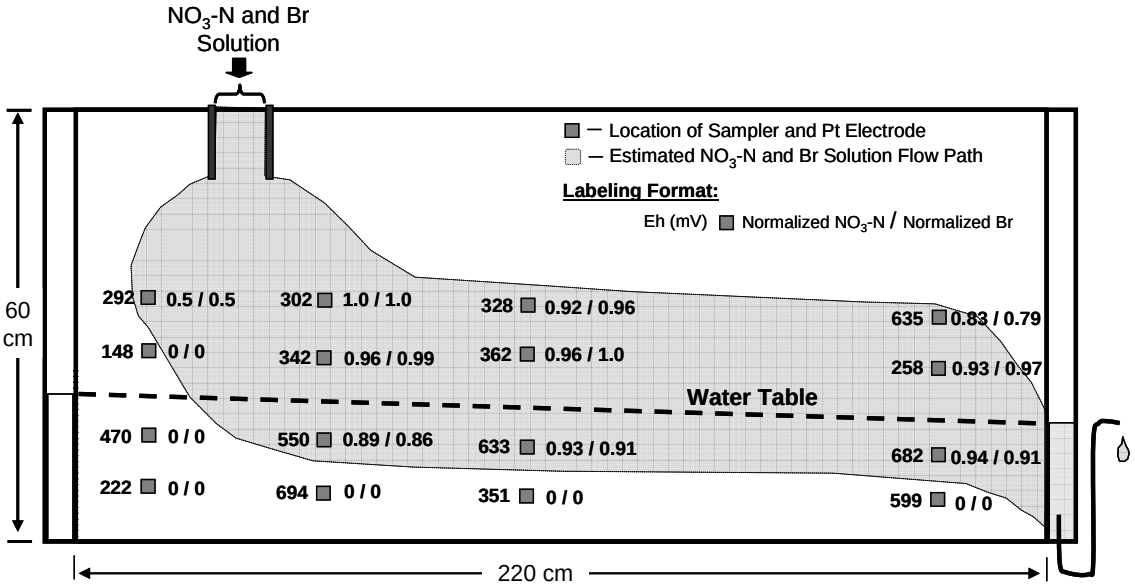

Figure 4. Schematic diagram showing final reduction potential (Eh) and normalized NO_3-N and Br concentrations at various locations in the medium sand packed flow cell subjected to a horizontal pore-water velocity of ~17 cm d^{-1}. The rate of solute application at the surface was 3.6 L d^{-1} and Eh values above 250 mV indicate oxic conditions.

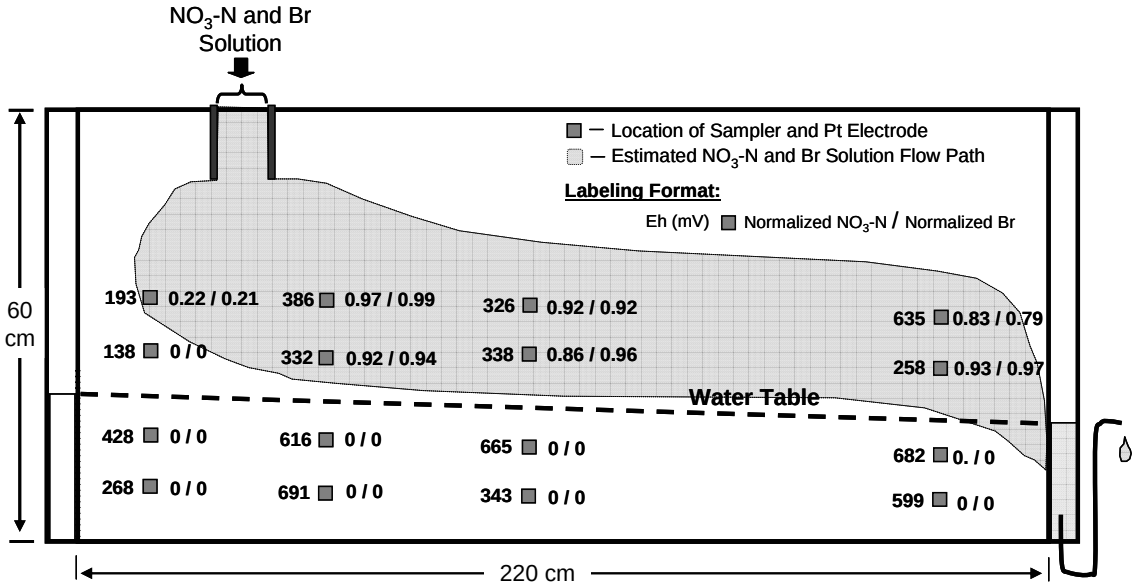

Figure 5. Schematic diagram showing reduction potential (Eh) and normalized NO_3-N and Br concentrations at various locations in the medium sand packed flow cell subjected to a horizontal pore-water velocity of ~43 cm d^{-1}. The rate of solute application at the surface was 3.6 L d^{-1} and Eh values above 250 mV indicate oxic conditions.

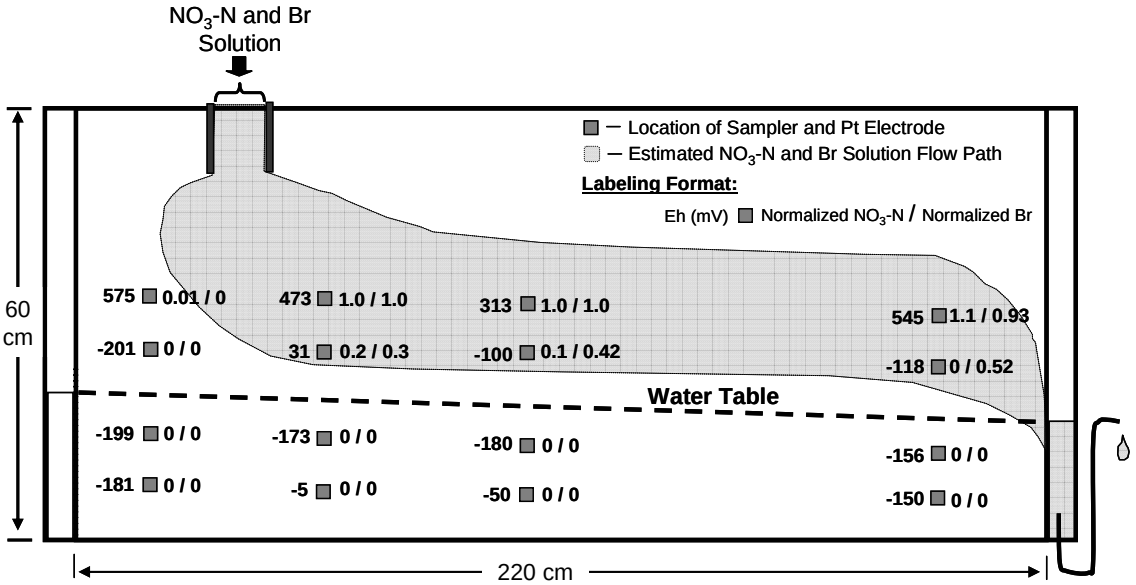

Figure 6. Schematic diagram showing final day reduction potential (Eh) and normalized NO_3-N and Br^- concentrations at various locations in the Leon soil-packed flow cell subjected to horizontal pore-water velocity of ~17 cm d^{-1}. The rate of application at the surface was 3.6 L d^{-1} and an Eh below 250 mV indicate that conditions are reduced enough to favor extensive denitrification.

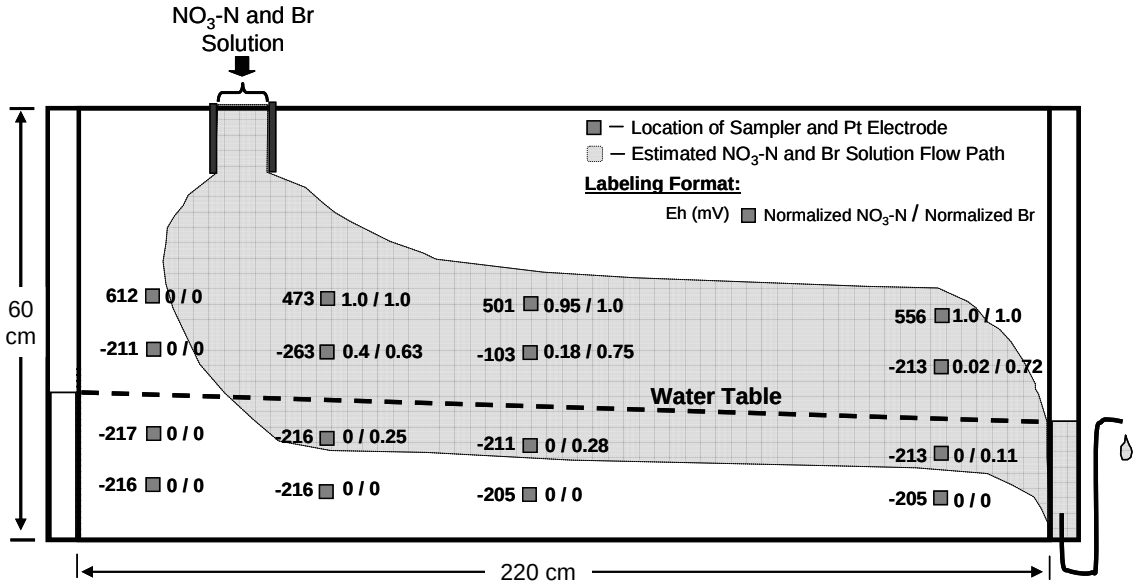

Figure 7. Schematic diagram showing final day reduction potential (Eh) and normalized NO_3-N and Br concentrations at various locations in the Leon soil-packed flow cell subjected to horizontal pore-water velocity of ~12 cm d^{-1} The rate of application at the surface was 3.6 L d^{-1} and an Eh below 250 mV indicate that conditions are reduced enough to favor extensive denitrification.

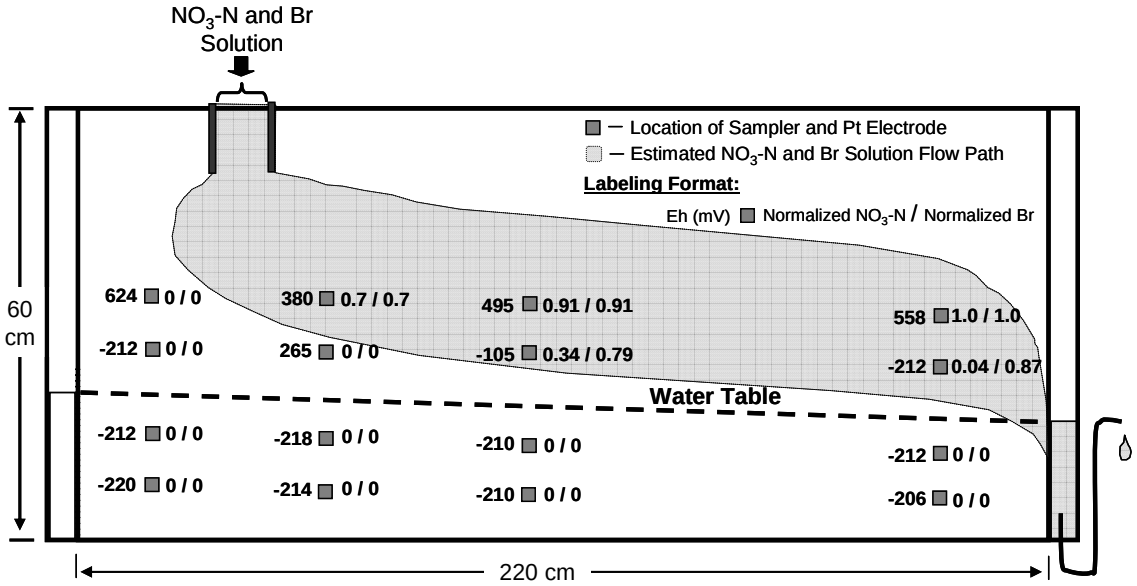

Figure 8. Schematic diagram showing final day reduction potential (Eh) and normalized NO_3-N and Br concentrations at various locations in the Leon soil-packed flow cell subjected to horizontal pore-water velocity of 29 cm d^{-1}. The rate of application at the surface was 3.6 L d^{-1} and an Eh below 250 mV indicate that conditions are reduced enough to favor extensive denitrification.

7. Appendix

Table A1. Selected properties of soils used in the experiment.

Soil	Texture	Ksat (m d^{-1})	TOC (g kg^{-1})	Percent N
Leon Ap	LS	3.0	35.4	0.12
Commercial Sand	Medium S	6.6	0.3	<0.02

Table A2. Bulk density of soils packed in the flow cell.

	Location (depth interval)	Bulk Density (g cm^{-3})
Leon Ap	Top (4-12 cm)	1.28
	Middle (23-31 cm)	1.37
	Bottom (40-48)	1.38
Commercial Sand	Top (4-12 cm)	1.51
	Middle (23-31 cm)	1.53
	Bottom (40-48)	1.62

Table A3. Descriptive statistics of dissolved organic carbon (DOC) and solution pH of samples collected from the medium sand Leon sand packed flow cells.

	DOC mg L^{-1}		pH	
	Medium Sand	Leon Soil	Medium Sand	Leon Soil
Mean	1.46	108.10	6.53	5.61
Range	4.18	299.10	0.63	1.07
Minimum	0.66	8.89	6.18	5.12
Maximum	4.84	308.00	6.81	6.19
Standard Deviation	0.79	74.86	0.12	0.25

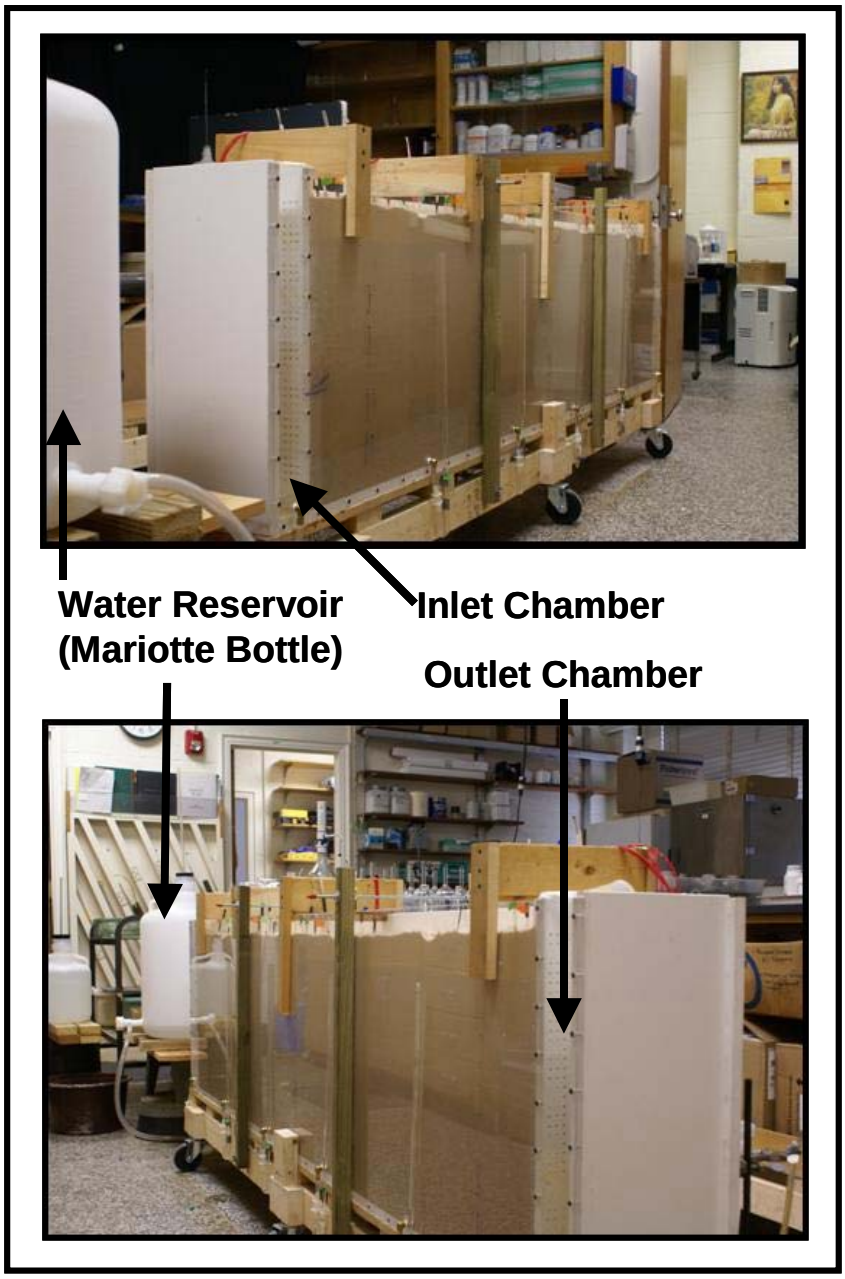

Figure A1. Photographs from two vantage points of the large flow cell used in the experiment.

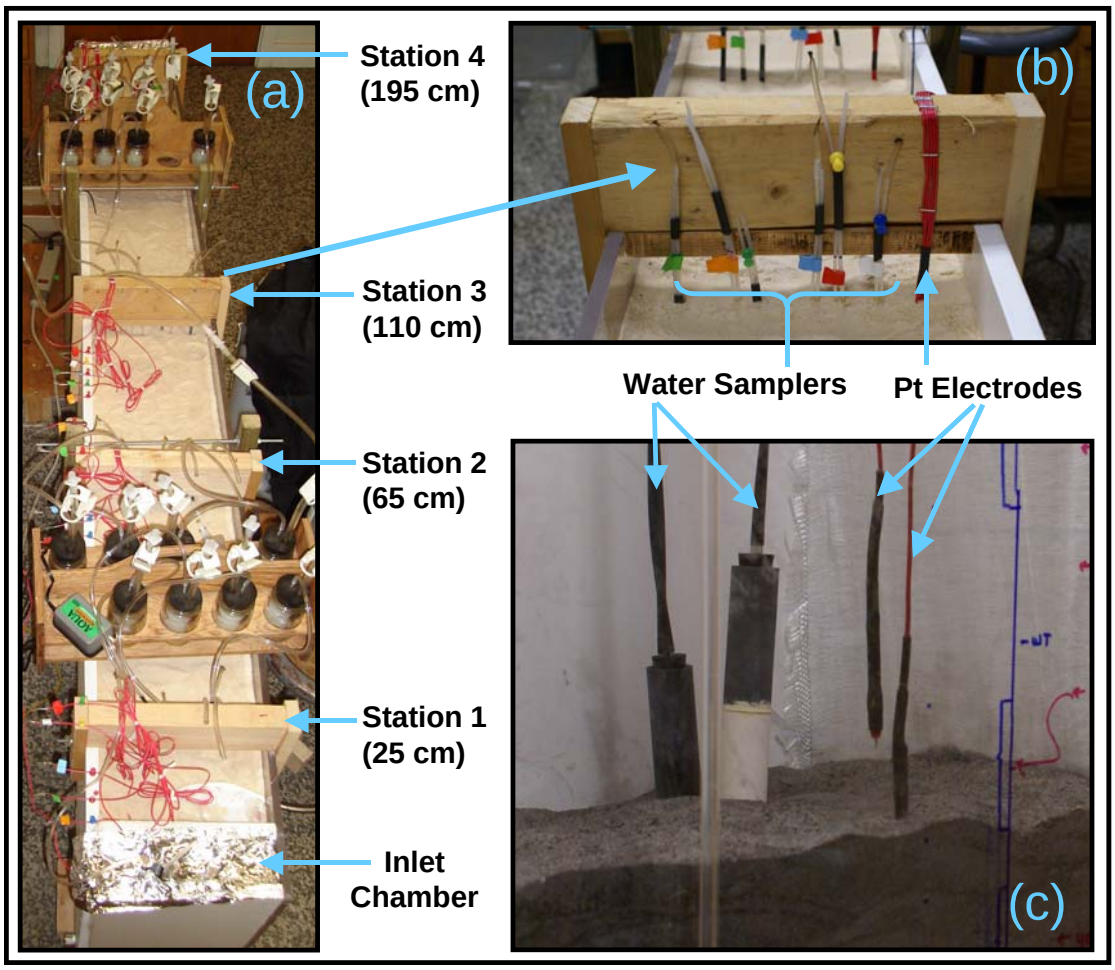

Figure A2. Photographs showing the top-view of the large flow cell (a), a sampling station (b) and water (tension) samplers and Pt electrodes hanging from the sampling station as soil is being packed in the flow cell (c). Note: The top of the flow cell was later covered with aluminum foil.

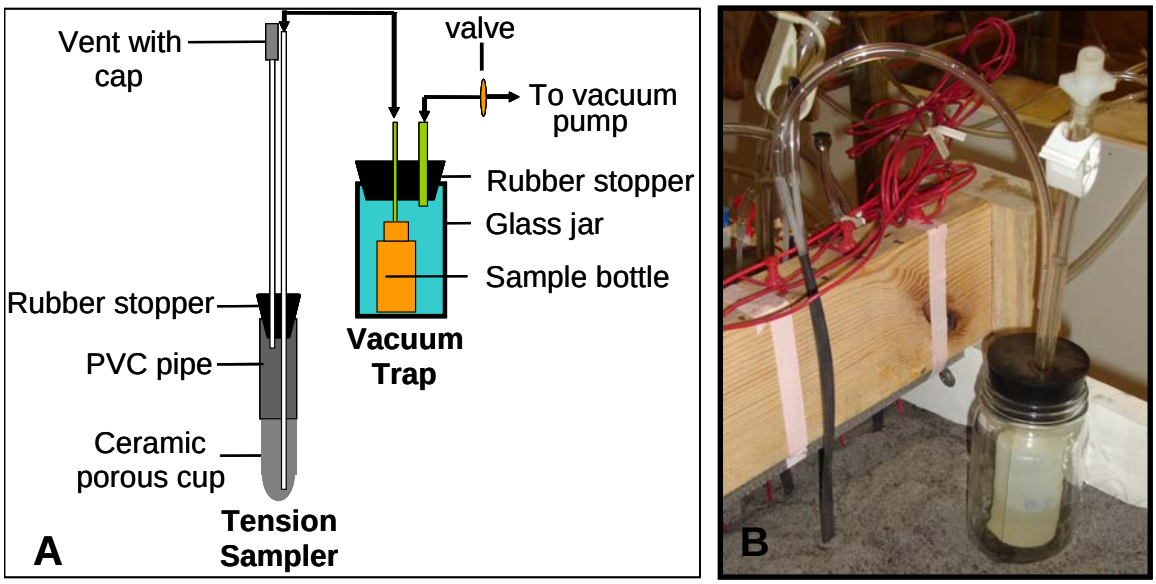

Figure A3. Diagram of the soil collection system (A) and photograph of the vacuum trap connected to a tension sampler (B).

CHAPTER 5

Dissolution of Phosphorus into Pore-water Flowing through an Organic Soil

Abstract

Phosphorus (P) loss from agricultural fields and restored wetlands can cause eutrophication in surface water bodies. Evaluation of P dissolution in organic soils present in agricultural fields and wetland restoration areas is important in devising management strategies to manage P losses. The objective of this study was to evaluate the dissolution of P in water flowing through the vadose zone-shallow ground water continuum of an organic soil. Three 90 cm × 50 cm × 8 cm flow cells were uniformly packed with Ponzer (Terric Haplosaprists) soil material collected from an area that had been in agricultural production for at least 30 years. The packed flow cells were instrumented with soil solution samplers and platinum-tipped redox electrodes at 5 cm below, and at 5 cm and 20 cm above a simulated water table (WT) to collect soil solution and monitor the reduction potential (Eh), respectively. Distilled water was continuously supplied at the constant rates of 1.2, 2.4 and 3.6 L d^{-1} to one side of the flow cells while maintaining a water table at approximately 12 cm above the bottom of each flow cell. These application rates corresponded to horizontal pore-water flow velocities of approximately 6, 12 or 18 cm d^{-1} across the respective dedicated flow cells, respectively. Phosphorus (P) concentration in the outflow solution was consistently above the USEPA water quality limit but the difference in pore-water velocity that a given volume of water flowed through the flow cell did not results in significantly

different amounts of P leached within the time frame of the experiment. Phosphorus dissolution at 5 cm below and 5 cm above the WT was significantly higher than at 20 cm above the WT. This indicated that much of the P that was leached out of the flow cell originated from 5 cm above the WT and below. Results from the analysis of dissolved reactive phosphorus, total Fe and dissolved organic carbon in soil solution combined with Eh data and the relatively high soil Al content point to the following possible mechanisms as largely responsible for the increase in soil solution P concentration: i) increased ligand exchange of dissolved organic matter (DOM) for mineral adsorbed phosphate (PO_4) and ii) DOM-enhanced dissolution of surface Fe and Al with concomitant release of PO_4. These results indicate that off-site exportation of P could be minimized if the WT in an agricultural field or a wetland restoration site containing high organic matter is kept below the P-enriched surface layers.

1. Introduction

Wetlands are destroyed through highway or public works projects, as well as private developments. Restoration of a wetland at another site to compensate for the lost wetland function resulting from these projects is required for permitting any wetland destruction. Areas that are commonly utilized for wetland restoration in North Carolina (and perhaps other states) are previous wetland areas that had been drained and devoted for several years to agricultural production.

Years of cultivation and fertilizer application of a previous wetland area lead to nutrient accumulation in near-surface layers. Four decades of cultivation of Histosols soils in the Hula Valley, previously an Eastern Mediterranean wetland in Northern Israel, resulted in at least 50% higher total P in the top 20 cm of the soil compared to underlying layers (Shenker et al., 2005). At least 30 years of fertilizer application to a Histosols soil in a drained Carolina Bay in North Carolina resulted in 173% higher Mehlich-extractable P in the top 20 cm of the soil compared to that in an undisturbed reference wetland (Ewing, 2003). In addition, the Mehlich-extractable P in a Spodosols soil at the same drained Carolina Bay increased by 138% (compared to a reference wetland) after 20 years of cultivation (Ewing, 2003). Given the elevated nutrient status in these areas, wetland restoration activities should include nutrient management strategies because re-flooding during restoration of wetland hydrology had been known to increase dissolution of P (Shenker et al., 2005). An increase in soil solution P is a concern as it may affect water quality in adjacent streams, rivers and lakes through its effects on eutrophication (Correll, 1998).

Many studies have shown that flooding of soils results in P release into solution that was largely attributed to reduction processes and dissolution of Fe-P minerals or to Fe-hydroxide dissolution and release of the adsorbed P (Patrick and Khalid, 1974; Sah and Mikkelsen, 1986; Vadas and Sims, 1997; Turner and Haygrath, 2001, Shenker et al., 2005).

Oxidation of organic matter becomes less efficient under anaerobic conditions resulting in the accumulation of dissolved organic matter (DOM) in pore-water (Fiedler and Kalbitz, 2003). At elevated DOM concentrations, additional P-dissolution mechanisms had been reported to influence pore-water phosphate (PO_4) concentrations. These include competitive adsorption of DOM and PO_4 by ligand exchange on mineral surfaces, and DOM-enhanced dissolution of surface Fe or Al with concomitant release of PO_4 (Hutchison and Hesterberg, 2004, Brownfield, 2007). Increase in pH associated with the development of reduced conditions also tends to reduce sorption of PO_4 (Hutchison and Hesterberg, 2004).

The above mentioned P-dissolution mechanisms are triggered by the development of anaerobic and reducing conditions. Monitoring of reduction potential (Eh) above and below the WT in a column study by Stall (2008) revealed that while Eh measurements indicate reducing conditions below the water table (WT), conditions at 10 and 30 cm above the WT were consistently oxidizing. A field study by Abit et al. (2008a) showed that while nitrate was lost probably due to denitrification below the WT, nitrate persisted in zones that were within the capillary fringe (CF) (within 30 cm above the WT) for most of the 84-day study period. Their field study indicated that while conditions below the WT were reducing, the CF remained generally aerobic. In a separate study that evaluated redox dynamics in horizontal

subsurface flow constructed wetlands, Dušek et al. (2008) reported a correlation between Eh and flow rate. This implied that pore-water velocity may be an important hydrologic parameter that influences the development of reducing conditions in the subsurface.

The jurisdictional wetland hydrology requirement in the United States is achieved if "saturation (i.e., condition below the WT) occurs within a major portion of the root zone (usually within 30 cm from the surface)" and this must occur "continuously for at least 5% of the growing season in most years" (US Army Corps of Engineers, 1987). This rule suggests that the WT does not have to be at the surface to meet the wetland hydrology requirement. This could also mean that the hydrology of the wetland restoration area could be managed to keep the WT from the phosphorus-enriched layers (i.e., the upper 20 cm of the soil) yet meet the wetland hydrology criteria. If this management strategy results in lesser P-dissolution in the P-enriched zones, then it could minimize the threat of P-exportation from the wetland restoration sites to their adjacent water bodies.

This study was conducted to test the hypothesis that P-dissolution in locations that are within 30 cm above the WT is significantly lower than in locations below it. Also of interest was the possible effect of pore-water velocity on the degree of P dissolution from a P-enriched organic wetland soil. The specific objective of this study was to evaluate the dissolution of phosphorus (P) in water flowing through the vadose zone-shallow ground water continuum of an organic soil.

2. Materials and Methods

2.1. Soil Material

Soil material was collected from the surface layer (Oap horizon; 0-10 cm) of a site classified as the Ponzer series (Loamy, mixed, dysic, thermic, Terric Haplosaprists). The site was in Juniper Bay, a drained wetland area in Robeson County, NC, that had been devoted to crop production for at least 30 years prior to collection of soil material. The soil was air-dried and passed through a 2-mm mesh sieve. A representative bulk sample was collected for soil analysis. Saturated hydraulic conductivity (K_{sat}) was measured by the constant head procedure (Amoozegar and Wilson, 1999) using uniformly-packed soil material in cylindrical cores (7.6 cm in diameter and length). Soil water retention between 0 and 400 cm pressure was measured by the pressure cell procedure (Dane and Hopmans, 2002) and bulk density was determined by the core method (Grossman and Reinsch, 2002) using the same intact cores used in the K_{sat} determination. The pH was determined using a 1:1 soil to water (mass basis) suspension ratio. Total elemental C and N were measured using a Perkin Elmer CHNS Elemental Analyzer (Model PE 2400) after combustion of oven dried soil samples that were passed through a 2-mm sieve (Nelson and Sommers, 1996). Total elemental C was considered equivalent to TOC in these acidic, non-calcareous soil samples (Essington, 2004).

2.2. Experimental Set-up

Three flow cells having length, width and thickness dimensions of 90 cm, 50 cm and 8 cm, respectively, were used in this study. The front side of each flow cell was constructed using a 0.64-cm thick transparent polycarbonate sheet while the bottom and other sides were

made of flat polyvinylchloride (PVC) sheets (Fig. 1; see photograph in Figure A1 in the Appendix). Two 2.5 cm-wide chambers, with perforated inner walls, were constructed on the two sides of the flow cell. The left and the right chambers were used as inlet and outlet chambers, respectively. The central portion of the flow cell (85-cm wide) that was bounded by perforated flat PVC sheets was packed with the soil material.

Packing was done by adding previously sieved air-dried soil in the flow cell and tamping uniformly with a flat-ended piece of wooden dowel. To minimize layering, the surface of the tamped soil was stirred before more air-dried soil was added on top of it. Packing was done in approximately 5 cm-thick sections at a time. As the packing progressed, two sets of solution samplers were installed at 32 cm and 53 cm from the inlet chamber. Each set had a solution sampler at 7, 17 and 32 cm above the bottom of the flow cell. These locations corresponded to 5 cm below a simulated WT and at 5 cm and 20 cm above the simulated WT as will be discussed later (see Fig. 1). This arrangement allowed collection of two samples from each of the three depths monitored in each flow cell. A blackened platinum-tipped redox electrode (Pt electrode) was also installed at the middle of the flow cell (42.5 cm from either the inlet or outlet chambers) at all depths that the solution samplers were installed. Locations where soil solution samples were collected are hereafter called "monitoring locations".

The top 5 cm of the flow cell was packed with commercially-available coarse sand. The coarse sand served as a capillary barrier that kept the packed soil from being wetted (via capillary action) all the way to the top. Having the capillary barrier also reduced the

likelihood of evaporative losses. The top of the flow cell was then covered with aluminum foil (with a few pinholes) to further discourage evaporative losses that could have encouraged upward flux of water in the flow cell.

Soil solution was collected using micro-samplers installed through holes at the front side of the flow cell (see Fig. 1). The hydrophilic porous polymer tube (Soilmoisture Equipment Corp, Sta. Barbara, CA) that were used for the construction of the micro-sampler in this study does not sorb P and has a bubbling pressure equivalent to approximately 200 kPa (2 atm). The micro-samplers were positioned horizontally inside the flow cell to collect water samples across the thickness of the packed soil (see Appendix Fig. 2 for an illustration of the micro-sampler). The holes on the flow cell through which the micro-samplers were installed were sealed with silicone rubber sealant.

Sealed 120-mL serum bottles were used for sampling. A drop of hydrochloric acid (HCl) was added to each bottle before it was covered with a rubber septum cap and clamped with an aluminum seal (Wheaton, Millville, NJ) to keep it air-tight. Air in the serum bottle was then evacuated using a pump to create a vacuum of 400 cm inside the bottle (hereafter referred to as “evacuated bottle”). To collect a sample, a dedicated evacuated bottle was attached to the sampler. This was accomplished by piercing a hypodermic needle that was attached to the micro-sampler (by a Luer-lock connector- see Fig. A2 in the Appendix) into the rubber cap of the evacuated bottle. A 20-mL solution sample was collected using this procedure for each sampling. After collecting a 20-mL sample using the pre-acidified serum bottles, a smaller non-acidified evacuated bottle (20-mL serum bottle with cap) was attached

to a dedicated micro-sampler to collect 5 mL of sample that was used for determination of soil solution pH.

The Pt electrodes used in the experiment were built according to the specifications in Wafer et al. (2004) and blackened using a platinizing solution (chloroplatinic acid hexahydrate and lead acetate trihydrate – Ricca Chemicals, Arlington, TX) as described in Jackson (1975). Blackened electrodes have been recommended for use in measuring reduction potential (Whisler et al, 1974; Quispel, 1947). Each Pt electrode was connected to a CRX10 data logger (Campbell Scientific, Logan, Utah) that was programmed to measure and record voltage measurements every 15 minutes. Electrodes were standardized in a ferrous-ferric iron solution or Light's solution (Light, 1979) before installation.

2.3 Flow-through Experiment

Before introducing distilled water into each flow cell packed with soil material, the outlet chamber was connected to a plastic tubing with an open end fixed at 12 cm above the bottom of the flow cell. The four inlet/outlet ports at the bottom of the flow cell and the inlet and outlet chambers were connected via a plastic tubing manifold to an aeration reservoir (Fig. 1, see Fig. A1 in Appendix for a photograph of the manifold). The aeration reservoir was connected to a 25-L distilled water reservoir (Marriotte bottle). The tip of the air inlet tube in the water reservoir was also set at 12 cm above the bottom of the flow cell (Fig. 1). A gel-filled Calomel reference electrode (Fisher Scientific, Pittsburgh, PA, ID No. 13-620-258) and the 3 Pt electrodes already installed in the flow cell were connected to a dedicated data logger.

Distilled water from the Marriotte bottle reservoir was initially supplied to the aeration reservoir while clamping the tubing that connected the aeration reservoir to the flow cell through the manifold. Using an aerator, air was bubbled through the distilled water in the aeration reservoir to keep it uniformly aerated. Once a static water level was established in the aeration reservoir, the tubing connecting it to the flow cell was unclamped allowing delivery of water through the manifold to the bottom and sides of the flow cell to establish a simulated WT. The soil material in the flow cell was saturated from the bottom to prevent air entrapment as the flow cell was flooded to the desired level. The reference electrode was immediately installed at the outlet chamber (tip of reference electrode submerged in water) as soon as water started to flood in it. The data loggers collected voltage measurements (between reference and Pt electrodes) every 15 minutes.

Four hours after a static WT was established 12 cm above the bottom of the flow cell, background soil solution samples were collected from all micro-samplers. One hour after collection of the background samples, the tube connecting the aeration reservoir to the bottom and sides of the flow cell were clamped. Distilled water was then introduced into dedicated inlet chambers to bring about horizontal flow across the packed soil. A pre-determined number of peristaltic pump tubes of different diameters was installed in a variable rate peristaltic pump for each flow rate. These tubes supplied distilled water from the aeration reservoir to the respective inlet chambers at rates of 1.2, 2.4 and 3.6 L d^{-1} that were equivalent to horizontal pore-water flow velocities of approximately 6, 12 or 18 cm d^{-1}

across a dedicated flow cell. The resulting average pore-water velocities (V_{ave}) in the experiment were computed using the formula:

V_{ave} = Flux/Water-Filled Porosity,

where Flux is the Darcian velocity, which is the total application rate divided by the cross sectional area of the flow path. The cross sectional area of the flow path included both the 12-cm saturated zone and the 30-cm thick CF. Since the CF is nearly saturated, the water-filled porosity was taken to be the same as the total porosity of 0.63 cm^3 cm^{-3}.

Outlet samples were collected daily and frozen until analyzed for pH, dissolved reactive phosphorus (DRP) and dissolved organic carbon (DOC). Outflow samples were filtered using 2.5-µm particle retention filter paper (Whatman International Ltd, Kent, UK, Whatman no. 42) prior to chemical analysis. Solution samples were collected from the monitoring locations at 3, 7, 14, 21 and 28 days after initial saturation. Soil solution samples were analyzed for pH, DOC, DRP and total Fe. When not collecting samples, the front side of each flow cell was covered with aluminum foil to prevent any impact that light could have on chemical/microbial activities.

Analysis of DOC was carried out using the Total Organic Carbon (TOC) Auto-analyzer (Shimadzu Corp., Columbia, MD) while DRP was analyzed using the Lachat Quickechem 8000 slow injection auto analyzer (Greenberg et al., 1992). Dissolved Fe was measured using inductively coupled plasma optical emission spectrometry (Perkin-Elmer ICP-OES 2000DV, Elmer, Germany). After 28 days, the flow cells were emptied, cleaned

and re-packed with the air-dried Ponzer soil material and subjected to the same mode of saturation, pore-water velocities and sampling schemes to duplicate the experiment.

3. Results and Discussion

The soil material used in the study contained 0.08 g kg^{-1} of Mehlich-extractable P, an expectedly high soil TOC content of 195 g kg^{-1}, and an extractable Fe of 10 to 63 mmol kg^{-1} depending upon the extraction procedure (Table 1). The soil also contained 130 mmol kg^{-1} of extractable aluminum (Al).

3.1 Outflow Solution Chemistry

Intuitively, P dissolution is expected to be higher at a relatively low pore-water velocity than at higher pore-water velocities. This is because slower pore-water velocities indicate a longer residence time of the water in the system, resulting in more time that the water is in contact with the soil and exposed to P-dissolution reactions. However, within the time frame of the experiment, the degree of P dissolution was not affected by the pore-water velocities employed in various flow cells. This was indicated by the absence of a significant difference between the mass of DRP leached-out of the different flow cells subjected to various pore-water velocities (Fig. 2). In effect, within the timeframe of the experiment, passing the same volume of water through a given volume of soil at pore-water velocities of 6, 12 and 18 cm per d^{-1} dissolved and leached a statistically similar amount of DRP from the soil. The absence of any significant effect of the pore-water velocities employed in this experiment on the degree of P dissolution may indicate that the resulting differences in residence time were not wide enough to cause any significant difference in the degree of dissolution.

It should be noted that regardless of the pore-water velocity, DRP concentrations of the outflow solution ranged between 0.217 to 2.69 mg L^{-1}, which exceeded the 0.1 mg L^{-1} USEPA water quality limit (USEPA, 1986). This indicates that water passing through Ponzer soil (or other similar soils) has a high probability of triggering environmental problems when drained to surface water bodies.

3.2 Phosphorus Dissolution

Given that water flowing through the Ponzer soil material yielded eutrophic levels of P in solution, the next question to ask is where in a vadose zone and ground water continuum P dissolution largely occurs with flowing water? Knowing this information is important as it could aid in devising possible management strategies to limit the degree of P exportation off-site during wetland restoration or (agricultural) drainage practices.

In addition to horizontal solute transport in the ground water, horizontal solute transport in the capillary fringe (CF), which is a part of the vadose zone, has been demonstrated in laboratory (Amoozegar et al., 2006; Silliman et al., 200; Henry and Smith, 2002) and field (Abit et al., 2008a, b) experiments. This indicates that P dissolution both in the CF and in the ground water could influence the amount of P that is leached out of the system.

Figure 3 shows a general increasing trend (with time) in DRP concentration of soil solution samples collected from the flow cells. The trend was observed across different pore-water velocities and the observed increase in DRP concentration was more obvious at the monitoring locations 5 cm below and 5 cm above the WT. In addition, detected DRP

concentrations at these two depths were consistently significantly higher than those detected (on the same day) at 20 cm above the WT. This suggests that much of the increase in DRP detected at the outlet was from the dissolution of P near the WT in both the saturated and vadose zones. The following discussions are largely focused on the results from the monitoring locations at 5 cm above and 5 cm below the WT as these were the zones where much of P dissolution occurred.

The observed increase in soil solution DRP concentration with time was coupled by a decrease in DOC concentration (Figure 4). This trend contradicts the information in the literature showing that an increase in dissolution of DRP is coupled by an increase in DOC (Hutchison and Hesterberg, 2004; Brownfield, 2007). The observed inverse relationship between DRP and DOC may be due to the fact that unlike the reactor/closed systems used in the above-mentioned experiments, wherein whatever carbon and P that were dissolved stayed and accumulated in the system, this study was conducted in a flowing system which presents the possibility that a fraction of the DOC and DRP could be leached with the flowing solution.

Results from the study of Hutchison and Hesterberg (2004) showed that an increase in DOC concentration from around 40 to 125 mg L^{-1} resulted in an 8 mg L^{-1} increase in dissolved DRP. Such observed increase in DRP was largely attributed to: i) competitive adsorption of DOM and PO_4 by ligand exchange, and ii) DOM-enhanced dissolution of surface Fe and Al with concomitant release of PO_4. These mechanisms are hereafter referred to as "DOM-triggered" mechanisms. Viewed differently, their results indicate that the DOM-

triggered P-dissolution mechanisms could proceed at DOC concentrations between 40 to 125 mg L^{-1}. Results from the reactor study of Brownfield (2007) involving the Ponzer soil indicated that an increase in DOC concentration from around 20 to 60 mg L^{-1} resulted in roughly 0.8 mg L^{-1} increase in DRP.

Despite the observed decrease in DOC in the flow cells with flowing water used in this experiment, DOC concentrations were consistently above 40 mg L^{-1}(Fig. 4). In fact, only once was the DOC observed to be below 50 mg L^{-1} in soil solution samples from the flow cells. In effect, despite the drop in DOC concentration in soil solution in the flow cells, DOC was still present in quantities that could cause the above-mentioned DOC-triggered P-dissolution mechanisms.

The amount of DOC in the system proved to be sufficient to encourage the progressive development of reducing conditions at 5 cm above and 5 cm below the WT (Fig. 5). Figure 5 shows that the Eh dropped below the hydric standard reduction line (below which Fe(III) reduction is expected to be extensive – USDA-NRCS, 2007) and remained very low (reducing conditions) despite the continued decrease in DOC in solution. Figure 5 also shows that the observed drop in Eh below the hydric soil standard reduction line was coupled by an increase in soil solution total Fe concentration. The observed spike in total Fe as the Eh dropped is most likely due to the reduction of Fe(III) resulting in an increased Fe(II) concentration in solution. However, after the initial spike (observed on day 3) total Fe concentration either essentially leveled-off or decreased throughout the remainder of the experiment. Figure 5 also shows that, at 20 cm above the WT, where the Eh reflected a

consistently oxidizing environment, no increase in Fe concentration was observed because conditions were not favorable for the reduction of Fe(III) to the soluble Fe(II) form.

In an Fe-P complex, one mole of Fe binds a mole of P. As shown in the idealized example reaction below, reductive dissolution of 1 mole of Fe^{2+} is accompanied by the dissolution of a mole of HPO_4^{2-}.

$$\text{Mineral--Fe--PO}_4 + e^- + H_2O \longrightarrow Fe^{2+} + HPO_4^{2-} + OH^-$$

This would mean that if P-dissolution was largely due to the reductive dissolution of Fe(III) minerals with associated PO_4 (hereafter referred to as "Eh-triggered" mechanism), then the number of moles of P that are released into solution should be similar to the increase in the number of moles of total Fe that gets dissolved. Figure 6 indicates that the increase in soil solution DRP with time was not largely due to the Eh-triggered mechanism. This was shown by the fact that solution DRP concentration (in mM) continued to increase at monitoring locations 5 cm above and 5 cm below the WT despite the fact that the total Fe concentration leveled-off or decreased after the 3rd day of the experiment. In other words, the increase in total Fe in solution under reducing conditions did not account for the increase in dissolved P as the experiment progressed.

It should be noted that the extractable Al content of the soil was at least double the extractable Fe. This suggests that much of the P in the soil was possibly initially complexed by Al rather than by Fe. This could also mean that much of the P that continued to be dissolved after total Fe concentration in solution stabilized or decreased resulted from the DOC-enhanced dissolution of Al with concomitant release of PO_4. Knowing that

contributions of Fe reduction to P dissolution was minimal, and that DOC was present at concentrations reported in the literature to be sufficient to cause P-dissolution (despite the observed decrease in DOC concentration), we believe that the increase in dissolved PO_4-P in our flowing system was largely due to the DOC-triggered mechanisms which were: i) competitive adsorption of DOC and PO_4 by ligand exchange, and ii) DOC-enhanced dissolution of surface Fe and Al with concomitant release of PO_4.

4. Summary, Conclusion, Recommendation and Practical Application

This study was conducted to evaluate the dissolution of phosphorus (P) in a vadose zone-shallow ground water continuum of an organic soil with flowing water. Passing equal amounts of water through a flow cell packed with Ponzer soil material at pore-water flow velocities of 6, 12 or 18 cm d^{-1} did not result in a significant difference in the amount of phosphorus dissolved and leached out of the system. However, regardless of the pore-water velocity, the concentrations detected at the outlet were consistently above the water quality limits and may cause eutrophication in adjacent surface water bodies. Dissolution of P was found to be significantly more extensive in monitored locations 5 cm above and 5 cm below the water table (WT) than at 20 cm above the WT. This indicated that much of the P leached out of the system was from 5 cm above the WT and below. The dominant mechanisms believed to contribute to P dissolution in the experimental system include: i) competitive adsorption of DOC and PO_4 by ligand exchange, and ii) DOC-enhanced dissolution of surface Fe and Al with concomitant release of PO_4. We recommend that Al concentration of soil solution be monitored if a similar study is conducted.

Phosphorus export had been reported when areas previously devoted to agriculture were restored into a wetland. Highest extractable P concentration in these agricultural areas usually occurs in the upper 10 cm of the soil. The wetland hydrology requirement is considered satisfied if the WT is within 30 cm from the surface for a required number of days during the growing season. Extensive dissolution and off-site exportation of P (especially in the first few years of wetland restoration when vegetation may not yet be fully established)

can be prevented while meeting the wetland hydrology requirement by managing the hydrology of the system. This can be accomplished by keeping the WT within 30 cm from the surface but below the layer of high extractable P content. It should be noted, however, that our study showed that P dissolution occurs in parts of the CF that are close to the WT (within 5 cm). To prevent P dissolution, the WT should be at least 5 cm below the P-enriched layer.

5. References Cited

Abit, S.M., A. Amoozegar, M. J. Vepraskas and C.P. Niewoehner. 2008a. Fate of nitrate in the capillary fringe and shallow groundwater in a drained sandy soil. Geoderma. 146:209-215.

Abit, S. M., A. Amoozegar, M. J. Vepraskas and C. P. Niewoehner. 2008b. Solute transport in the capillary fringe and shallow groundwater: Field evaluation. Vadose Zone J. 7:890-898.

Amoozegar, A., C.P. Niewoehner and D.L. Lindbo. 2006. Lateral movement of water in the capillary fringe under drain fields. In: Proc. 2006 Tech. Educ. Conf., Denver Co. 27-31 Aug. 2006. Natl. Onsite Wastewater Recycling Assoc. Sta. Cruz, CA.

Amoozegar, A., and G. V. Wilson. 1999. Methods for measuring hydraulic conductivity and drainable porosity. In: R.W. Skaggs and J. van Schilfgaarde (eds). Agricultural Drainage. Agronomy Monograph No. 38. Soil Sci. Soc. Am, Madison, Wisconsin.

Brownfield, C.S. 2007. Phosphorus dissolution in soil material from a Carolina Bay as affected by reducing conditions. Master's Thesis, Department of Soil Science, North Carolina State University, Raleigh, NC.

Correll, D. 1998. The role of phosphorus in the eutrophication of receiving waters: A review. J. Environ. Qual. 27:261–266.

Dane, J. H., and J. W. Hopmans. 2002. Water retention and storage. In: J. H. Dane, and G. C. Topp (eds). Methods of Soil Analysis Part 4: Physical Methods. No. 5 in Soil Sci. Soc. Am. Book Series. Soil Sci. Soc. Am., Madison, WI.

Dušek, J., T. Picek and H. Čížková. 2008. Redox potential dynamics in a horizontal subsurface flow constructed wetland for wastewater treatment: Diel, seasonal and spatial fluctuations. Ecological Engineering. 34(3):223-232.

Essington, M. E. 2004. Soil and Water Chemistry: An Integrative Approach. CRC Press. Boca Raton, FL.

Ewing, J. 2003. Characterization of soils in a drained Carolina Bay wetland prior to restoration. PhD Dissertation. Department of Soil Science. North Carolina State University, Raleigh, NC.

Fiedler, S. and K. Kalbitz. 2003. Concentrations and properties of dissolved organic matter in forest soils as affected by redox regimes. Soil Sci. 168:793-801.

Greenberg, A. E., L. S. Clesceri, and A. D. Eaton. 1992. Standard Methods for Examination of Water and Wastewater. 18th Ed. APHA. Washington, DC.

Grossman, R. B., and T. G. Reinsch. 2002. Bulk density. In: J. H. Dane, and G. C. Topp (eds). Methods of Soil Analysis Part 4: Physical Methods. No. 5 in Soil Sci. Soc. Am. Book Series. Soil Sc. Soc. Am., Madison, WI.

Henry, E. J. and J. E. Smith. 2002. The effect of surface-active solutes on water flow and contaminant transport in variably saturated porous media with capillary fringe effects. J. Contam. Hydrol. 56:247-270.

Hutchison, K.H., D. Hesterberg. 2004. Dissolution of phosphate in a phosphorus-enriched Ultisol as affected by microbial reduction. J. Environ Qual. 33:1793-1802.

Jackson, M.L. 1975. Soil Chemical Analysis. Published by author. Madison, WI. Page 661.

Nelson, D. W., and L. E. Sommers. 1996. Total carbon, organic carbon and organic matter. p. 961-1010 In: D.L. Sparks (ed.) Methods of Soil Analysis: Part 3. Chemical Methods. ASA and SSSA, Madison, WI.

Patrick, W.H. Jr. and R.A. Khalid. 1974. Phosphate release and sorption by soils and sediments: Effect of aerobic and anaerobic conditions. Science 186:53-55.

Quispel, A. 1947. Measurement of oxidation-reduction potentials of normal and inundated soils. Soil Sci. 63:265-275.

Sah, R.H. and D.S. Mikkelsen. 1986. Transformations of inorganic phosphorus during flooding and drainage cycles of soils. Soil Sc. Soc. Am J. 50:62-67.

Shenker, M., S. Seitelbach, S. Brand, A. Haim and M.I. Litaor. 2005. Redox reactions and phosphorus release in re-flooded soils of an altered wetland. European Journal of Soil Science. 56:515-525.

Silliman, S. E., B. Berkowitz, J. Simunek, and M. Th. Van Genuchten. 2002. Fluid flow and solute migration within the capillary fringe. Ground Water. 40(1):76-84.

Stall, C.J. 2008. Microbial fate and transport in a seasonally saturated North Carolina coastal plain soil. Master's Thesis. Department of Soil Science. North Carolina State University, Raleigh, NC.

Turner, B.L. and P.M. Haygrath. 2001. Phosphorus dissolution in re-wetted soils. Nature. 411: 258.

USEPA. 1986. Quality Criteria for Water. USEPA Bulletin 440/5-86-001. pp 240-243.

USDA-NRCS. 2007. Technical standards for hydric soils. Hydric Soils Technical Notes 11. USDA-Nat. Resour. Conser. Ser., at: http://soils.usda.gov/use/hydric/ntchs/tech_notes/index.html. Accessed: April 2009.

US Army Corps of Engineers. 1987. Corps of Engineers Wetlands Delineation Manual. Technical Report Y-87-1. Vicksburg, MS. pp. 30-32.

Vadas, P.A. and J.T. Sims. 1998. Redox status, poultry litter, and phosphorus solubility in Atlantic coastal plain soils. Soil Sci. Soc. Am. J. 62:1025-1034.

Wafer, C. C., J. B. Richards, and D. L. Osmond. 2004. Construction of platinum-tipped redox probes for determining soil redox potential. J. Environ. Qual. 33:2375-2379.

Whisler, F.D., J.C. Lance, and R.S. Leinebarger. 1974. Redox potentials in soil columns intermittently flooded with sewage water. J. Environ. Qual. 3(1):68-74.

Zelasko, A. J. 2007. Soil reduction rates under water saturated conditions in relation to soil properties. MS Thesis. Department of Soil Science. North Carolina State University, Raleigh, NC.

6. Tables and Figures

Table 1. Selected soil properties of Ponzer soil material used in study.

Soil Properties	Measurements
Mehlich 3-Extractable P (g kg^{-1})	0.08
Total Organic Carbon (g kg^{-1})	195.3 $\pm$ 9.7
Total Nitrogen (g kg^{-1})	5.7 $\pm$ 0.1
Iron * (mmol kg^{-1})	
Citrate Bicarbonate Dithionate-extractable	63 $\pm$ 3
Na Pyrophosphate-extractable	11 $\pm$ 0.8
Oxalate-extractable	10 $\pm$ 2.0
Aluminum (Citrate Bicarbonate Dithionate-extractable; mmol kg^{-1})	130 $\pm$ 3
pH	4.5 $\pm$ 0.2
Bulk Density (Mg m^3)	0.62 $\pm$ 0
Porosity (cm3 cm^{-3})	0.63 $\pm$ 0.01
Saturated Hydrauic Conductivity (K_{sat}) (m d^{-1})	1.17 + 0.1

*- Extractable Fe an Al values from Zelasko (2007)
Note: Bulk density, porosity and K_{sat} were measured from packed core samples

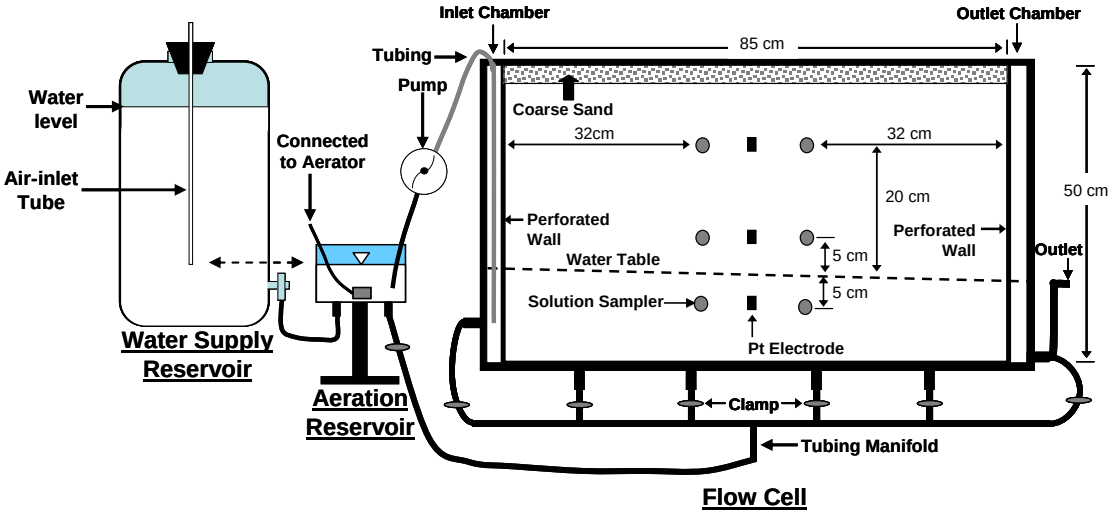

Figure 1. Two-dimensional representation of the set-up used in the experiment. Note: The flow cell is 8 cm thick and illustration is not to scale.

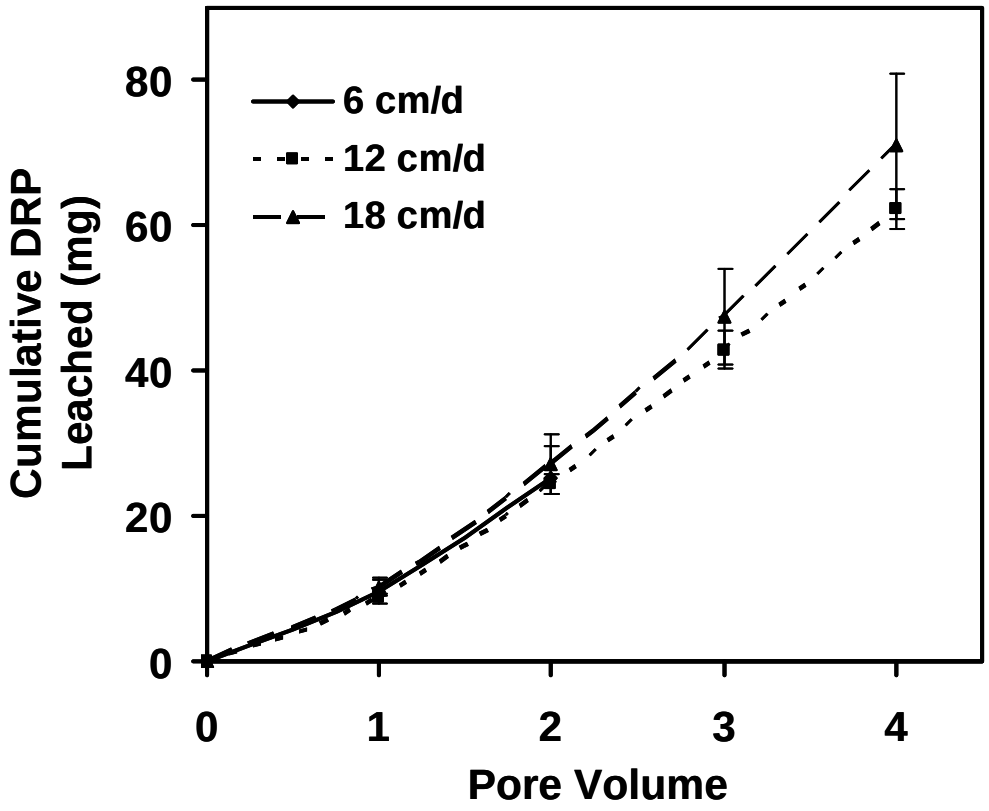

Figure 2. Cumulative amount of dissolved reactive phosphorus (DRP) leached out of the flow cell (pore volume basis) at various pore-water velocities.

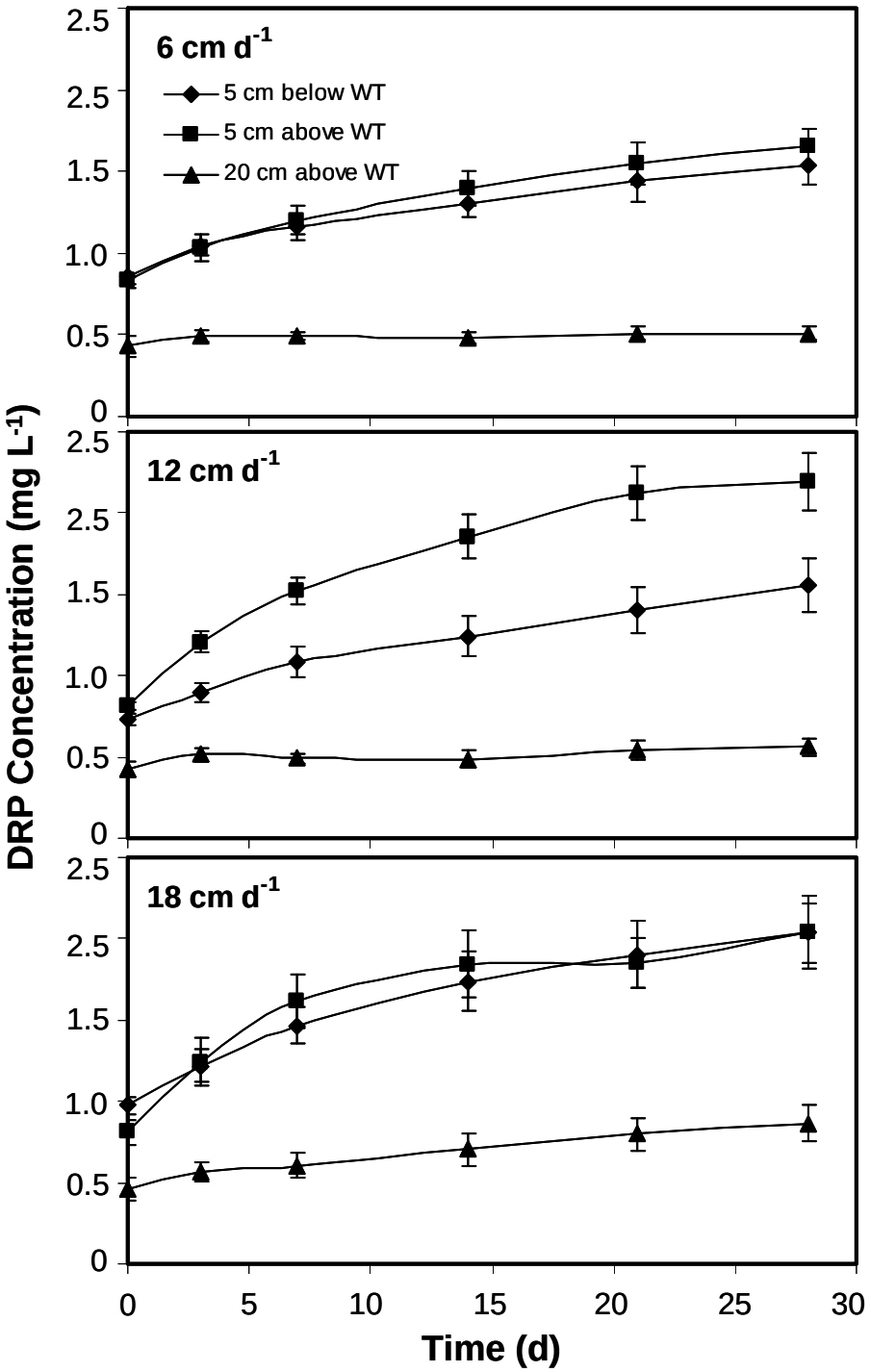

Figure 3. Soil solution DRP concentrations at various monitoring locations in flow cells subjected to various pore-water velocities.

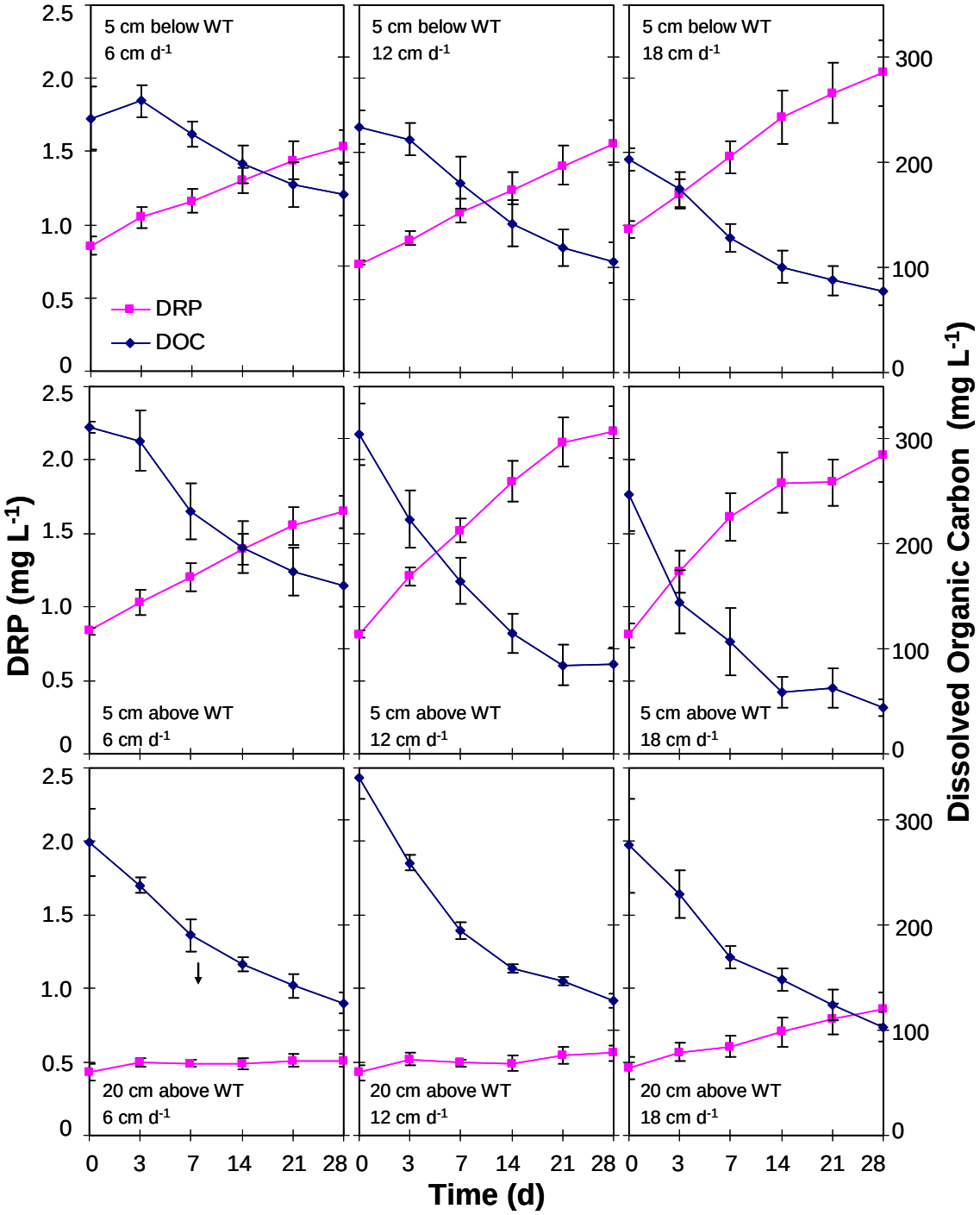

Figure 4. Changes in DRP and dissolved organic carbon (DOC) concentrations at various locations in the flow cells that were subjected to different pore-water velocities.

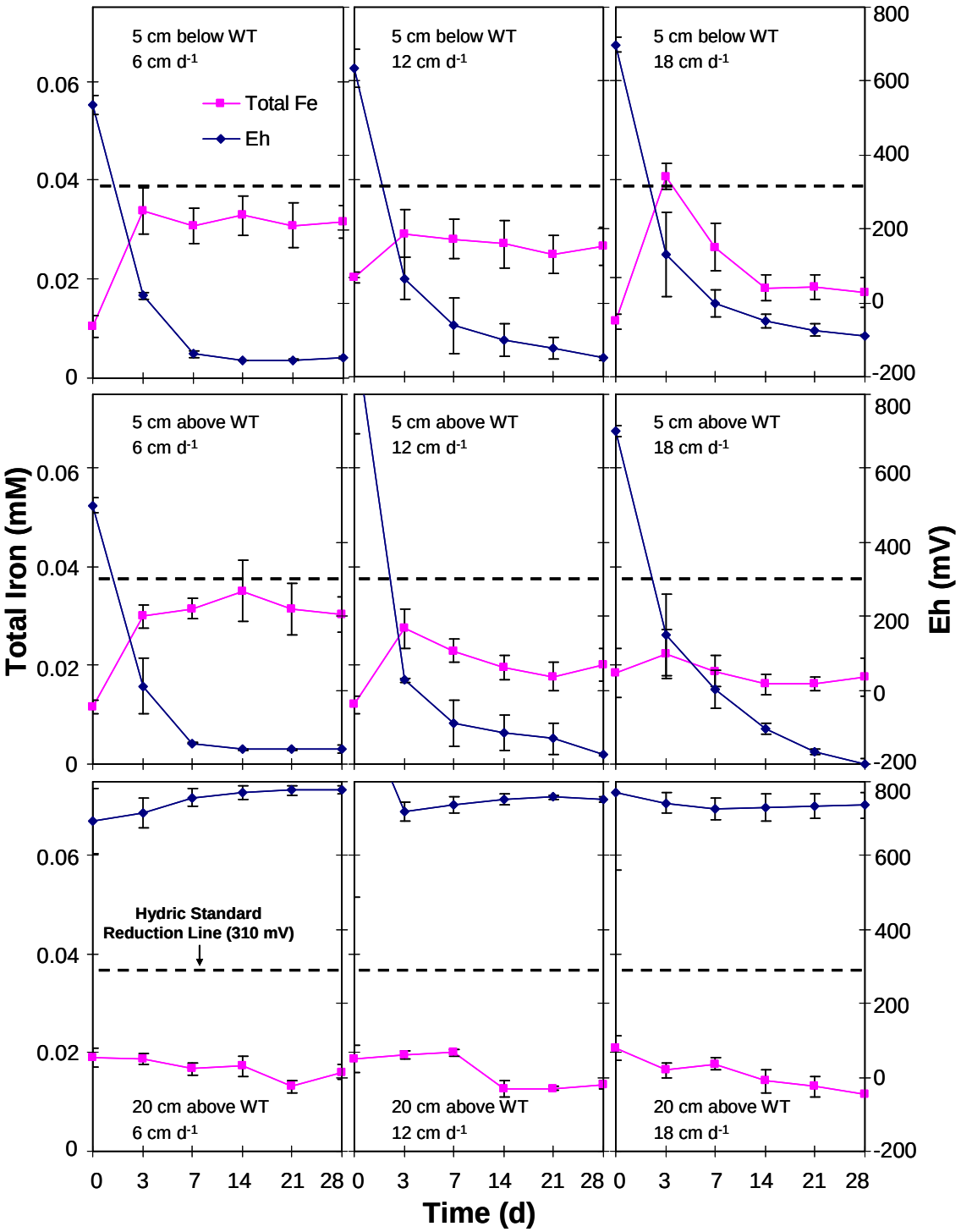

Figure 5. Changes in total iron (Fe) concentration and reduction potential (Eh) at various locations in the flow cells subjected to different pore-water velocities.

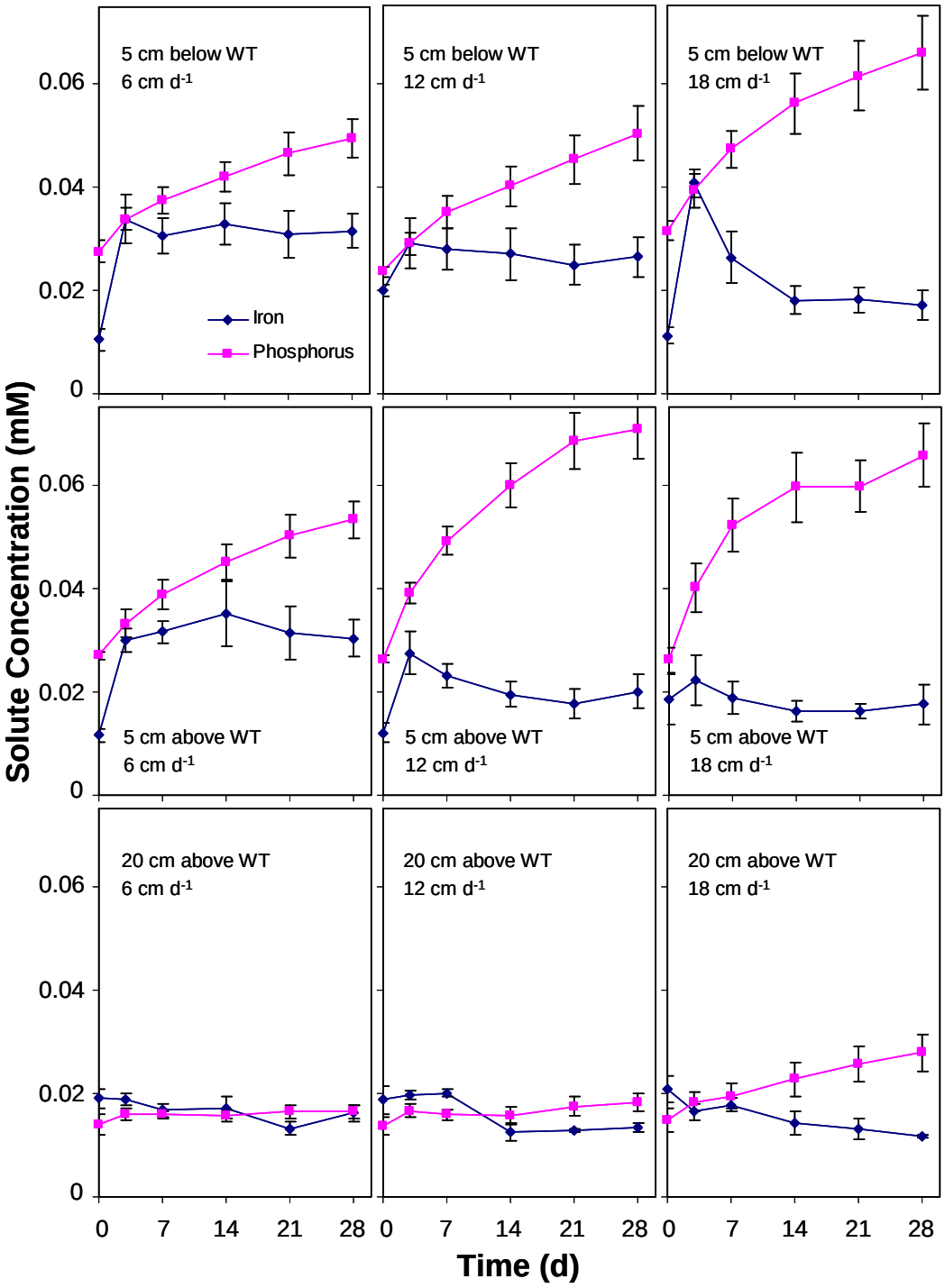

Figure 6: Comparison of DRP and total iron concentrations at various locations in the flow cells subjected to different pore-water velocities.

7. Appendix

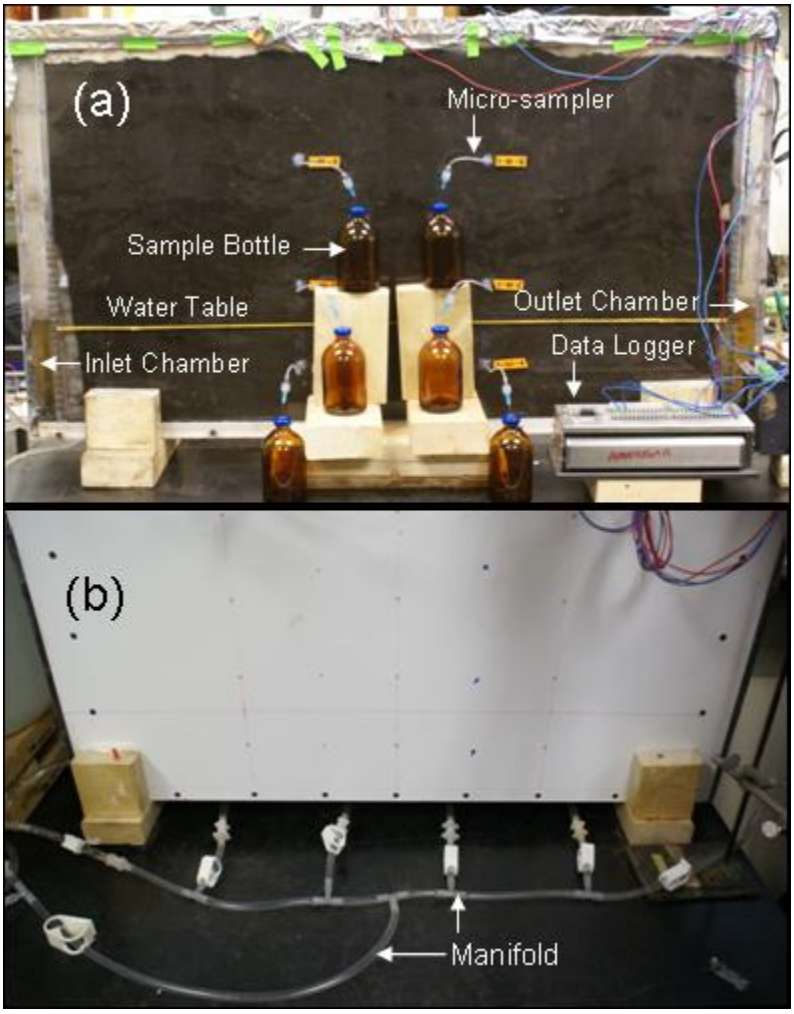

Figure A1. Photographs showing: a) flow cell with attached serum bottles. b) back-view of the flow cell showing the manifold used to supply water to establish a water table. Transparent side of flow cell was covered with aluminum foil when not sampling.

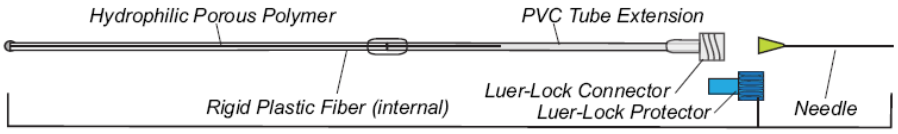

Figure A2. Illustration of the micro-sampler used in the experiment. Illustrations from Soilmoisture Equipment Corp.

CHAPTER 6

General Conclusions, Recommendations and Future Directions

Nutrients and pathogenic microbes in contaminated water resources could come from anthropogenic sources such as agriculture (crop and animal production), faulty septic systems and sewer lines, and surface-applied waste water or biosolids. The risks from these contaminant sources are expected to increase as demand for food as well as housing development continue to rise. This highlights the need for further study of their subsurface fate and transport, with the ultimate goal of being able to prevent these contaminants from causing ecological and human health problems.

Nutrient and microbial contaminants that are applied to the soil either sorb, degrade, transform or remain in solution or suspension. If contaminants remain in solution or suspension, they could be available for transport via the hydrologic system. The various experiments conducted in this research demonstrated that the hydrology of the system [e.g., pore-water velocity and water table (WT) fluctuation] affects the fate and transport of nutrient and microbial contaminants in the subsurface.

Horizontal subsurface transport of surface-applied solute and microbial contaminants occurred in the capillary fringe (CF) above the WT when the horizontal pore-water velocity of the ground water was relatively fast. The horizontal transport of solute and microbial contaminants was also fast when they were largely transported in the upper portions of the CF. This research also showed that surface recharge with water having solute and microbial contaminants resulted in WT rise even if the contaminants had not reached the original WT.

The subsequent drainage that resulted in a drop in WT was observed not to result in appreciable leaching of solute and microbial contaminants that were in the CF prior to drainage.

The aeration status at various locations in a vadose zone-ground water continuum where contaminant transport can take place was also influenced by the hydrology of the system. The development of reducing conditions tended to be slower when the system was subjected to faster horizontal flow velocities. In addition, while locations just above the WT and below it became progressively reducing after saturation, the upper portions of the CF remained aerobic.

The aeration status of the subsurface locations where water flow/solute transport occurred was also found to influence the fate (mainly transformation or dissolution) of nutrient compounds. In the case of surface-applied nitrate, the pore-water velocity dictated the subsurface flow path where it could potentially be transported (either both above and below the WT or the just largely in the CF). However, it was the aeration status of the flow path that influenced the fate of nitrate. Nitrate was lost completely, most likely due to denitrification, when surface-applied nitrate-containing solution reached the reduced regions below or just above the WT. In contrast, it was effectively transported horizontally, with relatively minimal loss, in the aerobic upper portions of the CF.

The fact that under certain hydrologic conditions dissolved nutrient compounds, such as nitrate and microbes can be transported solely in the CF, and that WT fluctuation does not result in effective leaching of solute and microbial contaminants in the CF to the ground

water implies that the non-detection of surface-applied contaminants below the WT does not definitively indicate that the contaminants are not in subsurface locations where they could be available for transport. They could indeed be lodged in the CF where they persist and transported horizontally across the subsurface. This poses a question on the efficacy of the current common practice of monitoring subsurface contamination by solely collecting water samples from the ground water. Collection of samples only from below the WT may lead to an erroneous conclusion that a contaminant of interest is attenuated and/or not transported horizontally in the subsurface. Protocols for monitoring subsurface contamination of solute and microbial contaminants has to be revisited and it is recommended that subsurface monitoring of nutrient and microbial transport include efforts to gather samples from the CF.

The aeration status in a subsurface location was also found to influence the degree of phosphorus (P) dissolution in an organic soil that had been previously received P-fertilizers. Dissolved reactive phosphorus (DRP) concentrations at aerobic regions at the upper locations in the CF were consistently lower than the DRP concentrations at reduced regions just above the WT and below it. Based on this, it was concluded that most of the P leached out of the system came from P dissolution at locations just above the WT and below it. These results imply that the hydrology of the system could be manipulated to lessen the extent of P dissolution and prevent extensive off-site P export. It is recommended that in order to prevent extensive P export, the hydrology of the area has to be managed so as to keep the WT below the P-enriched layers and prevent extensive P dissolution.

The effect of hydrology on whether horizontal transport of contaminants would occur in the CF (which is largely aerobic) or both in the CF and in the aquifer (which may be reduced), should have implications beyond the fates and transport of nutrient and microbial contaminants that were addressed in this research. Possible further research directions include the evaluation of fate and transport of other key contaminants in the CF, including: a) redox-sensitive heavy metals such as chromium and arsenic, b) chemical pesticides, c) pharmaceuticals and endocrine disruptors, and d) munitions. Also, field investigations need to be conducted to confirm the finding of this research under real world conditions.